ISSN 1307-3729

REHVA

Federation of European Heating, Ventilation and Air Conditioning Associations

The REHVA European HVAC Journal

Volume: 59 Issue: 6 December 2022 www.rehva.eu

CLIMA 2022 papers on Digitization

REHVA Brussels Summit

CO_2 and PM -sensors tested

Save the Date!

Get in touch with our sustainable future at ISH 2023

World's leading trade fair for HVAC + Water

ISH

13.–17. 3. 2023
Frankfurt am Main

messe frankfurt

The REHVA European HVAC Journal

www.rehva.eu

Volume: 59 Issue: 6 December 2022

SUBSCRIPTIONS AND CHANGES OF ADDRESSES
REHVA OFFICE:
Washington Street 40
1050 Brussels, Belgium
Tel: +32-2-5141171
info@rehva.eu, www.rehva.eu

PUBLISHER
TEKNİK SEKTÖR YAYINCILIĞI A.Ş.
Fikirtepe Mah., Rüzgar Sk. No: 44C
A3 Blok, Kat:11 D:124 Kadıköy/Istanbul, Turkey

Contents

Download the articles from www.rehva.eu -> REHVA Journal

Advertisers

Next issue of REHVA Journal

Instructions for authors are available at www.rehva.eu (> Publications & Resources > Journal Information). Send the manuscripts of articles for the journal to Jaap Hogeling jh@rehva.eu.

THINK PERFORMANCE

THINK...SUSTAINABILITY

THINK...FUTURE

Eurovent certified products for sustainable and energy efficient buildings & homes.

EUROVENT CERTIFIED PERFORMANCE
www.eurovent-certification.com

Visit our new website

SCAN ME

- Find & compare certified products
- Download full performance reports
- Verify product certificate validity
- Read & share our articles & news

www.eurovent-certification.com

Eurovent Certita CERTIFICATION

EPB standards under Systematic Review and update expected to improve the alignment with EPBD IV

In 2017/18 all EPB standards have been published. As usual for CEN and ISO standards, after 5 years the standards have to be reviewed to decide if the standards should stay as they are, be updated or withdrawn. Beginning December 2022 this review process has ended and it is up to the various involved TC's to decide on basis of the received reactions. Based on this and the already expected reactions it is clear that many standards need an update.

The still ongoing revision of the EPBD is also a driver to revisit the EPB standards.

Fundamental change of the standards is not expected. The allowance in the EPBD on the hourly approach which is needed for a proper grid interaction towards a total decarbonisation of our buildings, may require some adaption. More emphasis on IEQ declarations that could be reported at the building Energy Performance Certificate (EPC)

Will the expected improvements lead to more direct use of the EPB standards?

Yes, as they are already used in all EU MSs, but not always in a direct way and not always following the EPB standards for 100%. This leads to the situation that the energy labels in Europe cannot be compared, in fact there are 27 or more methods and not just one as intended by developing and publishing the set of EPB standards. Also, the EPC classification system (the A to G score) is not harmonised, which is expected to improve given the expected EPBD IV requirements. EPB experts working at national level on their national procedures confirm this. These experts are also in favour of having an EU universal software kernel available. A software package that is fully in line with the set of EPB standards. The task that then remains for experts and regulators at national level is to agree on the national input values, climate data, user patterns, IEQ classes for the different building uses, etc. For the software houses remains the task to build the user interface as they did for the current national methods. This national interface includes the national choses and is adapted for the typical national practises, languages, building traditions, with links to product databases including the data needed as input for the calculation etc. This all will contribute to the harmonisation of the EP assessment procedure. A great asset for our industry optimising their energy saving products and services. The current 27 different national procedures hamper a real open EU market in Europe. This leads to suboptimal solutions and higher costs of energy saving technology. A freely available EPB software kernel will overcome this and will lead to decarbonisation of the European building stock. It will also stimulate innovative solution as the way to reward them will be similar throughout Europe and possibly at more global scale. ■

JAAP HOGELING
Editor-in-Chief
REHVA Journal

CLIMA 2022 conference papers on the theme Digitization

Twenty CLIMA 2022 papers have been acknowledged as high ranking on the theme Digitization.

The following 7 are included in this issue:

Integrating BIM, BMS and IoT data on the Web: Lasitha Chamari, Ekaterina Petrova, Pieter Pauwels

Reinforcement learning for the occupant-centric operation of residential energy system: Amirreza Heidari, François Maréchal, Dolaana Khovalyg

A novel machine learning approach to predict short-term energy load for future low-temperature district heating: Thomas Ohlson Timoudas, Yiyu Ding, Qian Wang

From BIM databases to Modelica - Automated simulations of heating systems: Esben Visby Fjerbæk, Mikki Seidenschnur, Ali Kücükavci, Kevin Michael Smith, Christian Anker Hviid

Assessment of fouling in plate heat exchangers using classification machine learning algorithms: Seyit Ahmet Kuzucanli, Ceren Vatansever, Alp Emre Yasar, Ziya Haktan Karadeniz

Remote refrigerant leakage detection system for chillers and VRFs:Shunsuke Kimura, Michio Moriwaki, Manabu Yoshimi, Shohei Yamada, Takeshi Hikawa, Shinichi Kasahara

Control device for pumping one-pipe hydronic systems: Jiří Dostál, Tomáš Bäumelt, Jiří Cvrček

The other 13 papers can be accessed online::

An early prototype for fault detection and diagnosis of Air-Handling Units: Shobhit Chitkara, Alet van den Brink, Shalika Walker, Wim Zeiler

An ontology-based approach for building automation data analysis: Eunju Park, Sumee Park, Sebastian Stratbücker

Applying MTP-concept for the standardization of building automation and control systems: Michael Krüttgen (M. Eng.), Jochen Müller (Prof. Dr. rer. nat)

Automated energy performance diagnosis of HVAC systems by the 4S3F method: Arie Taal, Laure Itard

Deep learning for CFD analysis in built environment: Giovanni Calzolari, Wei Liu

domOS an "Operating System" for Smart Buildings: Junior Dongo, Dominique Gabiou, Amir Laadhara, Martin Meyer, Brian Nielsen, Frédéric Revaz, Christian Thomsen

Fault detection in district heating substations - a cluster-based and an instance-based approach: Jad Al Koussa, Sara Månsson

FDD method for a variable-speed heat pump with natural refrigerants: Ivan Bellanco, Francisco Belío, Manel Vàlles, Raphael Gerber, Jaume Salom

Improving the Calibration on Building Stock Level method by Comparing objective functions and optimization algorithms: Paula van den Brom, Samuel Smets, Laure Itard

Interoperability as a driver or barrier of smart building technologies?: Stijn Verbeke, Karine Laffont, David Rua

Interoperable interactions of HVAC components based on a capability ontology: Nicolai Maisch, Maximilian Both, Ralf Ulmer, Prof. Dr. Jochen Müller

Predict the remaining useful life in HVAC filters using a hybrid strategy: Hossein Alimohammadi, kristina Vassiljeva, Eduard Petlenkov, Tuule Mall Kull, Martin Thalfeldt

Transient analysis of individual return temperatures in hydronic floor heating systems: Simon Thorsteinsson, Henrik Lund Stærmose, Jan Dimon Bendtsen

Integrating BIM, BMS and IoT data on the Web

LASITHA CHAMARI
Department of the Built Environment, Eindhoven University of Technology, Eindhoven, the Netherlands
l.c.rathnayaka.mudiyanselage@tue.nl

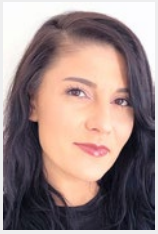

EKATERINA PETROVA
Department of the Built Environment, Eindhoven University of Technology, Eindhoven, the Netherlands

PIETER PAUWELS
Department of the Built Environment, Eindhoven University of Technology, Eindhoven, the Netherlands

Abstract: BIM, BMS and BIM data usually remain siloed and cannot be easily exchanged to perform cross-system analyses in buildings. Integrating these heterogeneous data sources provides ample opportunities to improve building performance. This study presents a methodology for integrating sensor data with a BIM model using Semantic Web technologies and open data models.

Keywords: Data integration, BMS, IoT, BIM, Semantic Web, Brick

Introduction

A building Management System (BMS) is used to centralize, automate, and manage HVAC, lighting, security, water, and energy subsystems. Internet of Things (IoT) devices are also extensively used in many new buildings [1], giving rise to a large volume of time series data about energy usage, ambient conditions (temperature, humidity, illuminance), as well as machine and equipment related parameters such as vibration, faults, alarms, etc. This data is useful in many applications such as reporting, monitoring, dashboards, fault detection, energy forecasting, etc., and also enables virtual representations of physical buildings, known today as "Digital Twins" [2]. Other than the time series data, Building Information Models (BIM) [3] are also essential components of the Architecture, Engineering and Construction (AEC) industry. A BIM model is a digital representation of a building that contains semantic information about the objects [4]. A properly developed and managed BIM model includes geometry, spatial location, and a broad representation of metadata about the properties of the building, its subsystems, devices, Mechanical, Electrical and Plumbing (MEP) equipment, etc. [5]. While time series data provides numerical values and patterns, BIM data provides the contextualization and semantic links between the systems of a building.

Data integration challenges

With the ever-increasing demand for smart building applications (such as Digital Twins) and real-time monitoring, there is a need to develop applications that combine the data available across multiple decentralized systems such as BIM and BMS. As a result, data integration becomes increasingly important. However, there is no straightforward way to integrate data across domains and systems, e.g., integrate a Honeywell BMS with a BIM model developed in Autodesk Revit. Such integration is not straightforward, because it relies on different modelling approaches, languages, and protocols, which makes it is incompatible by definition.

Therefore, a significant body of research in the AEC industry focuses on how to exchange and integrate heterogeneous data [2]. Many efforts revolve around Industry Foundation Classes (IFC), which is a vendor-neutral data model for the exchange of AEC data [2] relying on the EXPRESS schema language. IFC is an open international standard for BIM data that is exchanged and shared among software applications used by the various participants in the construction and facility management sectors [6]. However, not all aspects of the built environment can be modelled in IFC. For example, a crucial part of the operational phase of a building is the dynamic sensor data, which cannot be easily represented using IFC. Even though the IFC standard describes common systems such as Heating, Ventilation & Air Conditioning (HVAC), lighting, and sensor devices, they are not capable of representing the context of the devices contained within [7].

Using semantic technologies for data integration

Semantic technologies and linked data have shown promising results in integrating heterogeneous sources. IFC itself is also available as ifcOWL ontology [8]. Linked data models are built using formal ontologies and thereby allow extending and linking with other domain-specific ontologies, exchanging heterogeneous information [9], and deriving new information based on the semantic graph [7]. Linked Building Data (LBD) is an initiative with a focus on making building data web-ready [10], where a number of vocabularies and ontologies, such as BOT, PRODUCT, and PROPS, have been developed using a linked data approach [11]. Many other ontologies, such as SSN [12], RealEstateCore [13], Haystack [14], Brick [15], etc., have also emerged to formally represent different domains such as IoT sensors, business administration, BMS, etc., in the built environment. Semantic graphs, also referred to as knowledge graphs, are a representation of the built environment instantiated using such ontologies. These graphs can be queried using various query languages such as SPARQL [8], which allows information in the graph to be linked to other data sources and applications.

Status of data integration in buildings

Despite the availability of such technologies for data integration, their adaptation to buildings is quite slow. Data is often maintained in isolated silos, and there is little interaction between different datasets. For example, BIM models developed in the design phase often remain disconnected from the operational data. Most of the sensors and devices are also not included in the BIM models at the design stage. Again, although the spatial information is already available in the BIM model, this information is duplicated in the BMS due to the lack of interoperability. Therefore, despite the number of systems or amount of data being collected, it is difficult to interpret information across domains due to little interaction between islands of data [16]. Available data, their formats, naming conventions, and standards also differ significantly among each building and system vendor [17].

According to the literature [13, 14], a common use case is integrating sensor data into the BIM model using commercial BIM authoring tools like Revit or Navisworks. Although they may serve as appropriate tools for visualizing sensor data in a 2D or 3D environment, such approaches rely on vendor-specific software and do not provide reusable components for other applications. Alternative approaches rely on integrating datasets, including building geometry, the relationship between spaces, sensors and actuators, and time series data into a single semantic graph in Resource Description Framework (RDF) using Semantic Web approaches [20]. Sensor data is further retrieved for visualization in charts and colour-coded maps in 2D plans. Other studies [16, 17] suggest that retaining sensor data in a database that is optimized to store time series data is more efficient. Visualizing BIM models on the web has provided a vendor-neutral platform for collaboration and exchange of data, as well as means to integrate data across domains [10]. As such, a web-based server is proposed in [10], which allows users to upload BIM models in IFC format and visualize it in a graphical user interface. Attaching Linked Building Data (as graphs) to the project allows querying the BIM model based on the graph. However, implementations integrating systems, BIM, sensor data, and semantic graphs in a decentralized manner are still in their infancy.

Objective and scope

This paper presents the first outcome of the effort to integrate heterogeneous systems in a building using web technologies. We demonstrate how to integrate BIM models and time series data, two distinct systems in the built environment, in a distributed manner. The proposed approach uses an IFC file to create the initial graph, followed by another graph to represent the semantics of BMS sensors. This graph is used to integrate BIM and time series data. Each data stream remains in its optimum environment, and the connections are made via an Application Programming Interface (API) as opposed to file-based transfers. The demonstrated application is, therefore, entirely web based. The developed platform can be used to collectively view and query the building data in its entirety, browsing the BIM model and visualizing sensor data.

Case study: TU/e Atlas building

The TU/e Atlas case study building is a 12-storey renovated university building consisting of offices, study, and lecture rooms. It was renovated in 2019 and now contains a BMS, Energy Management System (EMS), and a Lighting Management System. The 4th to 11th floors of the building are considered a Living Lab and are used for research regarding Indoor Environmental Quality, energy efficiency, lighting, and Digital Twin implementations.

Time series data

The campus building has a Honeywell BMS. A data dump from the BMS containing occupancy, temperature, and CO_2 data is used for this study. They constitute 1,314,720 data points per month. Measurements are stored on an hourly basis, and the extracted data from the BMS is stored in spreadsheets (**Table 1**). The table columns contain the timestamps and the sensor IDs. Sensor IDs and their descriptions are also available in a separate mapping table as shown in **Table 2.** In here, sensor location is included in the description. For example, sensor 11NR008TE-001TRL is in room no.128 of the 8th floor.

BIM model

The BIM model used for this study represents the 8th and 9th floors of the case study building. It is developed in Autodesk Revit and includes space-related information (room name, room number, and the floor) and equipment-related information (sensors and lighting fixtures).

Implementation

This section describes the integration of the time series data and the BIM model. An overview of the underlying data conversion and storage infrastructure is shown in **Figure 1**. We demonstrate the implementation using graph snippets, and the full implementation of the RDF graph, BIM model, IFC file and XKT file is available in the ISBE-TUe/atlas-building-graph repository.

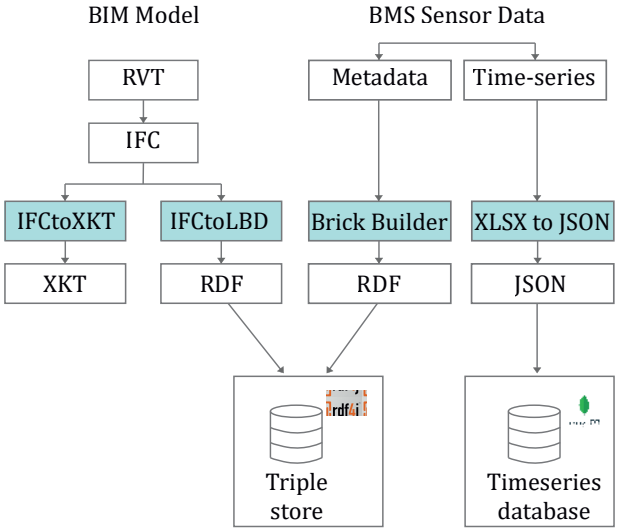

Figure 1. Data conversion and storage infrastructure.

Table 1. *BMS data extraction.*

Timestamp	11NR008TE-001TRL	11NR008TE-003TRL
28-02-2021 00:02:00	22.1	21.1
28-02-2021 01:02:00	22.0	20.9
28-02-2021 02:02:00	21.9	20.8
28-02-2021 03:02:00	21.7	21.2

Table 2. *BMS data point mapping table.*

Item name	Description
11NR008TE-001TRL	Room temperature 8_128
11NR008QT-040CO_2	*CO_2 measurement 8_323
11NR008LT-001PIRTM	Presence 8_128

Creating the semantic graph using IFC and sensor metadata

Several metadata representations that are useful in different phases of the building's lifecycle are available. IFC is an industry-wide standard data schema for BIM and covers many aspects of the design and construction phases of a building [2]. Geometry, building elements, and product properties are represented in IFC. The IFCtoLBD converter [23] is the tool used to generate RDF triples using an IFC STEP file. It makes use of the BOT, RDFS, and PROPS ontologies. The tool presented in [23] is used in this study to generate the RDF model of the building. Part of the IFC file containing information about the room "test 1 area" is shown in **Figure 2.** In IFC, there is a Globally Unique Identifier (GUID) for every element and `'0KLkXPBfvES9D1y7EjijkE'` is the compressed GUID of the space.

The above IFC file, when converted to RDF, is shown in **Figure 3.** "Space_1266" is a `bot:Space`, in which the number 1266 is related to the line number of the IFC file. The room can be uniquely identified by its compressed GUID represented using `props:hasCompressedGuid` relationship.

The Revit model of the building used for the study does not contain the BMS sensors; therefore, they are not available in the above graph. However, a mapping table was available, as shown in **Table 2**, which was used to find sensor metadata. The type of sensor and its location is available in this table. This study relies on the Brick Ontology to represent the BMS sensor data points. The RDF graph is created using the Brickbuilder [24] tool. A sample of the resulting graph with the relationships is shown in **Figure 4**.

The first RDF graph (**Figure 3**) semantically describes the context of the building, and the second graph (**Figure 4**) describes BMS sensors. These two graphs are stored in the RDF4J database [25] as two separate graphs. An instance of the resulting visual graph is shown in **Figure 5**.

Time series data

Timeseries data fits well in a time series database; therefore, MongoDB Timeseries Collection is used to store the timeseries data. Time series collection has the advantage of improved query efficiency and reduced disk usage for time series data, compared to normal document collections [26]. The ideal situation

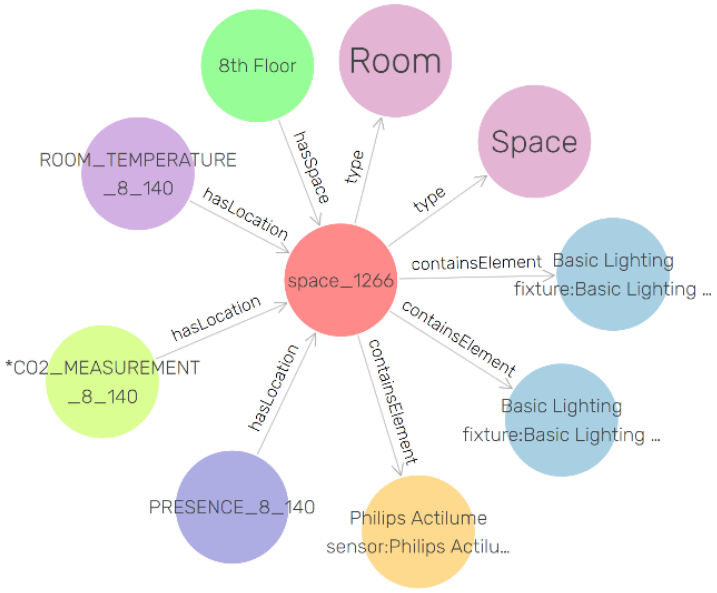

Figure 5. Graph representation of space_1266 using GraphDB.

```
1.  #1266= IFCSPACE('0KLkXPBfvES9D1y7EjijkE',#42,'9',$,$,#1245,#1263,'test 1 area',.ELEMENT.,.SPACE.,$);
```

Figure 2. Part of the IFC file containing IFCSPACE info.

```
1.  inst:space_1266 a bot:Space ;
2.  bot:containsElement inst:lightFixture_241729,
3.          inst:lightFixture_241879,
4.          inst:sensor_239793 ;
5.      props:hasCompressedGuid "0KLkXPBfvES9D1y7EjijkE"^^xsd:string ;
6.      bot:hasGuid "1456e859-2e9e-4e70-9341-f073adb2db8e"^^xsd:string ;
```

Figure 3. Part of the graph generated by the IFCtoLBD converter.

```
1.  inst:11NR008QT-301CO₂ a brick:CO₂_Sensor ;
2.      rdfs:label "*CO₂_MEASUREMENT_8_140"^^xsd:string ;
3.      brick:hasLocation inst:space_1266 .
```

Figure 4. Relationships defined among columns of the CSV file.

would be to integrate an already available API of the BMS time series database to retrieve time series data. However, access to such API for the Atlas building was not available so the time series data had to be duplicated in our own database.

BIM-SIM web application

BIM-SIM is the web application developed to support the above tasks. The front end is built using React, a JavaScript framework. One intended application functionality is to view the building geometry in 3D using a web browser. The proposed approach utilizes xeokit, an open-source JavaScript 3D graphics Software Development Kit (SDK) from xeolabs [27] [28] to render the 3D file in the browser. The IFC model can be transformed into XKT format, using several open-source command-line tools described in [29]. **Figure 6** shows the XKT file of the BIM model loaded in the web app.

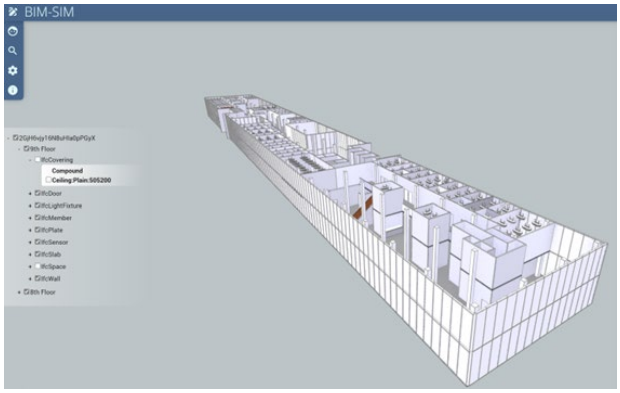

Figure 6. XKT file loaded in the web app.

Functionality

When a particular space is selected from the 3D model, the front end application picks the element's GUID, which is used to call the API, where a SPARQL query is executed to find all sensors in that space. A SPARQL query is sent in the request body in a POST request to the RDF4J server. Then the "Info window" is populated by the sensors in that space. These sensors are extracted from the RDF graph using the query shown in **Figure 7.**

This query results in three sensors contained in that space as shown in **Table 3**.

Then, selecting a particular sensor from the list calls the API with the sensor ID, which sends a query to the MongoDB database to retrieve historical data that belongs to the sensor ID. Then, the returned time series data is displayed in a chart as shown in **Figure 8**. When displaying sensor data, its metadata is also displayed. In this example, it is limited to the type of sensor (Brick CO_2 Sensor), but this can be extended to display the location and other relationships as well, when such are available.

Conclusion

This paper provides a vendor-neutral method for integrating time series data with a BIM model. The BIM model is used as the primary information source to develop the knowledge graph of the building. Second, BMS sensor semantics is introduced as another graph, using the Brick ontology. The IFC file is also used

```
1.  PREFIX brick: <https://brickschema.org/schema/Brick#>
2.  PREFIX inst: <http://linkedbuildingdata.net/ifc/resources20201208_005325/>
3.  PREFIX props: <https://w3id.org/props#>
4.  PREFIX rdf: <http://www.w3.org/1999/02/22-rdf-syntax-ns#>
5.  SELECT * WHERE {
6.      ?space props:hasCompressedGuid '0KLkXPBfvES9D1y7EjijkE' .
7.      ?sensors brick:hasLocation ?space .
8.      ?sensors rdf:type ?sensor_type .
9.   }
```

Figure 7. SPARQL query that runs in the API and retrieves the sensors in a given space.

Table 3. *SPARQL query results.*

	space	sensors	sensor_type
1	inst:space_1266	inst:11NR008LT-301PIRTM	brick:Occupancy_Sensor
2	inst:space_1266	inst:11NR008QT-301CO_2	brick:CO_2_Sensor
3	inst:space_1266	inst:11NR008TE-301TRL	brick:Temperature_Sensor

as the 3D model of the building, but it is converted to the XKT format, which is suitable for web-based visualization where the file size is reduced, but the geometry information is preserved. The developed web application provides the opportunity to interact with the knowledge graph, the 3D model, and the BMS sensor data. This integration is achieved by leveraging Semantic Web technologies, an open-source 3D graphics SDK, an API, and state-of-art web tools. This application can further be extended and improved, as discussed below.

The conversion of IFC to XKT [29] is adequately fast for the simple model used in this study. However, the conversion time and the completeness of the converted file have not been investigated in this study. This aspect can be further investigated in future extensions of the study.

In addition to the utilised historical data, an IoT sensor network is being developed to collect and display real-time temperature, humidity and illumination data. Integrating the real-time data with the web application is possible using the MQTT JavaScript client with WebSocket, which is currently under implementation.

Figure 8. Info window populated with sensors from the SPARQL query.

Although this study shows the implementation of an interactive monitoring application, other similar applications such as reporting on energy usage and indoor climate are also possible via the same resources. Most importantly, this platform needs to be extended to introduce data driven applications such as Fault Detection and Diagnostics (FDD), which can be implemented on top of the existing BMS infrastructure. The application shows potential for utilizing the BIM and time series integration to link the FDD results to the BIM model to visualize and locate faults in real time. Although basic semantics (location, type) have been used to describe BMS sensor data, the data model can be extended to include other metadata describing standardized semantic descriptions of the physical, logical, and virtual assets in buildings and their relationships, as required by data driven applications. However, while generating the semantic graph for the prototype implementation was a relatively easy task, the generation of a rich semantic graph with many systems can be a manual and time-consuming task. Recent developments to automate the generation of semantic graphs [30] can be used to improve the efficiency and effectiveness of this step.

In this study, the time series data is duplicated to our own database due to the lack of access to the actual BMS database by the time of writing this article. However, the API of existing BMS databases can be ideally used to access time series data. In that relation, adhering to the privacy, security and ethical data usage guidelines shall always be strictly followed when using building data, especially if the data contains sensitive information. ■

Acknowledgement

This project received funding from the Dutch Ministry of Economic Affairs and Climate Policy and Ministry of the Interior and Kingdom Relations under the MOOI program.

References

This article is based on the article "A web-based approach to BMS, BIM and IoT integration", presented earlier this year at the CLIMA2022 conference. Please find the complete list of references in the original article available at https://proceedings.open.tudelft.nl/clima2022/article/view/228

Reinforcement learning for the occupant-centric operation of residential energy system

AMIRREZA HEIDARI
School of Architecture, Civil and Environmental Engineering (ENAC), Ecole Polytechnique Fédérale de Lausanne (EPFL), Lausanne, Switzerland
amirreza.heidari@epfl.ch

FRANÇOIS MARÉCHAL
School of Architecture, Civil and Environmental Engineering (ENAC), Ecole Polytechnique Fédérale de Lausanne (EPFL), Lausanne, Switzerland

DOLAANA KHOVALYG
School of Architecture, Civil and Environmental Engineering (ENAC), Ecole Polytechnique Fédérale de Lausanne (EPFL), Lausanne, Switzerland

Abstract: This study proposes a Reinforcement Learning control framework that learns how to optimally control the building energy system by taking into account stochastic occupant behaviour and PV power production. Evaluations using real-world hot water use and weather data indicate an energy-saving potential of 7% to 22% compared to common practice.

Keywords: Reinforcement Learning, Space heating, Hot water, Occupant behaviour, Solar energy, Machine Learning, Occupant-centric, Control, Building, Temperature

Introduction

Optimal operation of building energy systems is challenging as there are several stochastic and time-varying parameters that affect building energy use. One of these parameters is occupant behaviour, which is highly stochastic, can change from day to day, and therefore is very hard to predict [1]. The occupant behaviour of each building is unique, and thus there is no universal model which can be embedded in the control system of various buildings at their design phase. To cope with this highly stochastic parameter, current control approaches are usually too conservative to ensure the comfort of occupants regardless of their behaviour. An example is hot water production, where huge volume of hot water with high temperature is produced in advance and stored in a tank to make sure enough hot water is available whenever it is demanded [2,3].

Another stochastic parameter affecting building operation is renewable energy. The share of renewable energy in the building sector is increasing, and is expected to get doubled by 2030 [4]. Due to the volatile nature of renewable energy sources, it will also increase the complexity of optimal energy management in buildings [5]. There are several other stochastic parameters, such as weather condition or electric vehicles charging that all affect the building energy use. The control logic of buildings should properly consider these stochastic parameters to guarantee an optimal operation.

Uniqueness of occupant behaviour in each building makes it challenging to program a rule-based or model-based control logic that can be easily transferred to many other buildings. Rather than hard programming a rule-based or model-based control method, a learning ability

can be provided to the controller such that it can learn and adapt to the specifications of that building and maintain an optimal operation. Reinforcement Learning (RL) is a method of Machine Learning that can provide this learning ability to the controller. RL can continuously learn and adapt to the changes in system such as variating weather conditions, volatile renewable energy, or stochastic occupants' behaviour [9].

The aim of this research is to develop a self-learning control framework that considers the stochastic hot water use behaviour of occupants, and variating solar power production, and learns how to optimally operate the system to minimize energy usage while preserving the comfort and hygiene aspects. Case study energy system is the combined space heating and hot water production, assisted by Photovoltaic (PV) panels.

The main novelties of the proposed framework are:

Integration of water hygiene: While the pervious study by authors [2] followed a simple rule to respect hygiene aspect, this study for the first time integrates a temperature-based model that estimates the concentration of Legionella in hot water tank at each time step. Estimation of Legionella concentration in real-time enables the agent to spend as minimum energy as required for maintaining the hygiene aspect.

Investigation on real-world hot water use behaviour: In this research, hot water demand of 3 residential houses is monitored to assess the performance of agent on real-world hot water use behaviour of occupants.

Stochastic off-site training to ensure occupants comfort and health: To ensure that agent would quickly learn the optimal behaviour with a minimum risk of violating comfort and hygiene aspects, an off-site training phase is designed in this study. This off-site phase integrates a stochastic hot water use model to emulate the realistic occupants' behaviour. Also, it includes a variety of climatic conditions and system sizes to provide a comprehensive experience to the agent.

The remainder of this paper is organized into four sections: Section 2 describes the research methodology, section 3 presents the results, and Section 4 concludes the paper.

Methodology

Figure 1 shows the components of an RL framework. The methodology section describes how each of these components are designed.

Environment design

Layout of residential energy system in this study is shown in **Figure 2**. This system uses an air-source heat pump to provide hot water in a tank, which is used for both hot water production and space heating through radiators. PV panels are also connected to the heat pump. PV panels are grid-connected, so the surplus power can be supplied to the grid. A dynamic model of the system is developed in TRNSYS.

Agent design

The agent is developed in Python using Tensorforce library [19]. An improved version of Deep Q-Network (DQN), known as Double DQN is used as it is proved to solve the issue of overestimation by typical DQN. Specifications of agent are provided in **Table 1**.

State, action and reward space

Parameters included in the state are presented in **Table 2**. Each parameter is a vector including the value

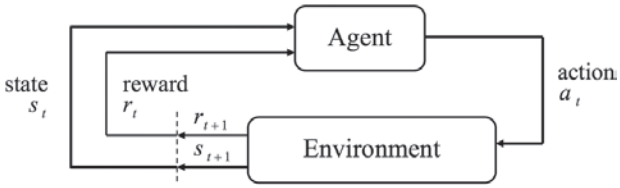

Figure 1. Interaction of agent and environment in Reinforcement Learning. [18]

Table 1. *Selected parameters for the agent.*

Parameter	Value
Learning rate	0.003
Batch size	24
Update frequency	4
Memory	48×168
Discount factor	0.9

Table 2. *Parameters included in the state vector.*

Parameter	Length of look-back vector
Hot water demand	6
Demand ratio	-
Outdoor air temperature (°C)	1
Indoor air temperature (°C)	3
PV power (kW)	6
Heat pump outlet temperature (°C)	1
Legionella concentration (CFU/L)	1
Tank temperature (°C)	1
Hour of day	-
Day of week	-

of that parameter during one or multiple previous hours. The demand ratio is the ratio of total hot water demand of the current day until the current hour, to the total demand of the previous day. Hour of day is a value between 1-24 indicating what is the upcoming hour of day. Day of week, similarly, indicates the current day as a value between 1-7, where 1 represents Monday. The values are normalized to a value between 0 to 1.

The agent has four possible actions: Turning ON the heat pump, Turning OFF the heat pump, selecting the indoor air temperature setpoint of 21°C (as an energy-saving setpoint) or 23°C (as an energy-storing setpoint). Based on the selected indoor air temperature setpoint by the agent, a two-point controller with a dead-band of 2°C tries to maintain the specified setpoint during the next hour.

Reward function includes 4 different terms. An energy term to penalize the agent for net energy use, hot water comfort term to penalize the agent if a hot water demand is supplied with a temperature less than 40°C, which is considered as the lower limit of comfort for hot water uses [2], space heating comfort term to penalize the agent if the indoor air temperature is out of the comfort region of 20°C-24°C, and a hygiene term if the estimated concentration of Legionella is above the maximum threshold of 500×10^3 CFU/L recommended for residential houses [20]. Equations 1-4 shows the formulation of energy, hot water comfort, space heating comfort, and hygiene terms.

$$R_{energy} = -a \times |HP_{power} - PV_{power}| \quad (1)$$

$$\text{if } T_{tank} \geq 40\text{: } R_{DHWcomfort} = 0 \text{ else } -b \quad (2)$$

$$\text{if } 20 \leq T_{indoor} \leq 24\text{: } R_{Indoorcomfort} = 0 \text{ else } -c \quad (3)$$

$$\text{if } Conc \leq Conc_{max},\ R_{Hygiene} = 0 \text{ else } -d \quad (4)$$

Where HP_{power} and PV_{power} are the power use of heat pump and power production of PV panels (kW), T_{tank} and T_{indoor} are the tank and indoor air temperature, $Conc$ and $Conc_{max}$ are the current and maximum concentration of Legionella in the tank (CFU/L), R_{energy}, $R_{DHWcomfort}$, $R_{Indoorcomfort}$ and $R_{Hygiene}$·a,b,c and d are set to 1, 12, 10 and 10 determined by a sensitivity analysis. The total reward is therefore the summation of all these terms.

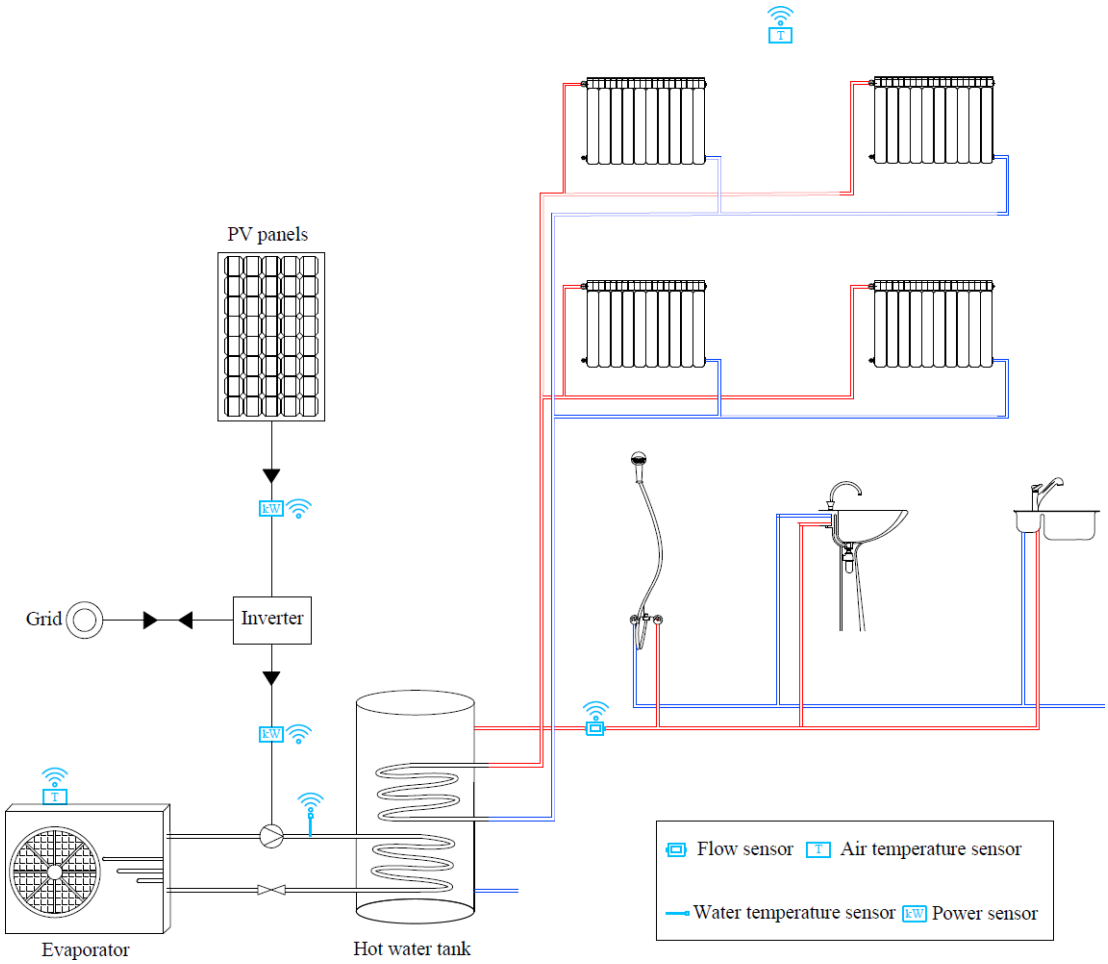

Figure 2. Layout of solar-assisted space heating and hot water production system.

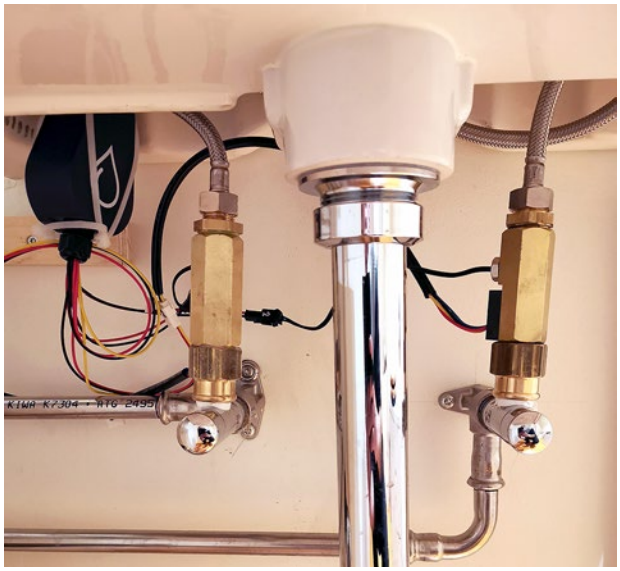

Figure 3. Flow and temperature sensor on a faucet.

Monitoring campaign

To perform a realistic test without disturbing the occupants, hot water use behaviour of people was monitored, and the collected data were used in TRNSYS simulation. For the current framework, as shown in **Figure 2**, only one single sensor at the tank outlet is enough to measure the hot water demand. In this study, to collect a comprehensive dataset, the hot and cold-water demand was monitored at all the end uses as shown in **Figure 3**.

Training procedure

Training and deployment stages are shown in **Figure 4**. To ensure occupants' comfort and health, first, the agent is trained on an off-site training process. In this stage, a virtual environment is provided to enable the agent to gain enough experience before being implemented on the target house. In this stage, a hot water use model [21] is used to emulate the hot water use

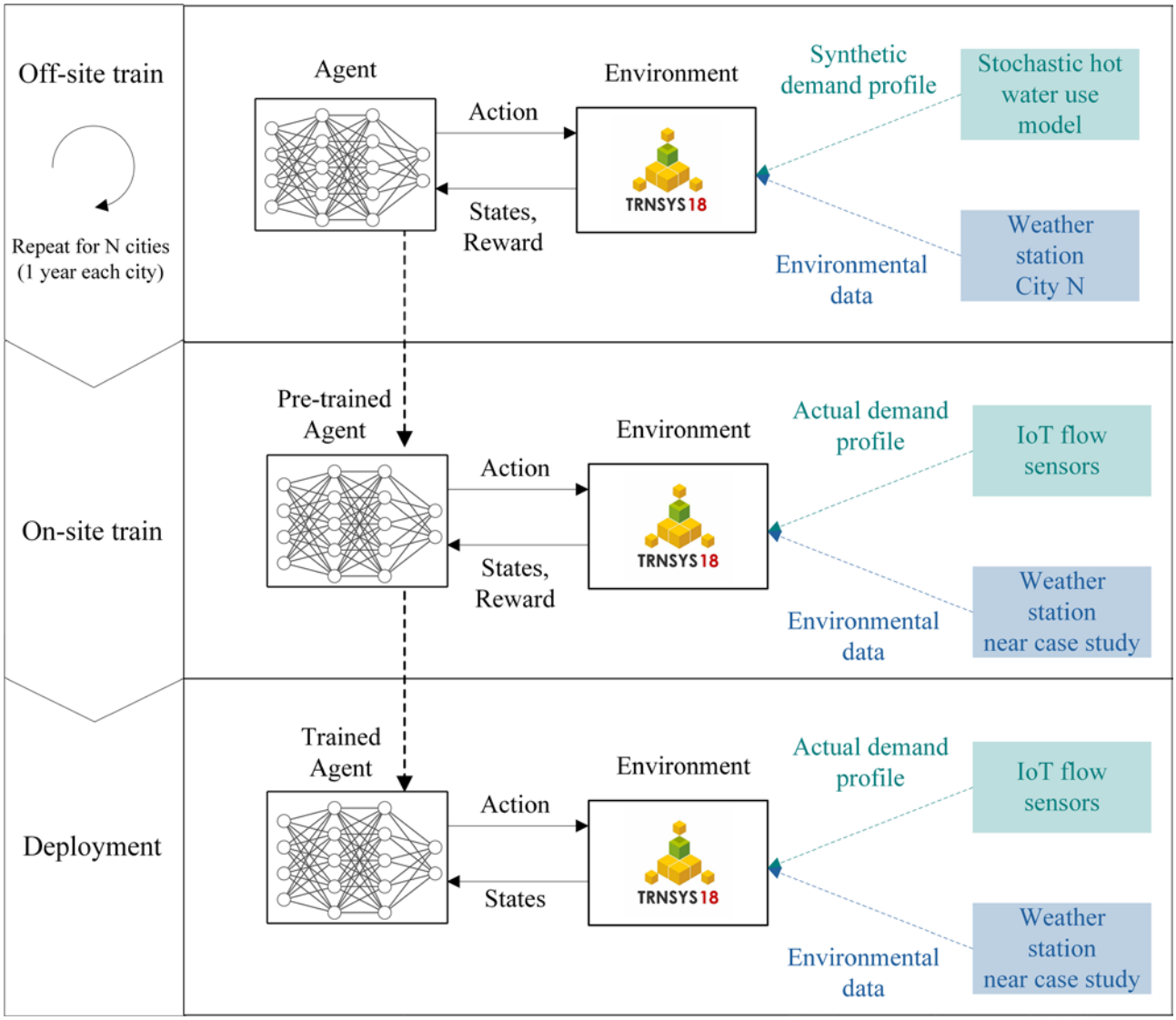

Figure 4. Training and deployment process.

behaviour of occupants and the agent is trained for 10 years. Next, the agent is trained on the target house for 16 weeks. The aim of training on the target house is to let the agent adapt to the specific characteristics of the target house, such as occupants' behaviour, systems sizes, or weather conditions. To simulate the target house, in on-site training stage the collected hot water use data, and also the weather data collected from a weather station near the case study is used. After the on-site training on the target house, the training process can be stopped and the agent starts the deployment stage, in which agent is no longer learning but only controlling the system. Duration of deployment phase is 4 weeks.

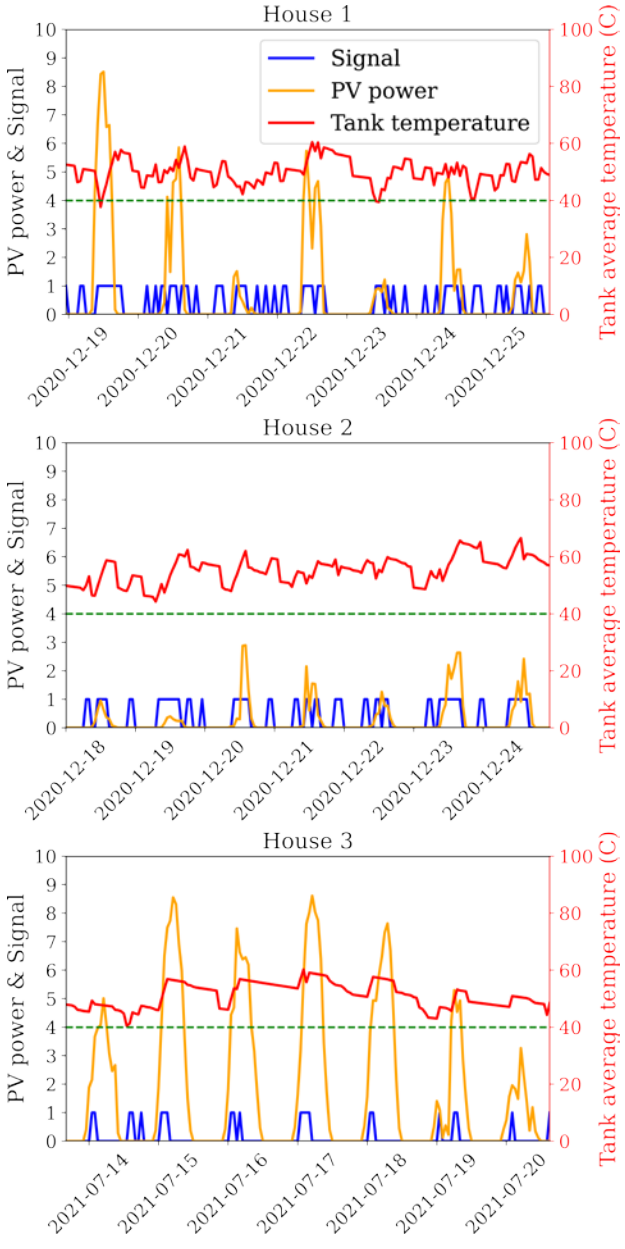

Figure 5. Control signal versus PV power production and tank temperature.

Results

Figure 5 shows the control signal, PV power production, and tank temperature over the deployment stage on three case studies. The deployment stage of houses 1 and 2 is during December, while the deployment stage of house 3 is during July. Therefore, the PV power production of the third case study is higher than others. In all of the case studies, it can be seen that the agent is trying to adapt the control signal to the PV power production and reduce the power use from the grid, by turning ON the heat pump more frequently during the hours of PV power production. This adaptation can be seen very well on house 3, where PV power production is significantly higher and the agent tries to turn ON heat pump only when there is a PV power production. In all of the case studies, the agent has learned how to keep tank temperature above 40°C to respect the comfort of occupants. It shows that agent could successfully learn and adapt to the occupants' behaviour, because none of the demands reduced the tank temperature below 40°C.

To better highlight how RL could better exploit solar power production, the contribution of PV power production in the total power use of the heat pump is shown in **Figure 6**. Two baseline scenarios are also

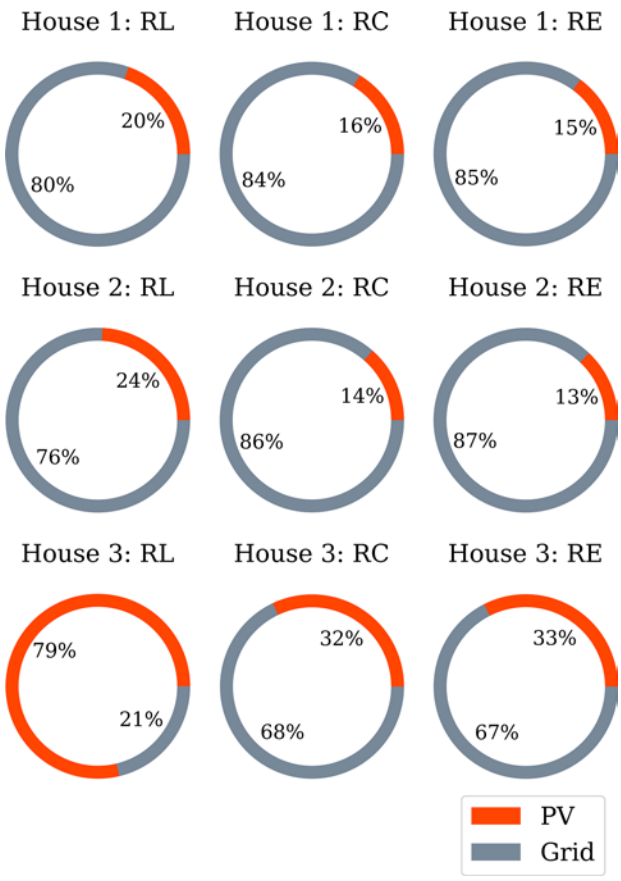

Figure 6. Contribution of PV power production in power consumption of heat pump.

modelled including RC (Conventional rule-based with 60°C setpoint for tank temperature and 22°C setpoint for indoor air) and RE (Energy-saving rule-based with 50°C setpoint for tank temperature and 22°C setpoint for indoor air). As can be seen, in all the case studies RL has used a higher contribution of PV power, compared to the RC and RE. In case of house 3, the contribution of PV power production is much higher than RC and RE, which is the why in this house the energy saving is much higher than other houses. It shows that a significant advantage of the proposed RL framework is to learn how to adapt the operation to the PV power production, and therefore potential energy-saving increases in regions with higher solar radiation.

RL has provided an energy saving of 7% to 22% compared to the RE framework.

Conclusion

This research proposed a model-free RL control framework that can learn the hot water use behaviour of occupants and PV power production, and accordingly adapt the system operation to meet the comfort requirements with minimum energy use. Different from previous studies, where RL is supposed to make a balance between energy use and comfort, in this study RL tries to make a balance between energy use, comfort, and hygiene. Inclusion of hygiene aspect is very crucial to ensure the health of occupants. Real-world hot water use data is monitored in three residential case studies and used to evaluate the performance of the proposed framework over the realistic behaviour of occupants. The RL framework is compared with two rule-based scenarios of RC and RE.

Results indicate the proposed framework could provide a significant energy saving, mainly by learning how to get the best use of PV power production. Therefore, the energy-saving potential is expected to be even more in regions with higher solar radiation than Switzerland. Also, the agent has successfully learned how to respect the comfort of occupants and water hygiene, so the potential energy saving is not with the cost of violating occupants' comfort or health. ■

References

Please find the complete list of references in the original article available at https://proceedings.open.tudelft.nl/clima2022/article/view/286

A novel machine learning approach to predict short-term energy load for future low-temperature district heating

THOMAS OHLSON TIMOUDAS
RISE Research Institutes of Sweden, Sweden
thomas.ohlson.timoudas@ri.se

YIYU DING
Department of Energy and Process Engineering, Norwegian University of Science and Technology (NTNU), Trondheim, Norway
yiyu.ding@ntnu.no

QIAN WANG
Department of Civil and Architectural Engineering, KTH Royal Institute of Technology, Stockholm, Sweden and Uponor AB, Sweden
qianwang@kth.se

Abstract: In this work, we develop machine learning methods to forecast the day-ahead heating energy demand of district heating (DH) end-users in hourly resolution, using existing metering data for DH end-users and weather data. The focus of the study is a detailed analysis of the accuracy levels of short-term load prediction methods. In particular, accuracy levels are quantified for Artificial Neural Network (ANN) models with variations in the input parameters. The importance of historical data is investigated – in particular the importance of including historical hourly heating loads as input to the forecasting model. Additionally, the impact of different lengths of the historical input data is studied. Our methods are evaluated and validated using metering data from a live use-case in a Scandinavian environment, collected from 20 DH-supplied nursing homes through the years of 2016 to 2019. This study demonstrates that, although there is a strong linear relationship between outdoor temperature and heating load, it is still important to include historical heating loads as an input for prediction of future heating loads. Furthermore, the results show that it is important to include historical data from at least the preceding 24 hours, but suggest diminishing returns of including data much further back than that. The resulting models demonstrate the practical feasibility of such prediction models in a live use-case.

Keywords: Low-temperature district heating, short-term load prediction, machine learning, Scandinavian climate.

Introduction

District heating (DH) plays a vital role for the operation of building energy supply systems, which accounted for 35% of global final energy use and 38% of energy-related CO_2 emissions [1]. However, existing DH networks in many cold climates still use

rather high supply temperatures, such as 75°C or above [2]. In the face of green energy initiatives, increasing shares of low-energy buildings, and case examples in mild climates, there is a pressing need to transform the existing DH networks toward low-temperature DH (LTDH).

Digitalization and the overall transition towards smart energy systems and cities are placing higher requirements on integration, communication, and cooperation with end-users (buildings) connected to such LTDH networks. As a result, future generations (4th and 5th) of LTDH networks will feature low operating temperatures, and greater integration with the end-users (buildings) and building-sized renewables. However, how to operate such integrations still rely fundamentally on a thorough understandings of heating loads.

Digital solutions for measuring and controlling the network will allow for higher degrees of system optimization with intermittent renewables and heat pumps. This means that short-term predictions of heating loads are essential. But updating all the legacy monitoring facilities is a very costly and lengthy process. There is still a pressing need for more knowledge about what tools are available, and how well these methods can be utilized for load predictions in LTDH applications. At the same time, there is still room for improvement and solutions that can work on top of the existing DH systems, using existing metering data, during this transition period.

In the studies investigating DH load predictions, a great amount of methods are based on linear regression models, due to the strong linear relationships of heating load with respect to outdoor temperature. These existing methods commonly have not taken full advantage of using data-driven approaches, such as emerging machine learning (ML) models to perform such predictions. Even within those limited publications in the respective areas, it is still not clear what are the key advantages of using such ML approaches, and to what extent the accuracy levels can be quantified, given limited dataset inputs. This study provides a practice of the above raised challenges.

In this work, ML methods was developed to forecast the day-ahead heating energy demand of DH end-users in hourly resolution, by using existing metering data for DH end-users and weather data. The importance of historical data was investigated – in particular the importance of including historical hourly heating loads as input to the forecasting model. Additionally, the impact of different lengths of the historical input data was studied. The feasibility of such models, and their accuracy, are evaluated using data from a live use-case in Scandinavian environment. A detailed analysis of the accuracy levels of short-term load prediction methods are in focus.

Methodology

The study applies combinations of a two-step approach:

Step 1. A thorough understanding of the DH network and building load on annual basis, namely load profiles. This provides an overall view and boundary conditions of DH networks.

Step 2. Based on the definitions of DH load profile, day-ahead prediction models are developed. The model is rooted as an Artificial Neural Network (ANN) model, varying the input parameters, and trained and evaluated using the DH dataset.

To measure and evaluate the performance of the models, the mean squared error (MSE), and the mean absolute error (MAE), were both recorded for each model after training had been completed, using the 2019 test data (that had not been seen by the models during training).

Data inventory

The heating load was measured and collected for 20 separate nursing homes in Scandinavian climate, all located in the city of Trondheim, Norway. All of these buildings are connected to the same DH network, and the measurements were obtained directly from the measuring equipment of the network operator. The data contains the hourly heating loads for each of the buildings, spanning the entire time period from January 1, 2016, to December 31, 2019, obtained from the energy monitoring platform of Trondheim Municipality [9].

For the model construction and evaluation, the average heating load per square meter (W/m²) was calculated across the 20 buildings for each hour. The data were supplemented with hourly outdoor temperature measurements obtained from the Norwegian meteorological station [10] in Trondheim, for the corresponding period.

Load profile development

The load profile was identified using an energy signature (ES) curve in the study. This method has been widely employed for planning and sizing purposes. An ES curve consists of a temperature dependent part, and

a temperature independent part, which are divided by changing point temperature (CPT) or heating effective temperature, defined as:

$$\text{If } T_t \leq \text{CPT}, \quad P(T_t) = p_1 \cdot T_t + p_2 + \varepsilon \tag{1}$$

$$\text{If } T_t > \text{CPT}, \quad P(T_t) = p_1 \cdot T_t + p_2 + \varepsilon \approx p_2 \tag{2}$$

where T_t is the outdoor temperature at time t, p_1 and p_2 are the coefficients of each ES curve model, and ε is the residual error. The heating demand follows the linear growth under the slope of p_1. Below the changing point temperature, it is the outdoor temperature dependent part and above the changing point temperature, it is the outdoor temperature independent part, when most of the heating needs go to domestic hot water (DHW) use.

For DH network monitoring, the load data are commonly aggregated as a combination of space heating and domestic hot water usage. Therefore, in the energy signature analysis, DHW load is extrapolated based on the existing studies [11], which has reported as a representative DHW profile for the given climate and resident types.

For modelling boundary conditions, daily heating degree hours (HDH) is calculated as the daily summation of the difference between balance temperature and hourly outdoor temperature, see below:

$$HDH = \sum_{t=t_o}^{t_o+23} \max(0, T_{bal} - T_t) \tag{3}$$

where t_o is the first hour of the day, the heating balance temperature t_{bal} is assumed at 15°C and negative summands are set to zero. From this, high-heating season, mild-heating seasons and non-heating seasons can be identified in the ES curve.

The day-ahead prediction models

In this study, short-term prediction is defined as 24-hours (day-ahead) time horizon. ANN-based models were developed to predict the short-term heating load, starting from a given hour, for each hour of the following 24-hour period. As mentioned, this serves as a decision-supporting tool for the operation purposes in future LTDH transitions. All of these models used as input the forecasted outdoor temperature for the corresponding 24-hour period. To study the importance of historical data, and the performance impact of different measuring scenarios, nine differentiated ANN models were created and compared.

The models differed in what additional input data were used. One of them used no additional inputs, i.e., only the forecasted outdoor temperature. The other eight models were split into two main categories:

- Half of them were additionally supplied with the historical outdoor temperature,
- The other half were supplied, in addition to that, with the historical measured heating load.

For both cases, the historical data were given in the same hourly resolution. Within each category, the models were further differentiated based on the number of hours of historical data stretched back: 12, 24, 48, or 72 hours.

These models had one input layer (the number of inputs varied between the models), one hidden Rectified Linear Unit (ReLU) layer with 64 nodes (this number was determined through hyperparameter search), and one output layer. All the layers were densely connected. Mean squared error (MSE) was used as the loss function, and Adam was used for the parameter optimization, with the maximum number of epochs set to 100.

Mathematical description of the models

The logic of the developed model is presented in **Figure 1**. Let Q_t and T_t represent the measured heating load, and the measured outdoor temperature, at hour t, respectively; and let $\theta_{t,s}$ and $\tau_{t,s}$ represent the predicted heating load, and the forecasted outdoor temperature, made at hour t for hour $t + s$ (defined for $s = 1,\ldots,24$), respectively. Let K be a parameter representing the number of hours of historical measured data to be used as input for the model. Introduce the shorthand notation as,

$$\theta_t = (\theta_{t,1}, \ldots, \theta_{t,24}) \tag{4}$$

$$\tau_t = (\tau_{t,1}, \ldots, \tau_{t,24}) \tag{5}$$

$$Q_{t,K} = (Q_{t-K+1}, \ldots, Q_t) \tag{6}$$

$$T_{t,K} = (T_{t-K+1}, \ldots, T_t) \tag{7}$$

θ_t, $Q_{t,K}$, τ_t, and $T_{t,K}$ represent, at the time instance t, the predicted heating load for the following 24 hours, the historical heating load for the preceding K hours (including t), the forecasted outdoor temperature for the following 24 hours, and the historical outdoor temperature for the preceding T hours (including t), respectively.

Each ANN model can then be expressed as either the function

$$\theta_t = f_K(\tau_t, T_{t,K}) \quad (8)$$

if historical heating load is not an input to the model, or as

$$\theta_t = g_K(\tau_t, T_{t,K}, Q_{t,K}) \quad (9)$$

if historical heating load is supplied, where f_K and g_K are abstract representations of our ANN models, and the parameter K takes either of the values 0, 12, 24, 48, and 72 (hours).

Training and evaluation of the models

As mentioned above, the different models were trained and evaluated using the same dataset, introduced in Section "Data inventory". The dataset was created from the original data by first considering every possible consecutive 24-hour window of both the outdoor temperature and the heating loads, and then appending the preceding K-hour window to it, both for the outdoor temperature and the heating loads. In the cases that did not consider the historical heating load, that part of the window was simply discarded. Each window is therefore split into input and output, according to **Figure 1**.

The data for the years 2016 and 2017 was used as the training set for the ANN, while the data for 2018 was used as the validation dataset, for the stopping criterion of the training. The resulting models were evaluated using the data for the entire year of 2019, the testing set, to ensure that the models were evaluated on a whole year of data.

Note that the model was evaluated using the actual measured outdoor temperature as the outdoor temperature forecast input. To improve statistical reliability, each model was trained from scratch ten times (using the same training data, but randomly initializing the weights each time), and the averages of these performance measures across the ten iterations were recorded.

Results

ES and load profile characteristics

Figure 2 shows the ES of the DH network. Around 12°C was found as the changing point temperature for providing a proper piece-wise approximation. It is found that outdoor temperature that are above the changing point temperature consists of 22.4% of heating seasons. **Figure 2** also shows that space heating loads are less temperature dependent at the mild-heating season (constant slope), and these small loads can be described by one regression line regardless of working hours and non-working hours.

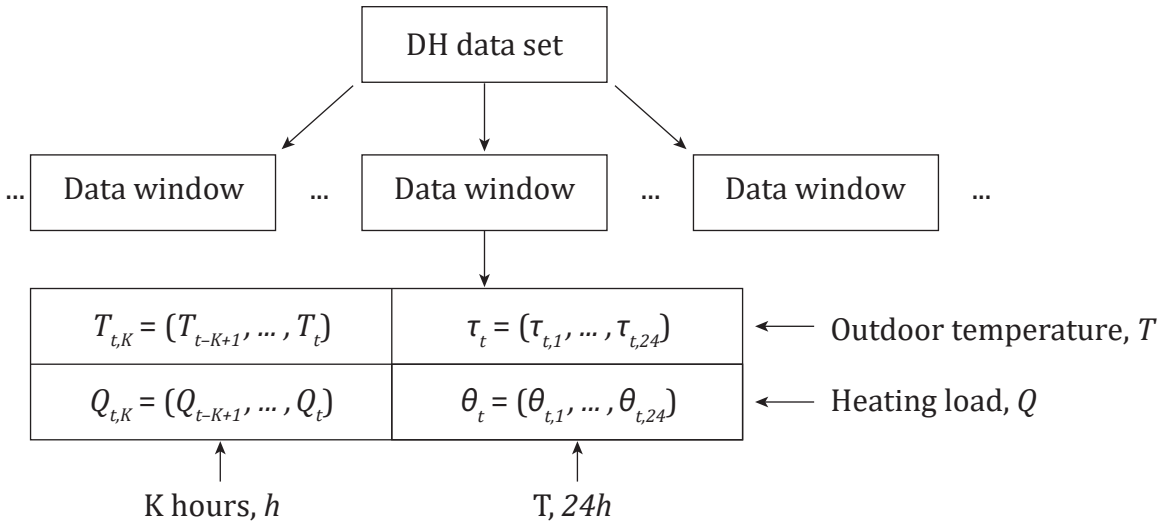

Figure 1. The logic of short-term prediction model.

The rest 77.6% of the time the outdoor temperature was below the changing point temperature, falls into high-heating season. Along the regression lines below the changing point temperature, there is a small region where non-working hour may need slightly higher space heating load than working hour under the same outdoor temperature (c.a. 10 – 12°C).

From the linear relationship between specific daily space heating and heating degree hours, as displayed in **Figure 3**, it shows the daily space heating operation follows the daily heating degree hours, without influences from day types or manual false operation/intervention. These results are expected, given the rather high-temperature/conventional DH networks in the study. This also provides the boundary conditions that the day-ahead predictions will be constrained by the operation scenarios, instead of allowing the network temperature drift freely with load variations.

Accuracy levels of day-ahead prediction

The evaluation errors of the models are shown in **Table 1**. Recall that the evaluation of the models was performed on the dataset covering the entire year of 2019, and that this data had not been previously seen by the model (during the training stage). The results show a clear difference between the models g_K that use the historical load data, and the models f_K that do not. In particular, the impact of including historical outdoor temperature data, but not historical load, as input to the model is relatively small, even when longer periods of historical temperature data are used, compared to also including the historical load data.

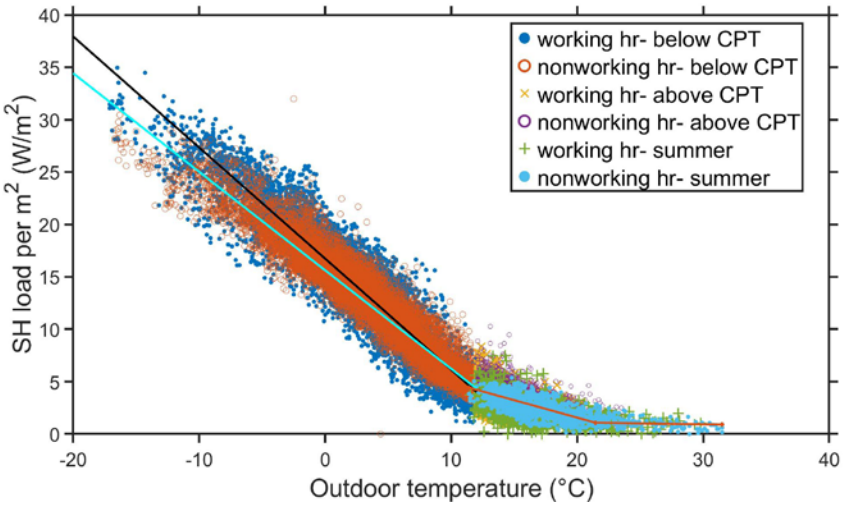

Figure 2. Energy signature (ES) curve for the district heating (DH) load profile.

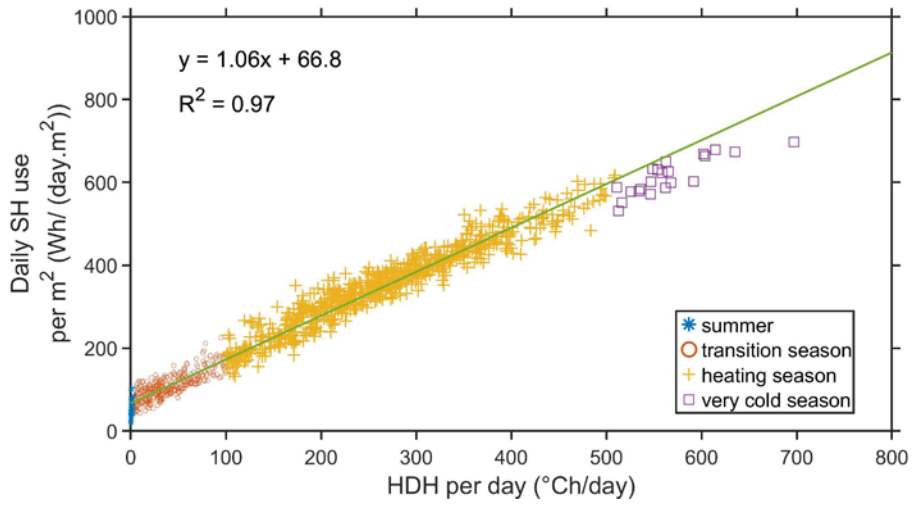

Figure 3. Load characteristics given the whole heating season, presented by heating degree hours (HDH).

Discussion

A significant difference can be observed between the models that use both historical heating loads and outdoor temperature as inputs, and the models that only use historical outdoor temperature. This difference is especially significant during the mild-heating season, when the heating load is dominated by domestic hot water. This is likely due to the relatively weak relationship between outdoor temperature and the total heating load during that period, compared to the high-heating season, when space heating demand is the dominant component. Another reason could be due to thermal inertia and storage effects of the buildings, as well as suboptimal control of the heating loads, in which case the historical heating loads could be useful to model.

This evidence provides a basis for how future LTDH should be operated under different climate conditions, when heating loads fall more into the mild-heating season regime, with perhaps only peaks fall into the high-heating season regime. These differences are also evident in **Table 1**, which shows the average performance over the whole-year period. The results demonstrate the importance of making historical heating load available to heating load prediction models. Yet, while historical hourly outdoor temperature is often publicly available, historical heating loads are in many cases only available with large delays or low temporal resolution, if at all. The results additionally demonstrate the importance of using historical data from longer time periods, although they seem to suggest diminishing returns beyond the data for the previous 24 hours. This optimal cut-off period will likely differ between different building types, due to differences in thermal inertia.

Table 1. Performance measures for the models, evaluated on the testing set of 2019.

Model parameter	Mean squared error (MSE)	Mean absolute error (MAE)
No historical data, i.e., f_o		
K = 0	0.0824	0.2275
Only historical outdoor temperature, i.e., f_K		
K = 12	0.0790	0.2213
K = 24	0.0770	0.2183
K = 48	0.0753	0.2161
K = 72	0.0698	0.2086
Including historical heating load, i.e., g_K		
K = 12	0.0307	0.1299
K = 24	0.0219	0.1106
K = 48	0.0231	0.1133
K = 72	0.0221	0.1112

It should be noted that the performance of the models was evaluated using the actual measured outdoor temperature as the forecasted outdoor temperature for the following 24-hour prediction. In practical applications, this forecast would typically be inaccurate. Such inaccuracies would lead to lower performance than observed in this study. As such, it is important that the base model is as accurate as possible, to reduce the propagation of such inaccuracies within the model.

Conclusions

This study demonstrates that, although there is a strong linear relationship between outdoor temperature and heating load, it is still important to include historical heating loads as an input for prediction of future heating loads. Accuracy levels are quantified by using ANN models with input parameter variations. Furthermore, the results show that it is important to include historical data from at least the preceding 24 hours, but suggest diminishing returns of including data much further back than that. The models developed in this study were evaluated on actual measured data from a live use-case, demonstrating the practical feasibility of such prediction models. ■

Acknowledgement

This work was financially supported by the Swedish Energy Agency with project No. 51544-1 and EU H2020 programme under Grant Agreement No. 101036656. Special thanks to Trondheim municipality, Norway, for providing data and user information.

References

Please find the full list of references in the original article at: https://proceedings.open.tudelft.nl/clima2022/article/view/319

Optimising energy efficiency through system accuracy

Discover the benefits of **sustainable indoor climate comfort**

With approximately 40% of the EU's energy consumption related to buildings and indoor climate systems, we are committed to delivering energy-optimised solutions that do not compromise the comfort demands of modern living. Our innovative range, that includes both low temperature hydronic systems and state-of-the-art electric heating systems, offers the best means to improve energy efficiency through high levels of system accuracy and function control, which results in precise temperature management. This accuracy enables the temperature to be adjusted quickly and consistently throughout the room, leading to optimal indoor comfort and lower energy consumption..

Discover more at www.purmogroup.com

PURMO GROUP

MYSON PURMO EMMETI FINIMETAL RADSON VOGEL&NOOT

From BIM databases to Modelica – Automated simulations of heating systems





ESBEN VISBY FJERBÆK[a] MIKKI SEIDENSCHNUR[a,b] ALI KÜCÜKAVCI[a,c] KEVIN MICHAEL SMITH[a] CHRISTIAN ANKER HVIID[a]

[a] Department of Civil Engineering, Technical University of Denmark, Kgs. Lyngby, Denmark, evifj@byg.dtu.dk, kevs@byg.dtu.dk, cah@byg.dtu.dk
[b] Rambøll, Copenhagen, Denmark, msei@ramboll.dk
[c] Cowi, Kgs. Lyngby, Denmark, alkc@cowi.dk

Keywords: BIM, Modelica, HVAC, simulations

Introduction

There is a large discrepancy between the estimated energy consumptions of buildings and the one measured, often leading to underestimated energy consumption [1, 2]. The issue, known as the performance gap, has many causes. One significant cause is the precision of building energy performance simulations (BEPS) used to estimate energy consumption. BEPS tools rarely consider HVAC systems in detail [3] or simply assume ideal performance of components and controls [4]. This means that commonly occurring phenomena such as oscillation or system imbalance, that create disturbances, are not identified by the BEPS models.

Modeling HVAC systems in detail ensures that all non-ideal performance is considered in the BEPS simulations, which increases simulation precision. In the design phase, this can help to evolve the design process from a steady-state practice, where the design of HVAC systems is based on a worst-case full-capacity situation, to a dynamic design paradigm, where requirements for part-load conditions and dynamic behavior define the design. Additionally, it will be possible to check that the detail of the design is sufficient for actual operation under all conditions. Today, this is ensured through guidelines provided by component manufacturers and empirical knowledge of practitioners. During operation, the detailed models can be used as digital twins for live monitoring of building performance.

Modeling HVAC systems can, however, be a laborious task with many manual processes. Often, the simulation models are built from diagrams of the systems, that the simulation engineer manually interprets and translates to the simulation model format. This error-prone process results in two separate models where changes to one does not affect the other.

Generating the HVAC simulation models from BIM data eases the burden of modeling. Integrating BIM and BEPS ensures that the BIM and simulation models share similar information. Several tools for using BIM as a basis for models in the open-source Modelica language [5] exist [6–8], but all of these have a primary focus on the envelope and thermal zone model. *IFC2Modelica* [8] includes an example for ventilation systems.

Common for all BIM to BEPS methodologies is their dependence on file-based BIM information. Several critics argue that the use of file-based BIM models limits interoperability and propose a change to web-based collaboration, where information is exchanged through open data formats and stored in centralized databases [9, 10]. This corresponds to BIM level 3 in the Bew-Richards BIM maturity model described in [11], where information exchange is handled through standardized, open data formats for integration with various tools.

Cloud BIM platform

The toolchain, presented in the following sections, is implemented in a cloud platform that stores BIM models in a database to allow cross-platform access to the models. The platform is built with a micro-service structure, which means that several *micro-services* for design and evaluation of HVAC systems can utilize the data. Amongst these is the Modelica micro-service, which creates models in Modelica language and simulates them with Dymola. As seen in **Figure 1**, the data flows back and forth between the micro-service and the database so that results are read and analyzed in the platform for analysis and visualization in the graphical user interface (GUI).

In the database, components and their relations are defined with the Flow Systems Ontology (FSO) [12, 13]. This ontology uses class hierarchies to define the type of component and its relation to other components. E.g., a pipe supplying water to a radiator would have the class *Segment* and have the property *ConnectedWith* equal to the radiator's unique tag. Selected classes relevant to this project are listed in **Table 1**, whereas the full list of classes and connections can be found online in [13].

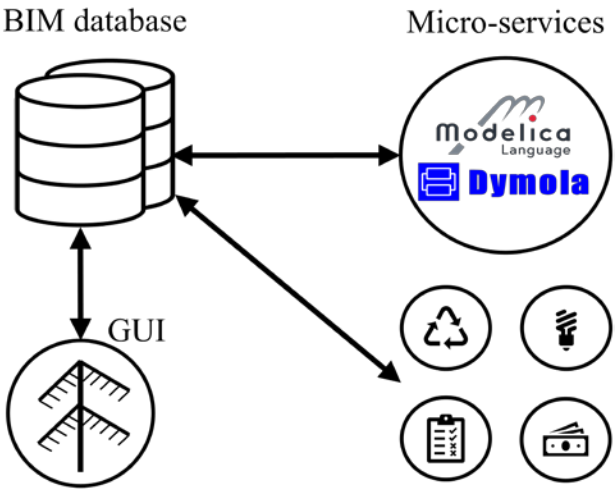

Figure 1. Several micro-services in addition to the Modelica service interface the BIM database platform.

Table 1. Selected component classes.

FSO class	Examples
Radiator	Radiators for heating
Segment	Pipe or duct segments
FlowController	Valves and dampers
FlowMovingDevice	Pumps and fans
HeatExchanger	Heating coils and heat recovery units

Toolchain

The toolchain automatically generates and simulates Modelica models of heating systems from BIM data. In **Figure 2** the main processes of the toolchain are shown along with the flow of data. On the left side, the tool is connected through an API (see **Figure 3**), that establishes an integration between the micro-service and the database. As seen in **Figure 3** the JSON format is used to parse data between the database and tool. As seen in **Figure 2** this is maintained throughout the tool, except for the last two steps, where the simulation environment needs a Modelica file and writes the results to a .mat file. Model data and results are sent back and forth between the toolchain and database an API, as depicted in **Figure 3**.

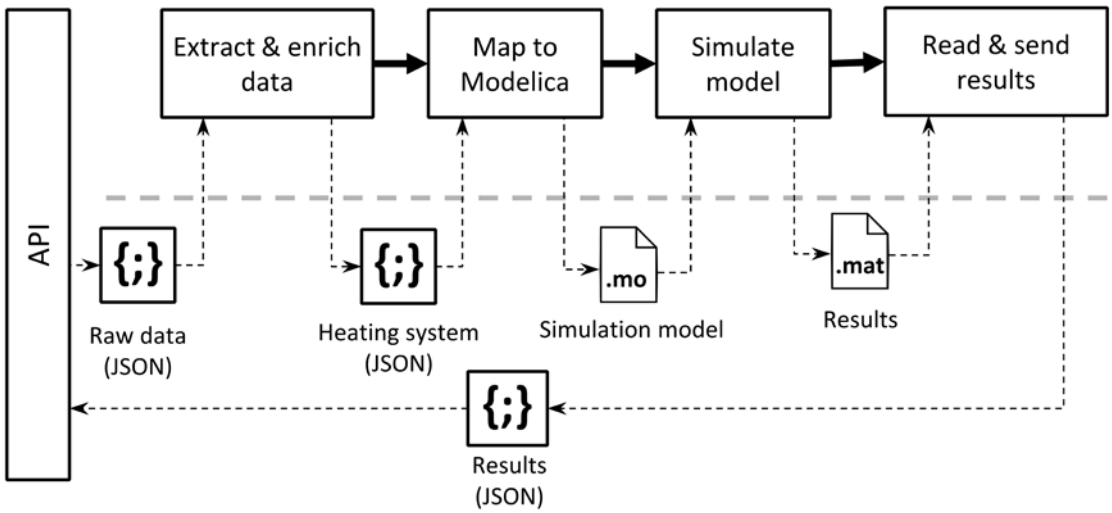

Figure 2. System architecture.

All functions are written with Python, since it is a straight-forward tool which is well suited for translation between data formats and since it is used in the BIM platform. Python does not carry out the simulations itself, but simply interfaces the simulation environment Dymola.

When the toolchain is activated the platform sends a Post request, including BIM data for the desired system(s) to the service's API as seen in **Figure 3** where all data exchange between the database, the API and the toolchain is seen.

Figure 3. Interaction between the database and the toolchain through an API.

In the following sections, each step in the tool is described.

System extraction and data enrichment

When activating the tool, BIM data for the heating system is sent from the database, through the API to the tool. As a precaution and for future scenarios with several systems the tool extracts all components in the heating system from the data. To support the following mapping process, minor changes are made to the data by adding certain parameters based on the component classes. E.g., the length of pipe segments is calculated from the component's start and end coordinates. The enriched/manipulated data is then sent to the mapping process for model generation.

Mapping

In the mapping step, the Modelica models are generated. This is where the original data format and classes are translated to Modelica language and classes. This step is be divided into two separate processes; in the first, the program loops through all components and maps them to a corresponding Modelica class and instantiates it in the model code. In the second, all connections between the components are translated to Modelica connectors. To handle the lack of information on control, this is also where default control connections are established.

In the mapping process, seven FSO classes are mapped to 10 different Modelica classes. Some FSO classes have been mapped to multiple Modelica classes, depending on the value of certain attributes. The full mapping and the translated attributes are seen in **Table 2**. The parameters are all required in the BIM data; if not, the program will fail.

All Modelica classes, except the bend model, originate from the Buildings library [14] which includes models for most components in HVAC systems in addition to detailed models of thermal zones. To simplify the mapping process, a purpose-built library with models that combine component models from *Buildings* was created. The combined models simplify the mapping process, since several Modelica models would otherwise have to be instantiated for each database component. Examples are the radiator model, which

Table 2. *Mapping between classes in the database and their corresponding Modelica classes.*

Component	Modelica
Segment	**model:** Pipe[a] **parameters:** nominal flow, insulation thickness, insulation lambda, diameter, length
FlowMoving-Device[d]	**model:** PumpConstantSpeed[b] **parameters:** speed, performance curve
FlowMoving-Device[d]	**model:** PumpConstantPressure[b] **parameters:** head, performance curve
Radiator	**model:** Radiator[b] **parameters:** nominal heat flux, nominal supply temp, nominal return temp, nominal room temp, nominal pressure loss
HeatExchanger	**model:** DryCoilCounterFlow[a] **parameters:** nominal air flow, nominal water flow, dp nominal air, dp nominal water, UA nominal
Bend	**model:** CurvedBend[c] **parameters:** angle, diameter, bend radius
Tee	**model:** Junction[a]
FlowControl-ler[d]	**model:** Valves.TwoWayLinear[a] **parameters:** nominal flow, Kv-value
FlowControl-ler[d]	**model:** CheckValve[a] **parameters:** nominal flow, Kvs-value
FlowControl-ler[d]	**model:** MotorValve[b] **parameters:** nominal flow, Kvs-value

[a] In Buildings.Fluid library
[b] In purpose-built library
[c] In Mocelica.Fluid library
[d] Mapping depends on component attributes

combines a radiator model and a thermostat, acting as a proportional controller and the MotorValve class, which combines a motorized valve with a PI controller and a setpoint.

In the connection process, the connections between components are translated from the database format to Modelica language. In the database, the connection between components are described in *connectors*, in the *ConnectedWith* attribute, as seen in **Figure 4** that shows an example of two connected pipes. All components have at least 2 connectors. Each connector defines the expected direction of flow (in or out) and the connected component's tag, among other properties not relevant to this project.

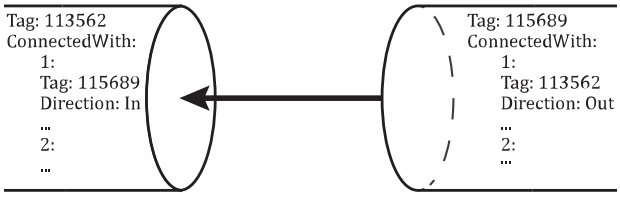

Figure 4. Example of connector definition.

The toolchain loops through all components and for every ingoing connector, a corresponding Modelica connector will be established. Only ingoing connections are considered to avoid duplicate connectors. In Modelica, components are connected through *ports*. The name of the ports vary depending on the component class, and hence, they are stored in the components during data enrichment.

Since the BIM data does not support definition of control logics, default controls are assumed for the components that need control. E.g., all components mapped to the MotorValve class (see **Table 2**) control the flow in a heating coil through a PI-controller.

For each component, a component model template is instantiated and added to a text string, containing the model information. After looping through all components, both for class mapping and connection establishment, the text string contains the entire model. The model is saved in a temporary model file for simulation.

Simulation

After mapping, the models are simulated with Dymola through *BuildingsPy* [15], which interfaces the commercial Modelica simulation environment Dymola. After simulation, the results are parsed to a JSON format and returned to the database.

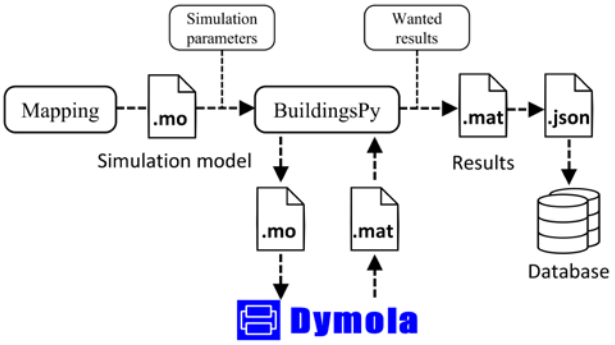

Figure 5. Simulation procedure.

Testing

To ensure that the tool is usable, it was tested on a small heating system model. The test did not focus on assessing the system's performance but merely to check whether the tool works, and the obtained results make sense and are of interest.

Test case description

The test case system, depicted in **Figure 6**, consists of a heating coil and a radiator, each in separate loops. The main pump supplies flow to both loops, and a secondary pump is connected to the heating coil. To simulate the dynamic behavior, both the heating coil and the radiator are connected to a generic room with the parameters given in **Table 3**. For simplicity, only heat loss through the walls and window was considered.

The radiator is controlled by a thermostatic radiator valve (TRV), connected to the room temperature. The TRV is not depicted in **Figure 6**, since it is considered a part of the radiator. To control the heating output of the heating coil, a PI controller adjusts the control valve position to change the heating supply temperature. This is based on the ventilation supply temperature to the room, which has a constant setpoint. For simplicity, both pumps are operated with constant speed, although under normal circumstances, such pumps would either be controlled for constant or proportional pressure. The heat source is not considered, and it is assumed that it supplies water at a fixed temperature of 70°C.

Table 3. *Room parameters.*

Parameter	Value	Unit
Floor area	30	m^2
Wall area	60	m^2
Window area (south)	4	m^2
Total envelope area	66	m^2
Wall U-value	0.27	$W/(m^2 K)$
Window U-value	1.31	$W/(m^2 K)$
Window g-value	0.73	[-]

Simulation results

By simulating the system through the toolchain, the overall temperature curves in **Figure 7** were achieved. **Figure 7** shows the temperature of the room and the ventilation supply air, compared to the external temperature. It is seen that the room temperature is stable, but that there is an offset from the setpoint. This offset is caused by the TRV, which in Modelica is modeled as a proportional controller, which will normally introduce an offset. Hence, this behavior is expected. The supply temperature is stable with no offset since it is controlled by a PI-controller.

Additionally, **Figure 7** shows the return temperature for both loops and the full system. The return temperatures are stable around 30°C, with a slight tendency to increase with lower external temperatures, as expected.

Discussion and gained experiences

The development process highlighted several points of attention during the mapping process. Most importantly, all needed data for the considered components must be available. If the parameters in **Table 2** are not available for all components, the simulations will fail. This puts high demands on the level of information in BIM, but with tools for system dimensioning and component databases, the amount of information is not unrealistic. The possibility to perform detailed simulations of, e.g., return temperatures may even motivate designers to populate BIM models with more information on hydronic components.

In the presented work, controls were handled by applying a set of assumptions suitable for the specific test case. To work expand the work to larger systems, unambiguous control relations must be established in the database. This can be handled in two ways. Either the existing data format is extended with component parameters for controls, such as process variables, set-points, etc., or a new data format for controls must be used. Work towards digitizing control information is in growth with several projects under development [9, 16]. Utilizing these existing frameworks to represent control logic in a database seems like a viable solution, but for simpler systems, the simple approach of added attributes may prove sufficient.

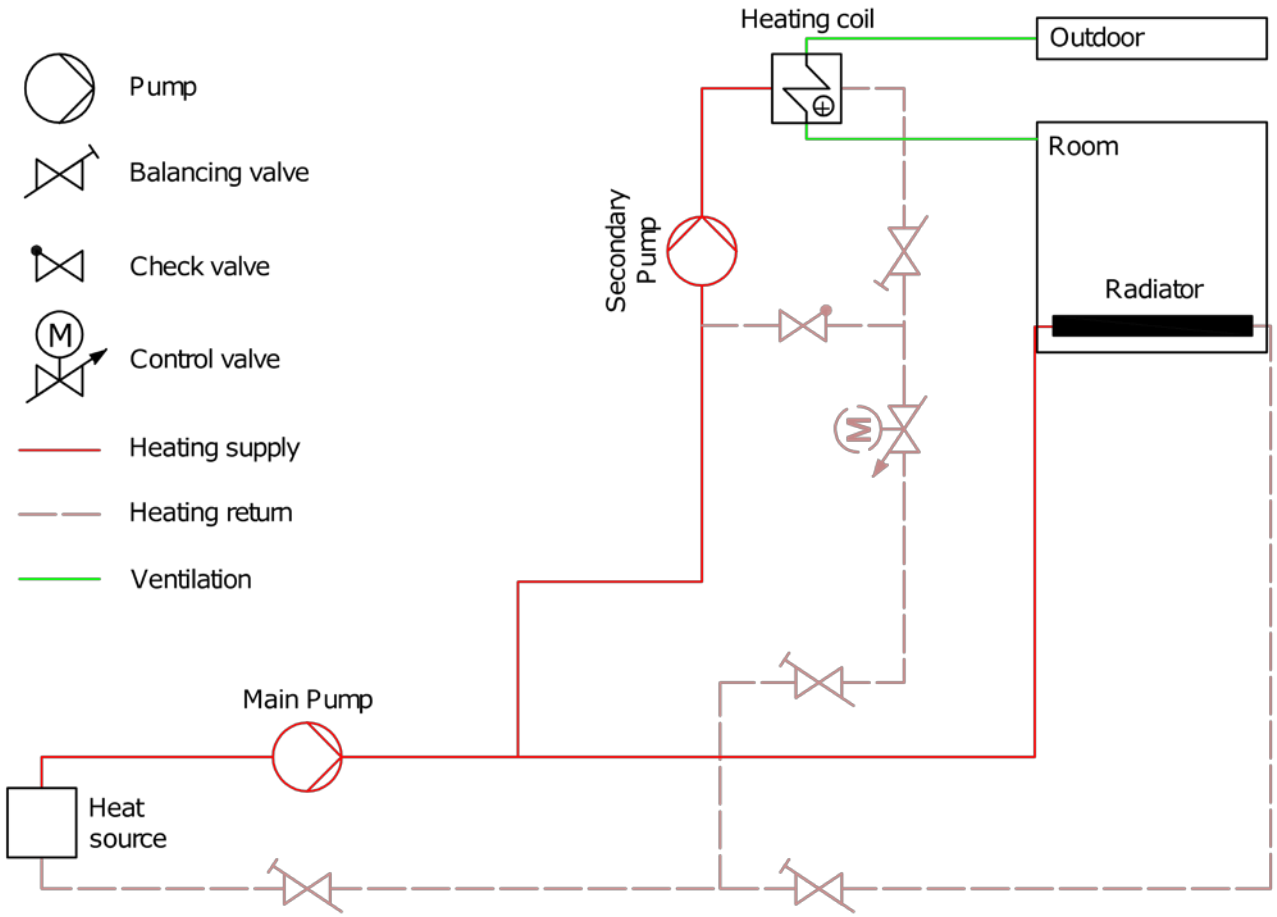

Figure 6. Heating system with one radiator and one heating coil used for testing the tool.

The connection between end units and rooms is a vital piece of information to correctly simulate the systems. Creating a link between end units and rooms may be a simple process in the BIM domain, but it requires additional mapping modules to include the rooms in the simulations.

Conclusion and future work

In this paper, it was proved that it is possible to create a tool for the simulation of heating systems based on BIM models. The simulations provided detailed and vital information on the performance of the individual components in the testing case. This showed the value of such simulations that are usually too time-consuming to be made. While the presented results may be trivial for a system as small as the test case, the same analysis for larger system will uncover results that are difficult for normal practitioners to quantify.

Several important attention points for a larger implementation were identified, the biggest being the lack of representation of controls in BIM models. These points resulted in several assumptions built into the tool, especially regarding control strategies. These assumptions mean that the tool is less flexible to different system configurations. By extending the data format to include the needed information on controls, the tool can easily be modified to simulate larger systems with both heating, ventilation, and cooling systems. When this work is done, the full models can be used in fault detection, detailed analysis of the dynamic effects of coupling the systems, etc. ■

Acknowledgement

This work was funded by the national IFD grant J.nr. 8090-00046B for the project "HEAT 4.0 - Digitally supported Smart District Heating", Elforsk grant 352-042, IFD grant J.nr. 9065-00266A for the project "Virtual Commissioning in Building Services" and "Databaseret energistyring i offentlige bygninger", EU Interreg-ÖKS 2020-2022.

References

Please find the full list of references in the original article at: https://proceedings.open.tudelft.nl/clima2022/article/view/365

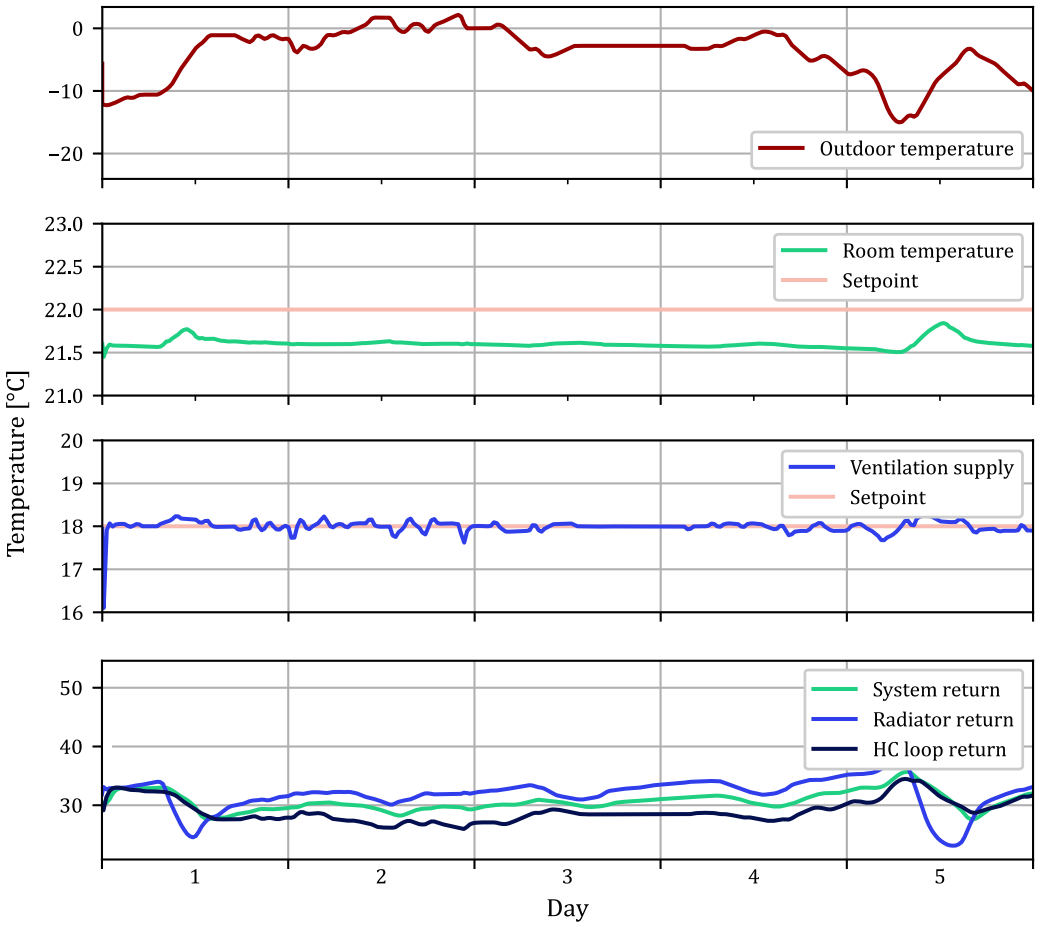

Figure 7. Results for the outdoor (t_{ext}), room (t_{room}) and ventilation supply (t_{vent}) temperature, including setpoints (SP).

Assessment of fouling in plate heat exchangers using classification machine learning algorithms




SEYIT AHMET KUZUCANLI
Department of Hydraulic Module R&D, Bosch Thermotechnology, Manisa, Turkey
ahmet.kuzucanli@tr.bosch.com

CEREN VATANSEVER
Department of Hydraulic Module R&D, Bosch Thermotechnology, Manisa, Turkey

ALP EMRE YASAR
Department of Hydraulic Module R&D, Bosch Thermotechnology, Manisa, Turkey

ZIYA HAKTAN KARADENIZ
Department of Energy Systems Engineering, İzmir Institute of Technology, İzmir, Turkey

Keywords: Fouling, plate heat exchanger, ML, classification, Naïve Bayes, k-nearest neighbours, decision tree.

Introduction

Fouling is the continuous deposition and accumulation of undesirable particles on heat transfer surface areas [1]. The primary heat exchanger (HC) provides heat transfer by combusting fuel to central heating (CH) water which is used to transfer heat to the domestic water via a plate heat exchanger (PHE). PHE consists of two channels that guide two immiscible fluids, CH and domestic water. Both sides of the PHE are under the influence of dirt accumulation from the system components. In addition, the domestic water side of the PHE is also affected by calcification due to existing calcium compounds in sanitary water. Crystallization and calcification of calcium compounds are investigated successfully by Lee et al. [2] and Pääkkönen et al. [3,4]

The CH side of the PHE is mostly influenced by the particles coming from the system components such as aluminium-made HC (HC). Due to the corrosion of HC and particles that come from the pipeline, particulate type fouling is encountered on this side of the plates. The main particle that is seen is Al_2O_3. Experimental and numerical investigations are published in the literature about particulate and composite fouling. [5–8]

Fouling modelling and prediction algorithms have mostly been based on statistical methods and ML techniques. Various ML algorithms are studied such as fouling prediction and detection algorithms based on support vector machines (SVM) [9,10], autoassociative kernel regression (AAKR) [11], autoregressive integrated moving average (ARIMA) [12] and artificial neural networks (ANN) [13–17]. Also, model-based fouling prediction research has been investigated by Kalman filter usage [18]. A predictive maintenance approach has been employed to predict fouling behaviour. Predictive maintenance system usually consists of data acquisition, pre-processing, fault diagnostics, and failure prognostics. Fault diagnostics generally focus on statistical approaches that provide classification and clustering. Most failure mechanisms can be associated with degradation processes [19]. The data acquisition process can be maintained by health system monitoring [20]. The ML algorithms used for classification are commonly Naïve Bayes, k-nearest neighbours (kNN), decision trees, and random forests. These algorithms are successfully studied to classify the faults of boilers using simulated data [21]. As a result, the decision tree algorithm gave the best result

with an accuracy of 97.8%. As can be seen from references, the ML techniques are commonly used in the HVAC sector, especially in heat exchangers but when the open resources are considered the classification ML algorithms on PHEs have been investigated rarely ever.

In this paper, a multi-classification study to determine fouling levels with an aim of to generate a warning on combi-boiler appliances is carried out for PHEs. The Naïve Bayes, kNN and decision tree ML algorithms are studied with cross-validation methods for experimentally acquired data. A comparison of multi-classification ML algorithms is provided as an introductory study.

Research methods

2.1 Experimental conditions

The algorithm development process starts with data acquisition regarding healthy and faulty conditions. To get a dataset for both conditions, PHEs are tested as stand-alone, i.e., separate from combi-boiler devices. Two PHEs one having 30 and the other 32 plates are considered to examine the clogging status. Each PHE is designed for a specific combi-boiler heating capacity and dynamic system behaviour. Specifications indicate that the given inlet and outlet temperatures and flow rates of the PHE should be in the desired range. Investigated PHEs are already meeting these specifications therefore they are considered as a reference.

The tests are conducted in the flow rates shown in **Table 1**. The domestic water inlet temperatures, i.e., domestic cold water (DCW), are kept constant at 10°C. The CH inlet temperatures are applied in a range of 72 ± 1°C.

The applied conditions of both PHEs represent the technical specifications of 30 and 32 plates (**Table 1**). The technical specifications of 30 and 32 plates PHE are applied to PHEs have different plate numbers, 28, 26, 24, 22, 20, 18 and 16. It is assumed that the effect of fouling on the performance of PHE is the same as the effect that would occur if the PHE with fewer plates was used. 50% clogged PHE as the maximum clogging percentage is considered by using technical specifications of 32 plate PHE that are implied to 16 plate PHE.

2.2 Experimental set-up

The experimental setup contains two lines representing CH and DHW circuits (**Figure 1**). CH line is a closed circuit. The static pressure of the circuit is 2 ± 0.1 bar which is measured inside the tank. A pump provides circulation through the closed circuit. A flow control valve is located on the CH line, together with the pump that can be controlled manually to adjust the required flow rates. On the CH circuit, there is a bypass line that is used for heating the water without preheating the PHE.

Table 1. *Experimental conditions applied to demonstrate the clogging behaviour of the PHEs.*

32 Plates		30 Plates	
CH Flow Rate (l/min)	DHW Flow Rate (l/min)	CH Flow Rate (l/min)	DHW Flow Rate (l/min)
29	18	26	10.3

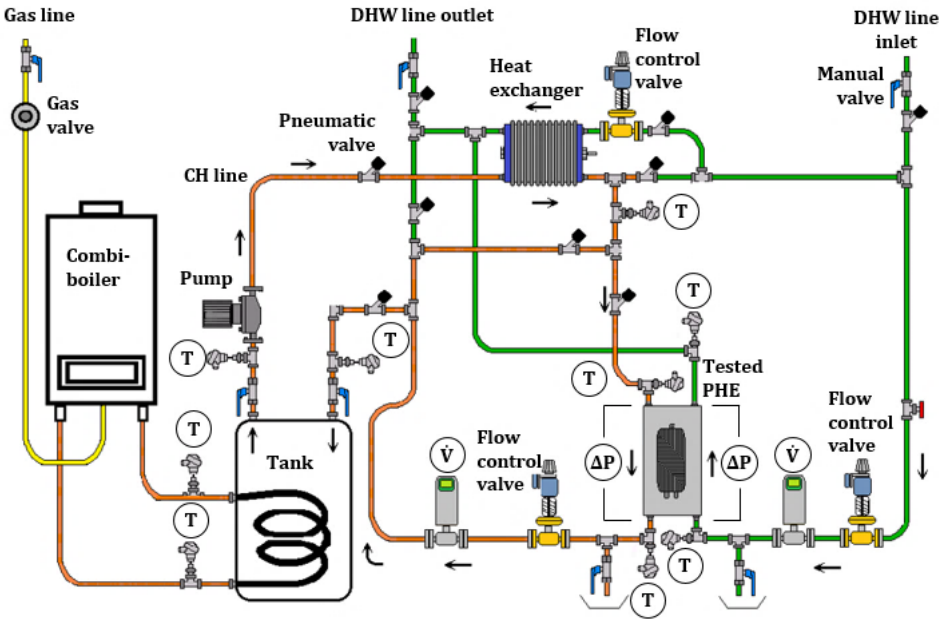

Figure 1. Schematic diagram of experiment set-up and its components.

CH line is interacted with a cold-water line to achieve the ability of necessary cooling with an additional plate heat exchanger. This cooling process control is carried out manually by a flow control valve located on the cold-water line. DHW line is supplied from a main chiller unit. The required flow rates are provided by a flow control valve manually. There are temperature sensors to measure water temperature at the inlets and outlets of the tested PHE besides important points such as the tank inlet and outlet. The sensor locations can also be seen in **Figure 1**. Flow sensors are located on both lines to measure the volume flow rate. Two differential pressure meters are placed to measure the pressure drop over the inlets and outlets of the tested PHE.

2.3 Data processing

The main effect of fouling on the PHEs is functional performance decreasing. The accumulated fouling particles create a film layer on the plates, which pretends like an insulation layer that results in degression of heat transfer. This film layer can be represented as fouling resistance regarding the thermal resistance concept. The logarithmic mean temperature difference (LMTD) method is used to calculate U (Equation. (1)). Heat transfer rates of DHW and CH sides are calculated by Equation (2) and (3). The material properties are taken at the average temperatures of the inlets and outlets for both fluids. The total heat transfer rate is determined by taking the average of the heat transfer rates of the CH and DHW sides. This method is also implied successfully by Zhang et al. [6]

$$\dot{Q}_{total} = U \cdot A \cdot LMTD \quad (1)$$

$$\dot{Q}_i = \dot{m}_i \, c_{p,i} \, \Delta T_i \quad (2)$$

$$\dot{Q}_j = \dot{m}_j \, c_{p,j} \, \Delta T_j \quad (3)$$

$$U = R_i + R_{wall} + R_j + R_f \quad (4)$$

Here, $\dot{Q}$ denotes the heat transfer rate. DHW and CH are indicated as i and j, respectively. Specific heat is indicated as c_p, mass flow rate is $\dot{m}$, temperature difference is ΔT. A denotes the heat transfer area. Fouling resistance (R_f) is obtained from equation (4), where R_i and R_j denote the convective thermal resistances of the DHW and CH sides, respectively. The above results are obtained from the CFD simulations generated by using the test conditions as boundary conditions. R_{wall} denotes conduction heat resistance which is neglected in this study.

2.4 Classification method

The main algorithm development method used is fault diagnosis to obtain the current fouling status of the PHE. Classification implied in this study is a type of supervised ML in which an algorithm learns to classify new data. The training data, from the experimental results, is used in an algorithm to teach the zones to be predicted. The zones that are the fault labels (1 to 8) of the algorithm represent the test conditions. Experimental conditions and measured parameters are predictors, while the zones are categorized responses in the classifier algorithm. While the deviation from zero-hour performance, initial status, is increasing, the deterioration of PHE will be increased also as expected. Zones represent the comfort loss and cost increase levels till the required maintenance time comes and finally when the PHE is needed to be changed. (**Figure 2**). As there are more than one classes to be predicted, multi classification algorithms are used.

Naïve Bayes, kNN (k-nearest neighbours) and decision tree algorithms are chosen due to their applicability to multi classification cases. The algorithms are applied to data by using Classification Learner App in MATLAB program. Before training of the algorithms,

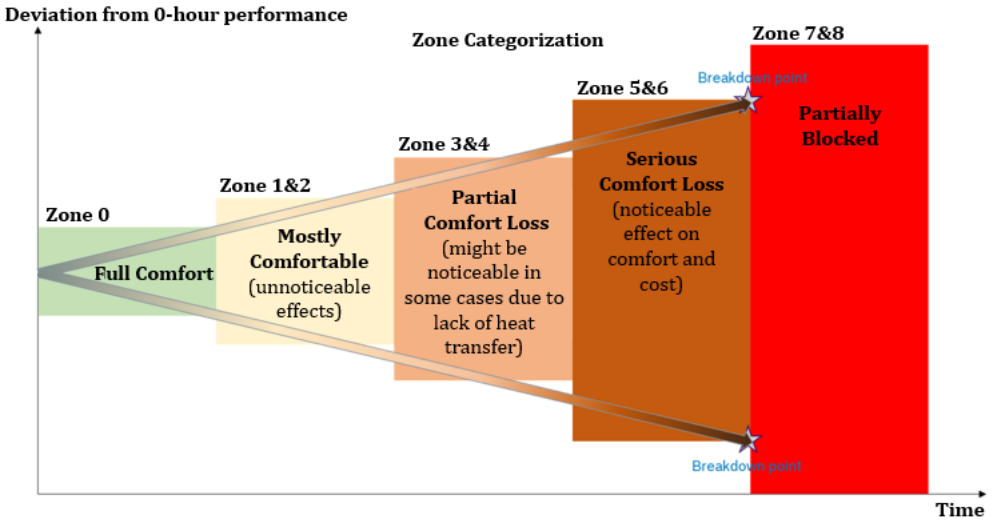

Figure 2. Zone categorization.

cross-validation is used in the process of creating the testing and training data. Cross-validation is a model assessment technique used to evaluate the algorithm's performance. Basically, this offers several techniques that split the data differently to be protected against overfitting. The k-fold cross-validation technique, which is used, partitions data into k randomly chosen subsets (or folds) of roughly equal in size as described in **Figure 3**. One subset is used to validate the trained model using the remaining subsets [22]. The average error across all k partitions is chosen to determine the overall accuracy percentage. The k value is chosen as 5 in this study for all used algorithms.

Naive Bayes is a classification algorithm that applies density estimation to the data. The algorithm uses Bayes theorem and assumes that the predictors are conditionally independent, given the class. Naive Bayes classifiers assign observations to the most probable class [23]. Kernel distribution is used as a numerical predictor where the kernel width is automatically determined using an underlying fitting function via MATLAB [24].

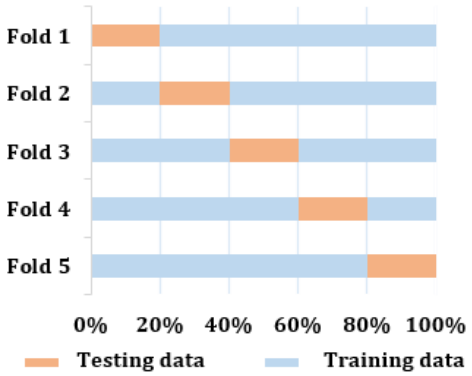

Figure 3. k-fold cross validation designation.

Given a data size of n number points and a distance function, the k-nearest neighbours (kNN) algorithm provides finding the k closest points in data [25]. Number of nearest neighbours (k) to find for classifying each point when predicting, specified as 10 in this study while Euclidean distance is implied as default in MATLAB Classification learner. Decision trees create a hierarchical partitioning of the data, which relates the different partitions at the leaf level to the different classes [26]. The hierarchical partitioning at each level is created using a split criterion. The Gini's diversity index is chosen as a split criterion in this study while the maximum number of splits is implied as 100.

Results and discussion

The experimental results are processed as grouped by classes to be predicted. Outlet temperatures of PHE and differential pressure between inlets and outlets of the PHE of both CH and DHW lines are presented in scatter plots for 30 and 32 plates (**Figure 4**).

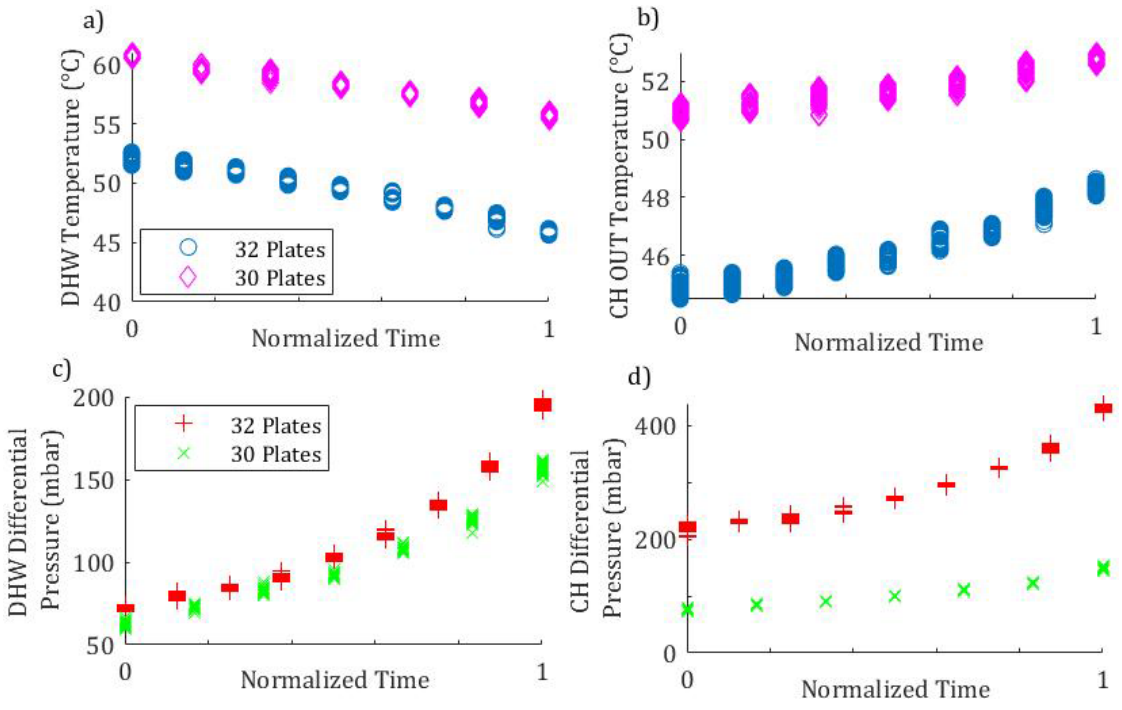

Figure 4. The performance trends for 32 and 30 plates a) DHW temperature behaviour b) CH outlet temperature behaviour c) Pressure drop behaviour of DHW d) Pressure drop behaviour of CH.

The results are presented in normalized time scale, here the normalized time axis represents the zones since they stand for the degradation of PHE from zone 0 to 8, respectively.

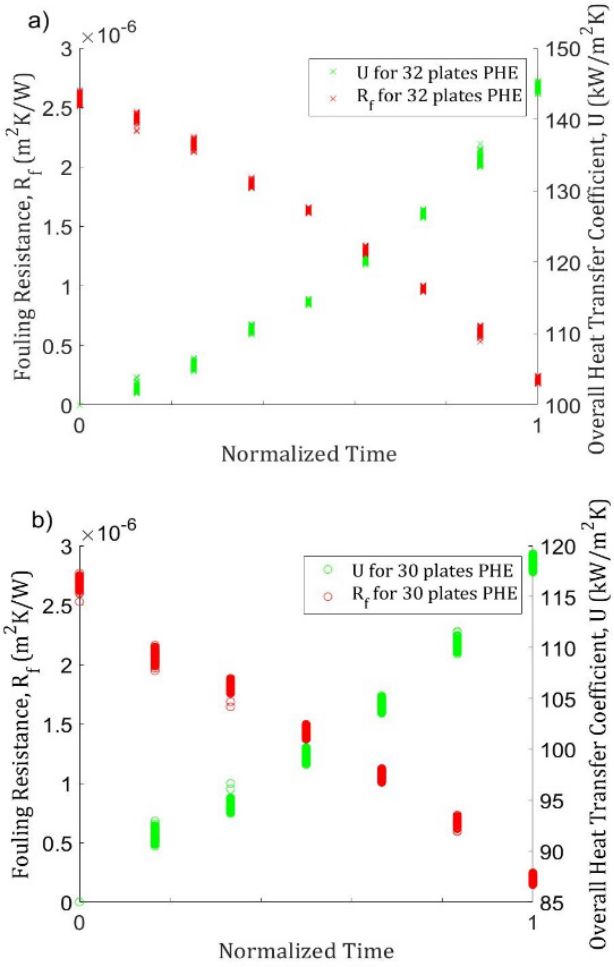

Figure 5. Fouling resistance and *U* behaviours a) for 32 plates, b) for 30 plates.

Since clogging of plates results in a performance decrease in PHEs, trends of DHW outlet temperature for both 30 and 32 plates decrease additionally, trends of CH outlet temperature and pressure drops of both CH and DHW lines for 30 and 32 plates increase as shown in **Figure 4**. The calculated overall heat transfer coefficients for both 30 and 32 plates are shown in **Figure 5**. The trends of U are decreasing as expected.

The fouling resistance values also follow the expected trends in contrast to the *U* as shown in **Figure 5**. In addition, fouling resistance graphs show similar trends to the study by Zhang et al. [6]

Additionally, the Reynolds number range is similar to the range in this study. [6] As a result, trends of the calculated fouling resistance can be considered as a realistic representation of the fouling behaviour with the help of the experimental method implied in this study.

The confusion matrices of the decision tree and kNN algorithms as the results of the predicted performances of the trained models are shown in **Figure 6**. Naïve Bayes predicted the response classes perfectly with 100% accuracy. As the decision tree algorithm can predict fouling with an accuracy of 99.2%, it is followed by the kNN algorithm with 96.7% accuracy. The true positive rates (TPR) and false negative rates (FNR) are designated in confusion matrices with the prediction accuracies portioned by classes. The standard deviation of the imported data can be seen in the parallel coordinates plot for Naïve Bayes trained model in **Figure 7**. In the figure, the classes show more distinguishable

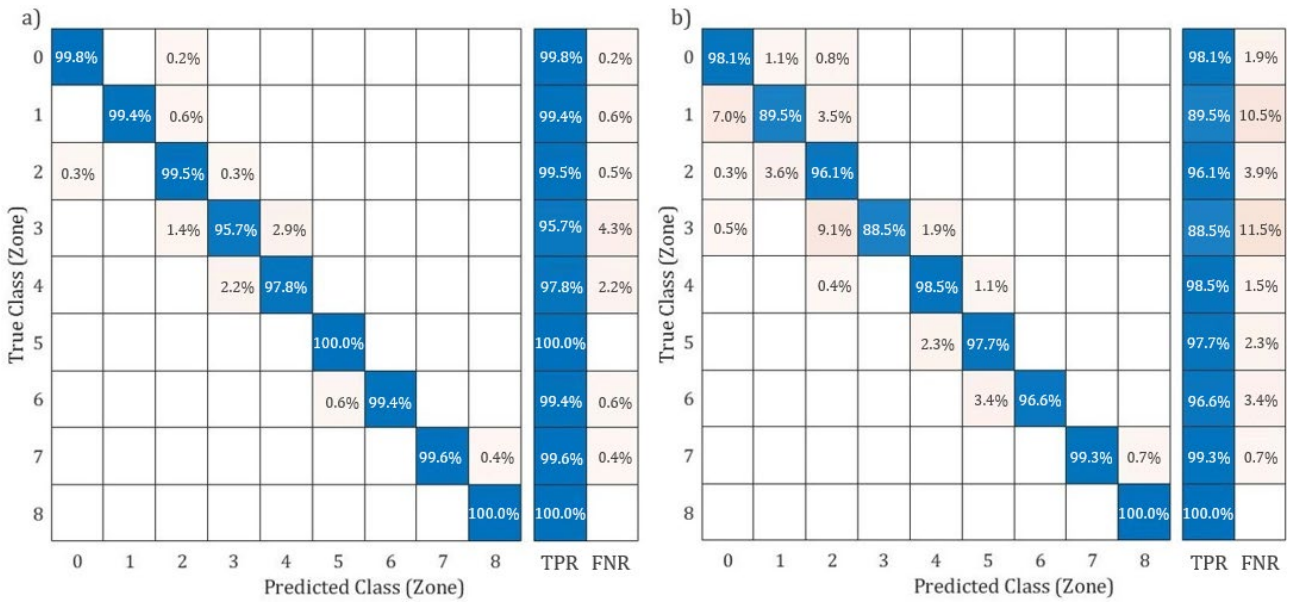

Figure 6. Confusion matrices of a) decision tree model b) kNN model.

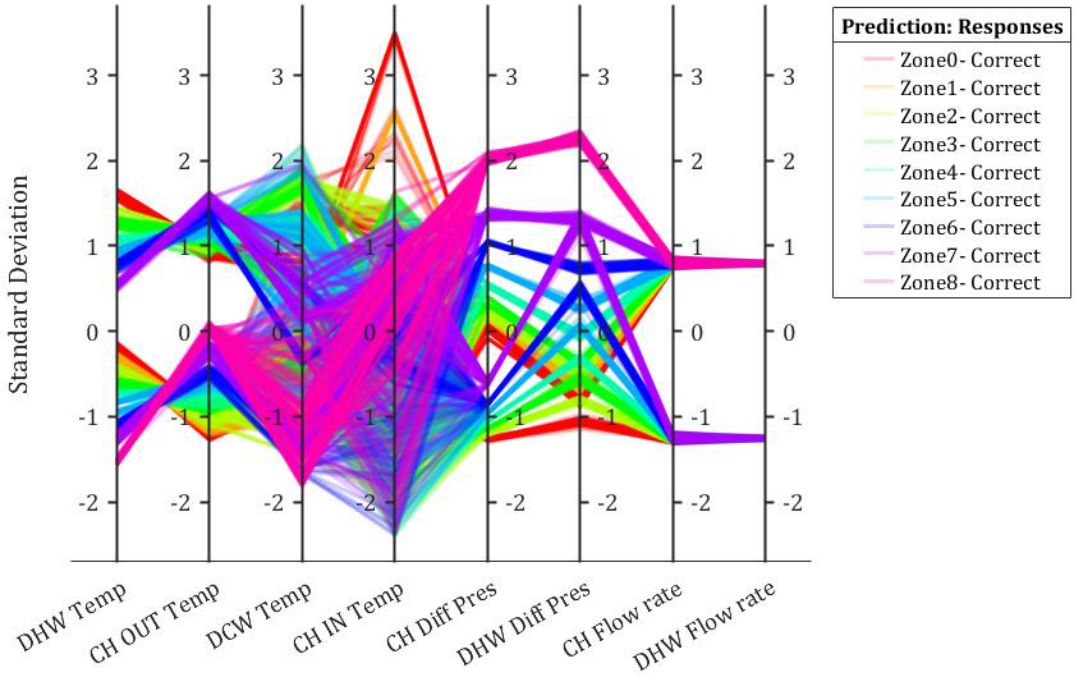

Figure 7. Parallel coordinates plot of experiment data shown in standard deviation scales for the Naïve Bayes model.

distribution on the CH and DHW pressure difference data rather than CH inlet and DCW temperatures. This results in the pressure difference is a more convenient parameter to predict classes correctly rather than other parameters. DHW and CH outlet temperature data are also helpful in distinguishing the classes according to the distribution shown in the parallel coordinate plot (**Figure 7**). With this representation of high dimensional experiment data, the relation of standard deviation between the predictors can be seen.

Conclusion

In this study, an algorithm is developed to imply on combi-boiler appliances with to generate a warning that indicates the fouling level of PHEs. Naïve Bayes, kNN and decision tree are used as the multi-classification ML algorithms.

The data is acquired from an experiment set-up for PHEs having 32 and 30 plates are tested. The experimental conditions are selected as the technical specifications of the PHEs. The experimental data is grouped by zones representing the fouling levels of PHE. The attempted models of ML algorithms result in that Naïve Bayes has better accuracy compared to other models and it is followed by decision tree algorithm with an accuracy of 99.2% and kNN algorithm with 96.7% prediction accuracy. The results of trained models with tested data are shown in confusion matrices. The standard deviation of the data can be represented in parallel coordinates plot which results in the pressure drop values being seen to have the best distinguishing feature among the predictors.

Overall, this study demonstrates the possibility of generating a warning for the current fouling level classification of PHEs in combi-boiler appliances by implying ML algorithms with high accuracy. Generation of fouling level warnings results in the possibility of releasing a feature that can be the major effect of cost saving by retrenching on maintenance.

The framework of this study can be refined by taking a time-dependent dataset into account to assess optimum time schedule of maintenance in future studies. ■

Acknowledgement

Sincere gratitude is expressed deeply to acknowledge the help provided by the technical and support staff in Bosch Thermotechnology.

References

Please find the full list of references in the original article at: https://proceedings.open.tudelft.nl/clima2022/article/view/127

Remote refrigerant leakage detection system for chillers and VRFs

SHUNSUKE KIMURA
Technology and Innovation Centre, Daikin Industries, Ltd., Osaka, Japan

MICHIO MORIWAKI
Daikin Comfort Technologies Manufacturing L.P., Texas, USA

MANABU YOSHIMI
Technology and Innovation Centre, Daikin Industries, Ltd., Osaka, Japan

SHOHEI YAMADA
Technology and Innovation Centre, Daikin Industries, Ltd., Osaka, Japan

TAKESHI HIKAWA
Technology and Innovation Centre, Daikin Industries, Ltd., Osaka, Japan

SHINICHI KASAHARA
Technology and Innovation Centre, Daikin Industries, Ltd., Osaka, Japan
Corresponding author:
Shinichi Kasahara
shinichi.kasahara@daikin.co.jp

Abstract: In Europe, owners of chillers and VRFs, are required by law to carry out regular inspections for refrigerant leaks. At the same time, the European F-gas regulation provides an incentive to halve the number of inspections by installing a leakage detection system. This paper reports on a highly accurate refrigerant leak detection system developed by the authors to obtain incentives.

Keywords: refrigerant leakage detection, chiller, VRF, machine learning

Introduction

The F-Gas Regulation, which came into force in Europe in 2006, was revised in 2015 [1] and penalties were implemented in many countries, which has energised the development of leakage detection systems. In recent years, the development of big data analysis technology has led to numerous proposals of machine learning based refrigerant leakage detection systems.

According to Hosseini *et. al.* [2], 82 papers have been published worldwide on machine learning based air conditioner fault detection systems between 2016 and

2020, 10 of which are on leakage detection. Out of these 10 papers on leakage detection, 6 papers are on VRF.

However, most of these papers were validated using simulations or experimental data obtained in laboratories, and only few of them were validated using actual on-site operating data. Therefore, a leakage detection system for VRF equipment during cooling/heating operation that uses machine learning operated on a remote monitoring system was developed, and its detection accuracy was validated using a large amount of on-site data [3-4]. Also, a leakage detection system for chillers was developed applying this technology, which has been launched in Europe. This paper presents a summary of these developed leakage detection system.

Overview of the detection system

The leakage detection system estimates the refrigerant charge amount from the operating data acquired from chiller and VRF equipment, and automatically detects leakages. **Figure 1** shows an overview of the developed system.

The leakage detection system calculates the *RLI* (Refrigerant Leak Index), an index strongly correlated with the refrigerant charge amount, from the operating data and detects leakages based on changes in this value.

The *RLI* used in chiller and VRF cooling operations is a dimensionless value defined as the ratio of the area of the liquid region to the area of the saturated region on the T-S diagram, as shown in **Figure 1**. As the refrigerant charge amount decreases due to leaks, the *RLI* also decreases.

During the heating operations, the degree of superheat of the compressor discharge temperature (*DSH*) is used instead of the above *RLI*. When the refrigerant amount decreases due to leaks, the discharge temperature rises and so does the *DSH*.

The *RLI* and *DSH* changes not only due to the refrigerant amount, but also due to external disturbances such as outside temperature and compressor speed. Therefore, even though there is no refrigerant leak, the *RLI* may drop due to the disturbances and the detection algorithm may misjudge it as a leak.

To prevent this, the disturbances from *RLI* is removed and the index Δ*RLI*, which represents only the variation of the refrigerant charge amount, is calculated. As shown in **Figure 1**, Δ*RLI* is the difference between the actual *RLI* calculated directly from the operating data and the predicted *RLI* under normal conditions. This predicted *RLI* is calculated by a prediction model created using machine learning (ML) from past normal operating data. The disturbances for *DSH*, which is an index for heating, is removed in the same way as above,

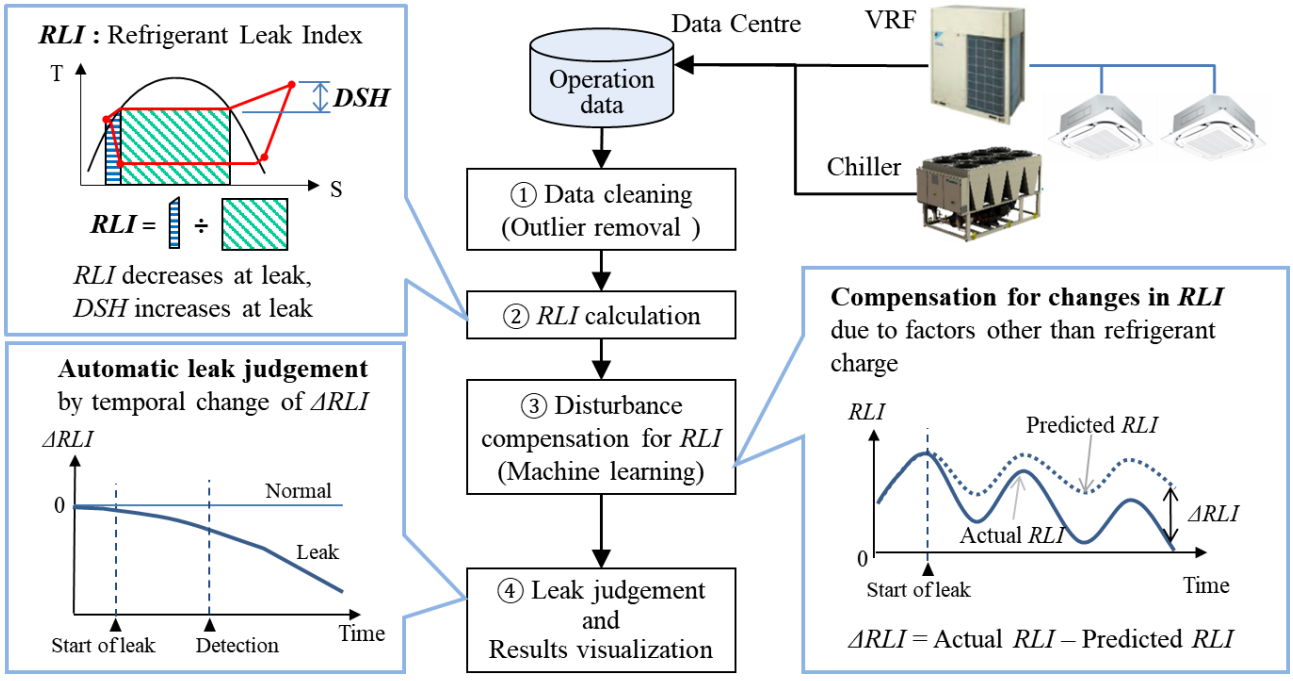

Figure 1. Overview of the leakage detection system.

and ΔDSH is calculated as an index of the changes in only the refrigerant charge amount.

Prediction models of leakage for VRFs

Since VRFs have enough operating data stored in the data centre, it is possible to create an *RLI* prediction model for normal conditions using these as training data. However, the stored data contain both normal data and anomalous data. Therefore, in the process of data cleaning, only normal data were extracted from the stored data as training data. The extraction was carried out in the following two stages.

First, the data of equipment without failure records and equipment with completed failure repairs were extracted. Next, the mean value of *RLI*, an index of refrigerant charge amount, was then calculated for each extracted equipment. The relative frequency distribution of these values is close to the black line of normal distribution curve shown in **Figure 2**.

This distribution is caused by the refrigerant charging process during installation and the refrigerant recovery and recharging process before and after maintenances such as component replacement.

The equipment with a value near the centre of the distribution curve (the red area in the figure) is the equipment charged with the appropriate amount of refrigerant, and its operating data is determined to be available for training.

Using the training data, a prediction model of normal *RLI* was created by LightGBM [5]. The explanatory variables used in the model were outdoor temperature, compressor speed, compressor current, and opening of the expansion valve for subcooling heat exchanger control. The normal *DSH* prediction model for heating was also created in the same way: the explanatory variables were outdoor temperature, compressor speed, total capacity of indoor unit in operation and opening of the expansion valve for subcooling heat exchanger control.

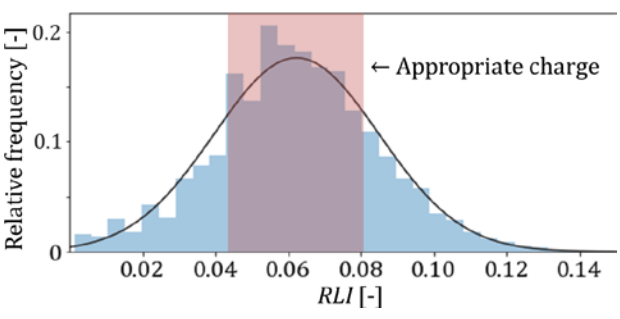

Figure 2. Distribution of RLI.

The leaks found in the first process and the data during the failure period were labelled according to the failure and used as the anomaly data for the validation of leakage detection accuracy.

Prediction models of leakage for chillers

The prediction model for the chiller was created in a different way from that for the VRF. For chillers, there was almost no stored data for *RLI* calculation. Therefore, a chiller was installed in a climate chamber, and tests were carried out under various conditions simulating actual operating conditions to obtain training data.

The four test conditions to be varied were outdoor temperature, compressor load ratio, leaving water temperature (*LWT*) and refrigerant charge amount as leak condition.

If the conditions are set to cover the entire variation range of all parameters uniformly, the number of test man-hours will be huge. Therefore, to create an accurate prediction model while reducing the number of test man-hours, the test conditions were chosen from the frequently occurring operating conditions from the on-site data.

Considering both characteristics, the combinations of test conditions set within the variation range of outdoor temperature and compressor load ratio are shown in **Figure 3**.

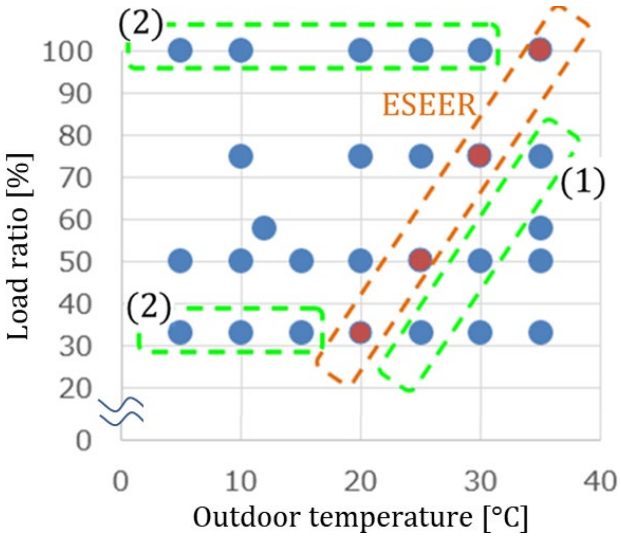

Figure 3. Combination of outdoor temperature and compressor load ratio set for the test

In the 27 conditions set, priority is given to the ESEER (European Seasonal Energy Efficiency Ratio) condition and the area below the ESEER condition (1), which has a high frequency of occurrence in air-conditioning applications, and to the area (2), which has a high frequency of occurrence in process temperature control applications.

For the *LWT* data, four conditions of 5, 7, 11 and 13°C were chosen, focusing on the areas with the highest frequency of occurrence.

The data obtained from the tests carried out based on the above test conditions were used as training data, and a normal *RLI* prediction model was developed using random forest regression. The six explanatory variables are outdoor temperature, compressor load ratio, *LWT*, main expansion valve opening, economizer expansion valve opening and compressor current.

The training data for the prediction model are randomly selected from 70% of the data with 100% refrigerant charge amount. The remaining data with 100% refrigerant charge amount and the data with 120, 90, 85 and 80% refrigerant charge amount were used as the test data for the validation of leakage detection accuracy.

Automatic leakage detection logic

The automatic leakage detection logic outputs judgement results of leakage based on the decrease in Δ*RLI*. **Figure 4** shows an overview of the logic for the automatic judgement of refrigerant leakage.

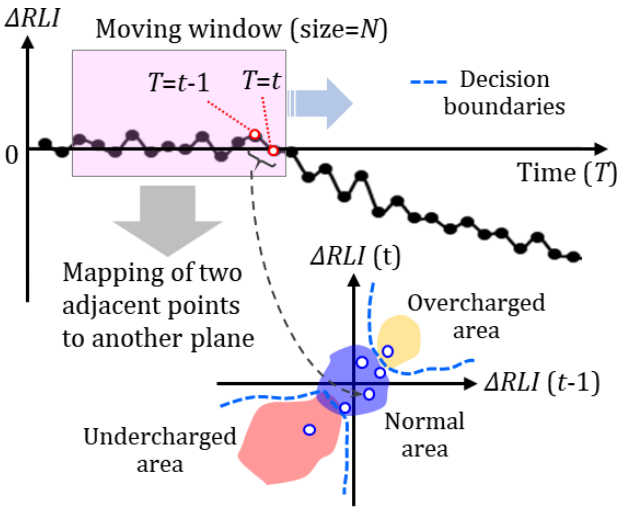

Figure 4. Overview of the automatic leakage detection logic

The detection logic consists of a moving window with *N* terms, a planar mapping section, an anomaly calculation section and a judgement section. The planar mapping section maps the points whose coordinates are two adjacent points Δ*RLI*(*t*-1) and Δ*RLI*(*t*) onto the plane whose axes are Δ*RLI*(*t*-1) and Δ*RLI*(*t*) at any given time.

The mapping plane is pre-classified into normal, undercharged, and overcharged areas based on the decision boundaries plotted by machine learning. The undercharged area is in the third quadrant and the overcharged area is in the first quadrant. The anomaly calculation section calculates the anomaly score defined by the following equation (1) when the *N*-1 points created from the *N* data in the moving window have been mapped to another plane.

$$\text{Anomaly score} = \frac{\text{Number of points in undercharged region}}{N-1} \quad (1)$$

When this value exceeds a certain threshold, it is judged that there is a leak. If the distribution of points is mapped in the undercharged area from the beginning of operation, it is judged to be undercharged initially. If the distribution of points is mapped in the overcharged area from the beginning of operation, it is judged to be overcharged initially.

In the case of heating, the leakage index is Δ*DSH*, which increases opposite to Δ*RLI* during leakage, thus the undercharged area is distributed on the first quadrant.

VRF data validation results

The responses of Δ*RLI* and Δ*DSH* in VRF equipment were evaluated. **Figure 5** shows the leak detection results; the upper plot is for cooling operation of equipment where 15% of the refrigerant charge amount was recovered to simulate a leak: the lower plot is for heating operation of leaking equipment.

In both figure, the red line represents the actual *RLI* and *DSH* calculated directly from the operating data, the blue line represents the *RLI* and *DSH* predicted by the normal prediction model and the grey line at the bottom represents their differences Δ*RLI* and Δ*DSH*, the red areas labelled "Leak" are the period during which the detection logic judged as a leak.

In normal operation period, the actual values for both cooling and heating are close to the predicted values

and the differences, ΔRLI and ΔDSH are almost 0. On the other hand, during leak period, the actual values for both cooling and heating differ significantly from the predicted values. Thus, the ΔRLI and ΔDSH values are sufficient for the automatic detection logic to detect the leak correctly.

Next, the leakage detection was carried out for several test data obtained from the stored data and the accuracy of the detection was evaluated from the confusion matrix of the detection results. The confusion matrix is a combination of the correct and incorrect judgment results for the actual equipment state (normal or leaking), and its definition is given in **Table 1**. The judgment performance was evaluated by two indices, accuracy and false discovery rate (*FDR*), as shown below.

$$\text{Accuracy} = \frac{TP + TN}{TP + TN + FP + FN} \quad (2)$$

$$\text{False discovery rate (FDR)} = \frac{FP}{TP + FP} \quad (3)$$

The accuracy is the ratio of correct predictions among the total number of test cases. The *FDR* is the proportion of normal equipment misclassified as leaks among the equipment classified as leaks.

When assuming the actual operation of a refrigerant leakage detection system, it is important to keep the *FDR* as low as possible. This is because misjudgement of normal equipment as leaking equipment not only increases operating costs due to the unnecessary dispatch of service personnel, but also leads to a loss of user confidence in the detection system. Considering these factors, the target accuracy and *FDR* of the current fault diagnosis by remote monitoring is set to be 80% or higher and 10% or lower, respectively.

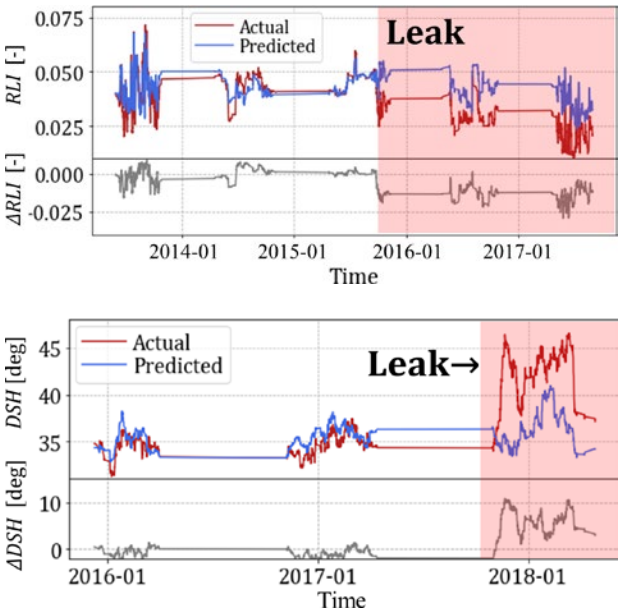

Figure 5. RLI and DSH responses at leaking equipment for cooling and heating operation.

Table 2 show the confusion matrices for cooling and heating. Each element of the confusion matrix in the table shows the incidence rate of normal and leakage detection against the actual number of normal and leak equipment. The number in () is the number of detections.

The accuracy and the *FDR* calculated from equations (2) and (3) are shown in **Table 3**. The accuracy of 80% or higher and the *FDR* of 10% or lower were achieved in both cooling and heating. The incidence rates in **Table 2** were used for the calculations. The reason is that if there is a large difference between the number of normal equipment and the number of leaking equipment, the judgment result is affected by it. By using the incidence rates, this effect can be eliminated.

Table 1. *Definition of confusion matrix.*

		Predicted	
		Normal	Leak
Actual	Normal	TN (True Negative)	FP (False Positive)
	Leak	FN (False Negative)	TP (True Positive)

Table 2. *Confusion matrix of leakage detection evaluation results for cooling and heating.*

			Predicted	
			Normal	Leak
Actual	Normal	Cooling	93.7% (119)	6.3% (8)
		Heating	98.8% (82)	1.2% (1)
	Leak	Cooling	14.9% (7)	85.1% (40)
		Heating	21.5% (6)	78.5% (22)

Table 3. *Accuracy and FDR in cooling and heating operation.*

	Operation mode	
	Cooling	Heating
Accuracy	89.4%	88.7%
FDR	6.9%	1.5%

Finally, the sensitivity of leakage detection was evaluated by obtaining estimates of the leakage amount at the time when the automatic detection logic judged a leak for true positive (TP) equipment. In this paper, the definition of refrigerant leak rate is the ratio of leaked refrigerant amount to the initial charge amount, as commonly used in refrigerant regulations. To estimate the leakage amount at the time of the detection, the conversion coefficient of the changed refrigerant charge amount (% of total refrigerant amount) and *RLI* and *DSH* were determined first. To do this, the data of equipment for which the leakage amount could be identified from the repair records etc. were used. The leakage amount was calculated by multiplying the change in *RLI* and *DSH* by the conversion coefficient. The relative frequency distribution of the estimated leakage amounts and the dotted line approximating it with a normal distribution are shown in **Figure 6**. From the mean μ and standard deviation σ of the normal distribution, the mean detection sensitivities were defined as μ and the worst detection sensitivity as $\mu+3\sigma$, resulting in the sensitivities shown in **Figure 6**. Since the current detection logic for VRF has a detection sensitivity of more than 50%, this method improves the detection sensitivity by 30% over the conventional method.

Chiller data validation results

The responses of Δ*RLI* in chiller equipment were evaluated. **Figure 7** shows the leak detection result for cooling operation of leaking equipment. The legend is the same as in **Figure 5**. The detection result was as good as for the VRFs. In this case, the detection was obtained immediately after the leakage occurred and the leakage point was repaired in only 10 days.

For chillers, there are few stored data on leaking equipment, the evaluation in a confusion matrix was done with the test data in the climate chamber.

Table 4 shows a confusion matrix of the results obtained by performing the same evaluation as above on the test data for various operating conditions varying outdoor temperature, compressor load ratio, *LWT* and refrigerant charge amount. The breakdown of test conditions is 56 conditions of normal data with 100% refrigerant charge amount, and 52 conditions of leak data with 85% and 80% refrigerant charge amount. 86.5% of the accuracy and 0% of the *FDR* are calculated by the same method as VRF.

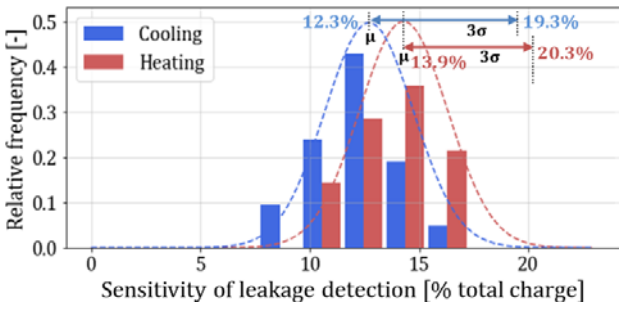

Figure 6. Sensitivity of leakage detection in cooling and heating operation.

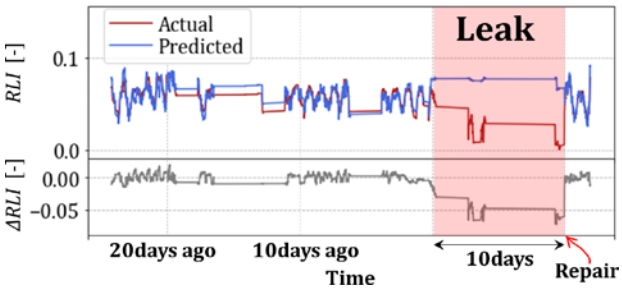

Figure 7. RLI responses at leaking equipment for cooling operation.

Table 4. *Confusion matrix of leakage detection results.*

		Predicted	
		Normal	Leak
Actual	Normal	56	0
	Leak	14	38

Conclusions

An indirect refrigerant leakage detection system based on machine learning was developed and its performance was validated on VRFs and chillers. The detection sensitivity was normally distributed according to the operating conditions and equipment characteristics and was able to detect leaks of 15% of the initial refrigerant charge amount on average and 20% at worst. There is room for improvement in accuracy by modifying the machine learning model and the training data. The next target is to improve the accuracy to detect 10% of leaks in the future. ■

References

Please find the full list of references in the original article at: https://proceedings.open.tudelft.nl/clima2022/article/view/373

Go Blue with Uponor bio-based PEX pipes

AND A REDUCED CO2 FOOTPRINT OF UP TO 90%.

Our latest initiative, Uponor PEX Pipes Blue, are the first bio-based PEX pipes on the market. They feature a reduced carbon footprint of up to 90% compared to fossil-based PEX pipes. Certification by the independent ISCC ensures traceability and transparency across the entire supply chain. Find out how PEX Pipes Blue will allow for construction projects to be more sustainable in the future and how you can achieve your own sustainability goals: **Visit https://www.uponor.com/en-en/products/pex-pipe-blue**

uponor | Moving › Forward

Control device for pumping one-pipe hydronic systems



JIŘÍ DOSTÁL TOMÁŠ BÄUMELT JIŘÍ CVRČEK

Czech Technical University in Prague, University Centre for Energy Efficient Buildings, Buštěhrad, The Czech Republic
Corresponding author: jiri.dostal@cvut.cz

Abstract: The article presents the development and algorithms behind an active control device for pumping one-pipe (or primary-secondary pumping) systems. The main feature of such a system is the series connection of thermal loads/sources and a small pump by each load/source, as opposed to classical two-pipe systems with a parallel connection and throttling valves. Our main contribution is an integration of all necessary components into one device and the ability to infer mass flow in a secondary circuit without a flowmeter. By measuring a temperature drop, we can estimate and control heat flow and provide remote thermal and hydraulic diagnostics of a connected heat terminal. It is powered and communicates through the Ethernet and contains a wet-rotor BLDC pump controlled by the field-oriented control method. A Kalman filter provides a mass flow estimate, and a robust distributed parameter system controller regulates the heat flow.

Keywords: One-pipe, single-pipe, primary-secondary pumping, heat flow control, Q-pump

Introduction

This article focuses on one-pipe hydronic networks, also called single-pipe or referred to as primary-secondary pumping systems. Nowadays, however, mostly two-pipe hydronic heating systems are used. The most widespread is quantitative control, where varying hydraulic resistance in a branch controls flow through a heat terminal. The easiest quantitative control actuator is a manual valve; however, nowadays, legislative norms (e.g. [1]) no longer allow its use. At least automatic thermostatic valves have to be utilized. A thermostatic valve controls its opening mechanically, depending on the room temperature. A more up-to-date solution is the use of Pressure Independent Control Valves (PICV, [1]), which are utilized mostly in fan-coil unit (FCU) applications. A PICV contains a spring mechanism for maintaining a constant pressure drop across an adjacent control valve; the flow, therefore, depends only on the valve opening and not on any pressure variations [1].

Another way to control a hydronic system is to pump heat transfer liquid where needed instead of throttling it where not required. This solution is already available on the market [2,3] and uses a small pump for each heat terminal. Let us call systems with throttling valves "passive" or "throttling" and systems using the pumps "active" or "pumping". Wilo AG has also established a terminology where throttling systems are called "supply oriented" and those with pumps "demand oriented". It is also possible to meet the term "centralized" for systems with a central pump and "decentralized" for decentralized pumping systems.

Although there is also a two-pipe variant of a decentralized pumping system [2,4], this article expands only on the one-pipe pumping hydronic network and its designated control device.

The article presents a pumping one-pipe network and the control device development, algorithms and real-life validation.

Pumping one-pipe hydronic network

Pumping one-pipe systems, also referred to as "primary-secondary pumping" [5], are mostly used to connect heat sources but can also be utilized on the load side. In short, from the main pipe in a circuit branch out two closely-spaced T-fitting to where a secondary (the "small") pump with a heat source/terminal is looped in. The heat sources/terminals are connected in series on the main (primary) piping. The main piping loops from, say, heat load to a main circulator, heat source (or hydraulic separator) and back to the heat load. See **Figure 1** for a schematic depiction.

The advantages of the pumping one-pipe hydronic system are:

- the system generally contains only two pipe diameters (primary and secondary),
- time and material savings (fewer pipes, connections, valves and plumber's work),
- one type of pump in the secondary loop can control a wide range of load capacities; i.e. the system is robust against design inaccuracies/changes,
- the amount of the overall dissipated pumping energy is the lowest of all possible topologies,
- one-pipe system contains less heat transfer liquid (water, glycol) than a comparable two-pipe system.

The disadvantages are:

- practitioners mostly hold the impression that one-pipe systems are inefficient and problematic. This is based on the long-surpassed throttling one-pipe heating variant with its real higher operational cost and low comfort [5]. It harms, beforehand, the reputation of pumping one-pipe systems,
- temperature relations among secondary loops shall be considered during system design. There is a one-pipe network design and validation tool [8,9] available. But solutions for retrofitting two-pipe systems also exist,
- this solution became feasible only recently as canned wet rotor pumps, and electronically commutated motor became available. There are not many installations proving the performance of the system. Despite that, dozens of pumping one-pipe systems are in service in the US, e.g. [3].

For more hydronic network topologies details and a one-pipe network design tool description, resort to [6].

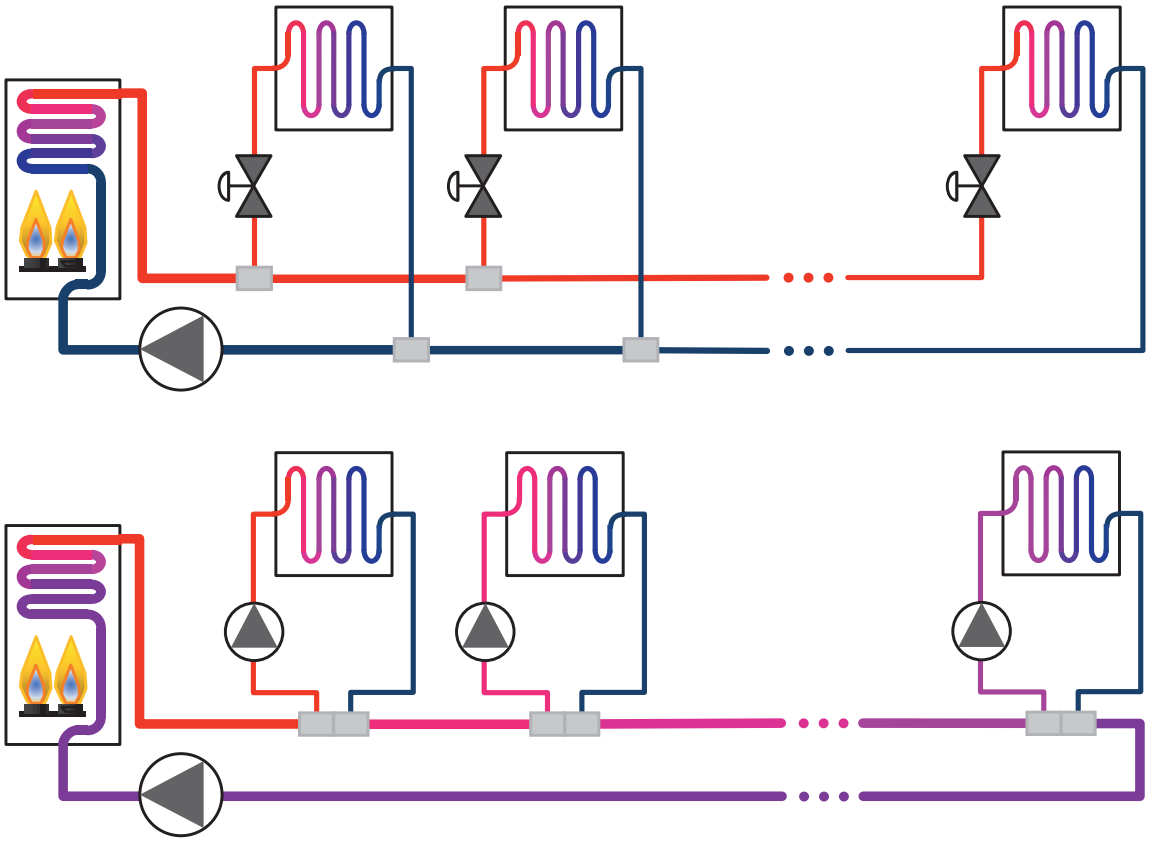

Figure 1. Hydronic topologies: two-pipe throttling system (top), pumping one-pipe system (bottom).

One-pipe control pump device

The speed of the secondary pump controls the power output of a heat terminal in the pumping one-pipe network. And as there is no variable hydraulic resistance in the secondary circuit, the secondary flow is governed solely by this speed.

Such conditions enable us to infer flow from pump power readings, as **Figure 2** depicts. Knowing the pump speed, power, and power-flow characteristics is the main predisposition to estimate the absolute volumetric/mass flow through the pump and consequently through the whole secondary circuit, i.e. the heat terminal. A heating/cooling power can be calculated by adding a pair of temperature sensors on a supply and return secondary pipe.

Our patented invention [7,8], with the business name Q-pump (Qp), bundles the two closely-spaced T-fittings, a pump housing, a check-valve and a pair of temperature sensors together into one device. Such a device directly connects a heat source/terminal to the main pipe. See **Figure 3** for a schematic depiction.

Note: Although the same principles generally apply to heat sources, the one-pipe control pump devices will only be depicted in the heat distribution to the heat terminals. Also, even though only heating will be addressed further, similar principles apply to the distribution of cooling power.

Design and Manufacturing

The EU directive [9] recommends designing heat sources for a typical building load (instead of a maximal load), with a complimentary heat source to cover for extreme conditions. Applying the same principle to heat distribution, the main pipe has been chosen DN32 with G5/4 threads, which renders an economic pressure drop [10] for supplying one floor of 75% of commercial buildings in the EU [11]. The other 25% of establishments with higher loads shall, but only for 6% of operation time [12], experience higher main pipe velocities than 1.2 m/s and, therefore, higher pressure losses.

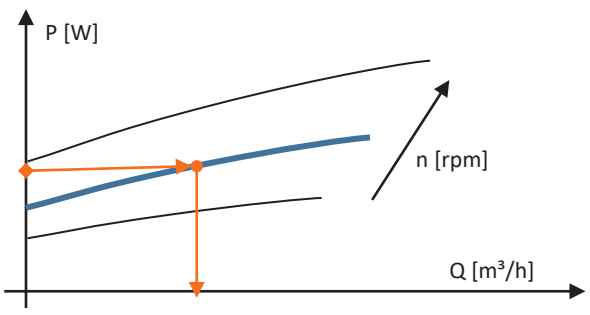

Figure 2. The basic principle of inferring flow from a pump electrical power reading.

The device's secondary piping and pump are sized for a load of 10 kW with an average weighted hydraulic conductivity of 0.8 bar/m³/h. The secondary ports are DN15 with G1/2 threads, the standard connection for most heat terminals. See **Figure 4** for results from the research on typical design operation conditions (normalized using EN 442-1:1995) and specific loads.

A D5-sized pump [13] (used in, for example, solar-thermic installation or hot water recirculators) serves as the secondary pump. It is a spherical-shaped wet-rotor electronically commutated pump with four rotor poles and six stator coils on a magnetic core ring.

The Qp body (**Figure 5**) consists of the main pipe, from which a pump housing extends with its suction hole. The pump outlet directs perpendicularly away from the main pipe axis. The secondary outlet port houses a spring check valve and a secondary supply temperature sensor. From the same direction comes the secondary inlet, where the secondary return temperature sensor is housed and which connects back to the main pipe.

The Qp body was made as symmetrical as possible from the primary-pipe point of view to enable directing the secondary ports to the right or left regardless of the flow direction in the main pipe. Which means that the direction of flow in the main pipe does not alter hydraulic conditions in the secondary piping.

The first prototypes were manufactured using 3D printing. The final prototypes are cast from brass using ceramic moulds (created on top of 3D printed masters). The final body design is fully brass-castable and machinable by standard machining techniques. ▶

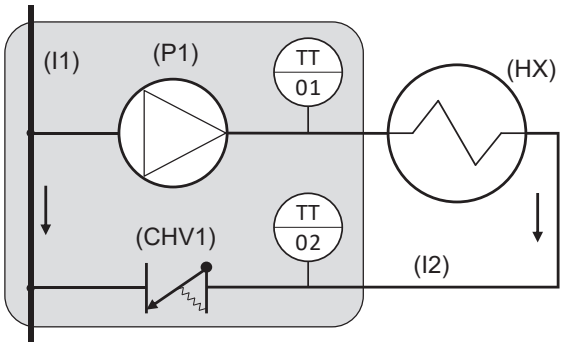

Figure 3. One-pipe control pump device scheme. HX – heat exchanger, CHV – check-valve, I – pipe, P – pump, TT – temperature sensor.

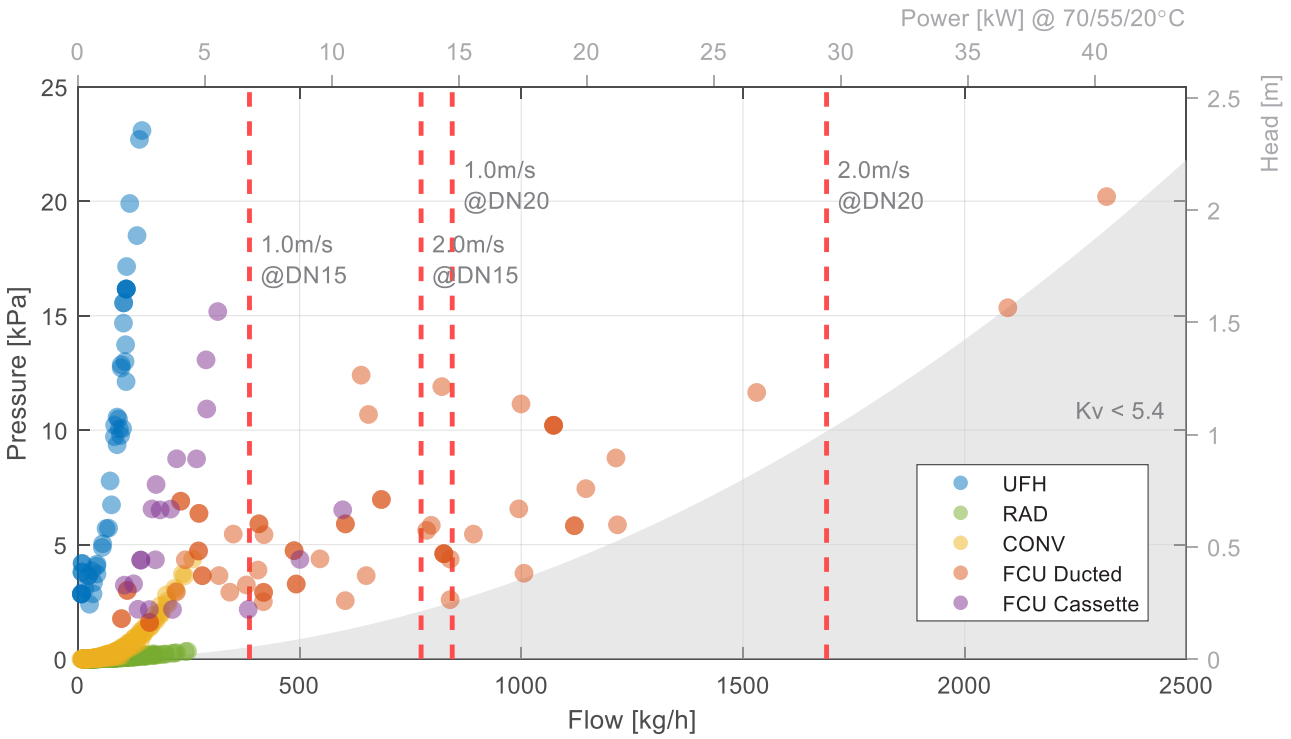

Figure 4. Typical design operation conditions for underfloor heating (UHF), radiators (RAD), convectors (CONV) and fan-coil units (FCU). All datasheet values normalized to conditions 70/55/20°C using the norm EN 442-1:1995.

- The electronics cover is designed to be injection-moulded without any special cores. It is designed to comply with IP44 and cable-pull protection.

Figure 5. One-pipe control pump device: brass-casted and machined body with injection-mould-manufacturable electronics cover.

Electronics and software

The electronics utilizes an NXP i.MX-RT microcontroller with built-in motor control features. The pump speed and electrical power acquisition are performed by vector control methods (FOC) [14], allowing for efficient device control in the whole range from zero to maximal flow.

The processor runs FreeRTOS and allows for temperature readings, heat power estimation, controller calculations and communications.

Mass flow estimation

Mass flow estimation is the key component of the one-pipe control pump device. Being able to determine flow without the use of a flow meter enables cost-effective implementation of the following features:

- Heat flow estimation
- Heat flow control
- Heat metering
- Thermal diagnostics

Looking at the schematic of the secondary circuit (**Figure 3**), there are three main features from the hydraulic point of view: the double T-fitting (connection to the primary circuit), the pump body

with a check-valve and the hydraulic load - the heat terminal with its piping. The T-fittings are spaced closely together not to create a pressure source for the secondary circuit. Changes in the primary flow do not influence the secondary flow (verified by measurement, variation is less than 5 ℓ/h per 1000 ℓ/h change in the primary flow) – hence the two circuits are hydraulically separated. This simplifies the secondary hydraulic circuit to just two components: the pump and the load.

The Qp device sizing doesn't change up or down with the capacity of the load; the control authority is always full, as we control the flow directly. Precision speed control of the pump means sufficient flow control precision for any load capacity. Therefore, the QP body, with its pump housing, check valve and ports, is of a fixed size and can be described precisely by its head-flow (HQ) and power-flow (PQ) characteristics. **Figure 6** presents the measured data and the polynomial model. Fitting was performed under an L1 norm with shape constraints [15].

Mass flow estimation is based on the underlying mathematical model of the circuit (**Figure 7**), the fixed but unknown hydraulic load and the fixed and known pump with its housing.

The pump model is mainly given by the head and power polynomials; partial effects have the inlet water and motor coil temperature. The dynamic behaviour is primarily governed by the speed controller, flow inertia and impeller inertia. The latter ones are, however, fast enough to enable coarse approximation by first-order dynamics.

The quadratic Darcy-Weisbach law mainly gives the model of the load. The hydraulic conductivity is unknown but considered only very slowly changing. The dynamical flow model is derived from an analogous inertance model, where the head difference between input and load is the flow change driving potential. The hydraulic conductivity K is mildly dependent on mean water temperature.

The model is non-linear, with one parameter and two states to be estimated. The states, pump speed S and most importantly, the flow Q, altogether with the hyd. conductance of the load K are estimated by an extended Kalman filter (EKF). The resulting flow estimate is denoted $\widehat{m}_w$.

Heat flow control

A heat terminal, e.g. FCU, is generally a distributed parameter and distributed time-delay system governed, when simplified, by a one-dimensional hyperbolic PDE [16]. Additionally, temperature measurements are situated at the Qp device, so there is a possibly significant transport delay due to the secondary piping length.

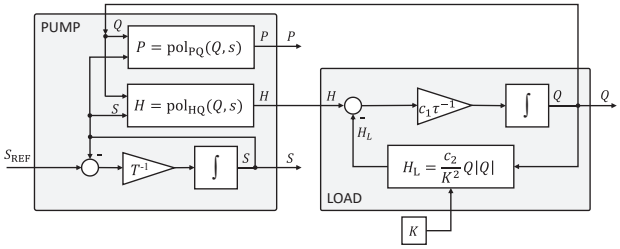

Figure 7. Simplified scheme of the dynamical model used for mass flow estimation

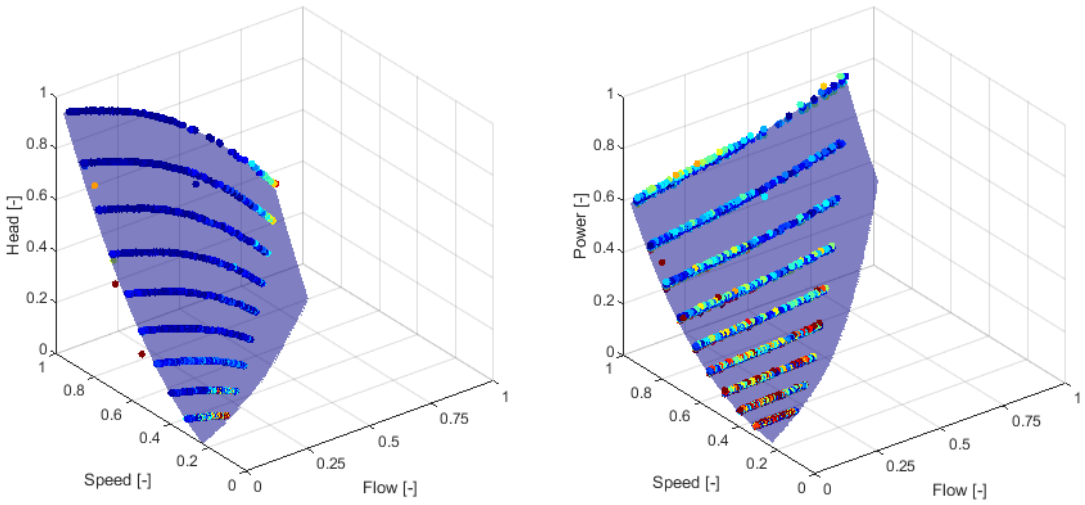

Figure 6. the Qp device characteristics fitting for HQ plane (left) and PQ plane (right).

Standard PID feedback control is not suitable for such a system. However, a controller by Sandoval [17] is specifically designed for robust velocity control of convective spatially distributed systems, e.g. heat terminals.

The control problem statement is to find a controller that drives the heat control error e to zero.

The stabilizing control law is defined as

$$\dot{\zeta} = k_I \mathrm{sg}(e)\theta(|(u-\zeta)\zeta| + |\dot{e}|)$$
$$u = \zeta + \theta\psi(e), \quad (1)$$

Where $\mathrm{sg}(e) = 1$ for $e \geq 0$ and $\mathrm{sg}(e) = -1$ otherwise.

The two constants k_P and k_I are tuning parameters for proportional and integral action, respectively. The controller can be considered a PI controller with a variable integral gain. An anti-windup modification has been utilized to prevent wind-up situations.

In our scenario, the heat control error is given as

$$e = \widehat{m_w} c_p (T_{wi} - T_{wo}) - Q_{REF} \quad (2)$$

where c_p [J/kg/K] is the specific heat capacity of the heat transport fluid (assumed water, a statistical test for the presence of water can be performed), T_{wi} and T_{wo} [°C] are supply and return temperature measurements in the Qp device. Heat flow reference Q_{REF} [W] is given by a supervisory temperature controller – a wall module or a zone temperature MPC [18].

Validation

The development of the Qp device would not be possible without a precise and multifunctional testbed.

Testbed

The hydronic testbed for hydronic control devices with temperature feedback (**Figure 8**) contains three connected circuits.

The primary hydronic circuit starts with the main pump and passes through a hot-water tank, the primary side of the Qp device, set of PT1000 temp. sensors and electromagnetic flowmeter routes back to the primary pump.

The secondary circuit starts at the Qp device secondary ports and passes through an actuated valve, a Coriolis flowmeter, a set of PT1000 temp. sensors to a water-to-air heat exchanger and back to the Qp device. A precise differential pressure sensor connects to the Qp ports on the secondary or the primary side.

An airstream starts with a straight duct with a Wilson grid flowmeter and continues through a controlled fan and a set of PT1000 temp. sensors into the water-to-air heat exchanger, from where it leaves the testbed.

The testbed also contains a small tank holding water of significantly different temperature to realize sharp temperature changes. It connects to the primary pipe via an old Qp prototype.

An ADRC controller controls the heating tank, and airflow and primary water flow are controlled by regular PI controllers. See **Figure 8** for a depiction of the testbed.

Two-pipe throttling actuators with temperature feedback may also be developed/tested here.

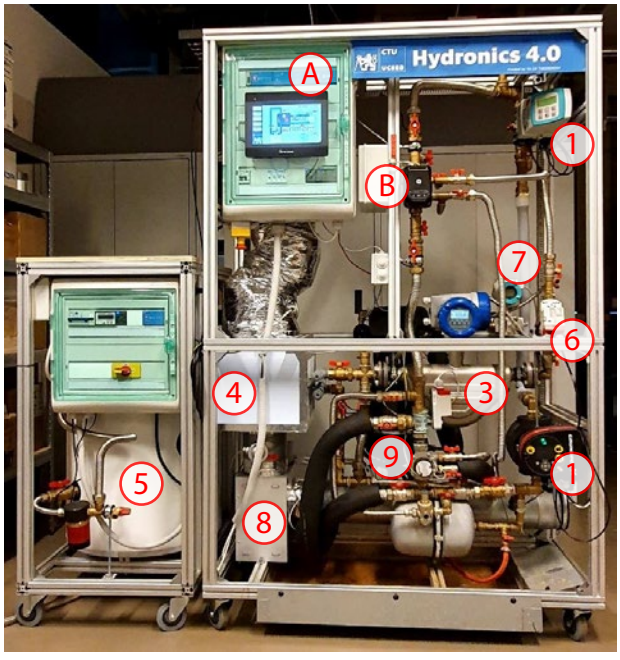

Figure 8. Hydronic Testbed. A) testbed controller, B) one-pipe control pump device, 1) primary pump, 2) primary induction flowmeter, 3) secondary Coriolis flowmeter, 4) water-to-air heat exchanger, 5) main tank, 6) actuated valve, 7) differential pressure sensor, 8) controlled fan, 9) second tank for sudden temperature changes.

Results

Figure 9 presents flow estimation precision. The data were obtained by ramping the pump speed up and down, preceded by three load steps, where the EKF identified the hydraulic load. The actuated valve connected to the secondary circuit was randomly positioned to represent an unknown hydraulic load. The standard deviation in the whole range for the actual hydraulic load is 3.91 ℓ/h; however, the estimation in the low-flow region is not entirely accurate due to the lack of feedback from the pump's electrical power reading, as the PQ characteristic is flat here.

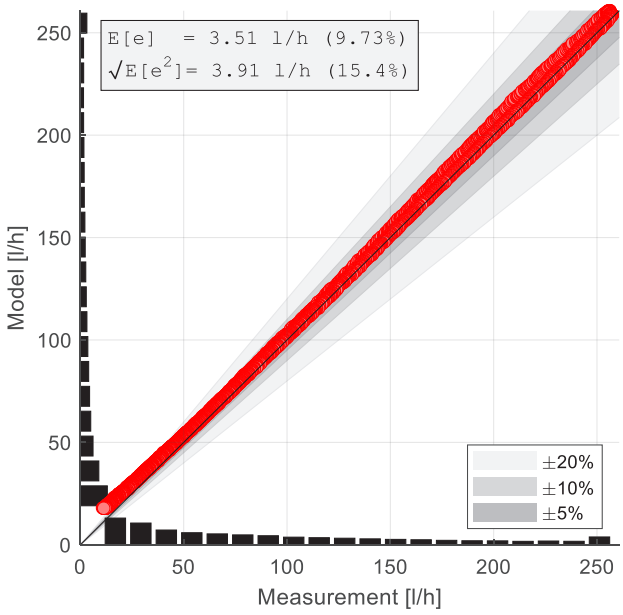

Figure 9. Flow estimation precision for a random fixed position of the actuated valve in the secondary circuit.

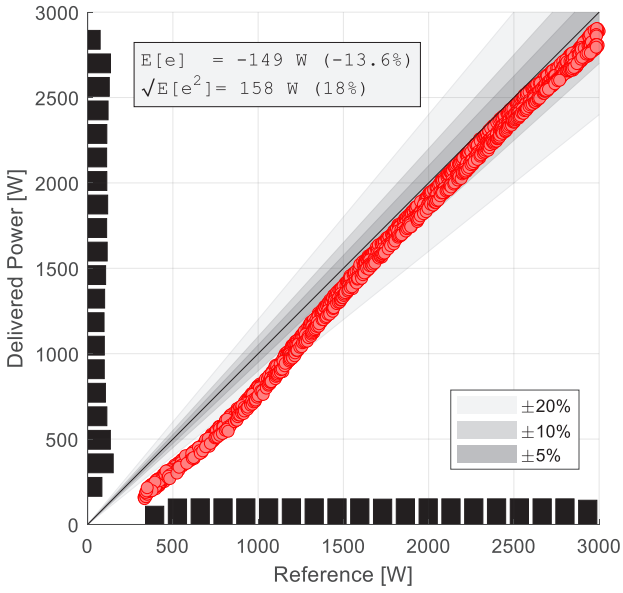

Figure 10. Steady-state heat flow control precision for the heat terminal present at the hydronic testbed.

Figure 10 presents the heat flow control of the water-to-air heat exchanger. The results were obtained by ramping up and down the absolute heat reference value. The standard deviation over the whole range of the heat terminal was 158 W. However, the tracking precision at low heat flows is not very satisfactory due to multiple factors.

First and foremost, the error in mass flow estimation is a factor. Second, the delivered (real) heat is calculated from wet-well water temperature sensors positioned directly on the heat exchanger inlet and outlet. In contrast, the estimated power is calculated from dry-well temperature sensors onboard the Qp device, and there is a good portion of uninsulated piping in between. Note that the heat flow controller always tracks the heat estimate exactly to the reference, but the estimated power differs from the real one. The systematic power control error in the higher flows is likely due to the heat dissipated by secondary piping (not insulated) and other errors in temperature measurements; the flow estimation error adds up to the latter in the low flow region.

Conclusion

This paper presents the results of a three-year-long development of the one-pipe control pump device: a Q-pump. We have built a well-working testbed suitable for developing temperature feedback hydronic actuators (valves, pumps) and have designed and built the Qp device according to the patented ideas. The paper presents the mechanical development process and the core working principle from the estimation and control point of view. Measurements validate the method to be sound, although there is still room for improvement in details. Future development will be directed towards thermal diagnostics, mainly detecting diminishing heat transfer due to dust build-up in an FCU. ■

Acknowledgement

This research was funded by the Technology Agency of the Czech Republic, grant number TK01020024.

References

Please find the full list of references in the original article at: https://proceedings.open.tudelft.nl/clima2022/article/view/349

BIM-based tools for energy-efficiency renovations

DIMITRIOS ROVAS
Dr, Associate Professor
UCL Institute for Environmental Design & Engineering, The Bartlett School of Environment, Ener-gy and Resources, University College London

Introduction

According to the IEA, energy efficiency is the 'first fuel' and a key element in the transition to net zero and better energy security. In the 2030 Climate Target Plan, the EU has set ambitious targets to cut carbon emissions by 2030 by at least 55% compared to 1990 levels. With 75%–85% of existing dwellings standing in 2050, it is imperative to focus on renovating an ageing building stock. The current renovation rate is modest at ≈ 1.2%/year; this rate should increase to 3% or more if we hope to achieve these targets.

For many buildings, especially ones that existed before the digital era, digital documentation is scant or even non-existent. Achieving health and well-being benefits requires consideration of aspects beyond energy, such as comfort (thermal, visual, acoustic), life-cycle costs and recording of user preferences. Even though there is significant evidence of unintended consequences, an excellent evidence-based knowledge base of best (and worst) practices does not exist. Very often, there is no post-renovation evaluation to quantify the benefits of specific interventions. The renovation market is quite fragmented, with multiple stakeholders with different and often conflicting interests. The fragmentation is reflected in the communication and information exchanges between stakeholders. All these factors are exacerbated when analysing the *associated risks and costs, leading to reluctance to invest in energy renovation and* low renovation rates.

The whole renovation process should be improved and can benefit from increased use of digital engineering tools to support stakeholders throughout the renovation process of existing buildings, from project inception to delivery. Within the recently completed EU research project BIMERR[**1**], we have been developing an ICT-enabled Renovation toolkit to support a streamlined and improved approach to planning and delivering renovations and retrofits.

The primary aim of the BIMERR project is to deliver on this vision of the *Digital Twin* in the context of renovation. The term '*Digital Twin*' refers to the digital replica of physical assets, processes and systems. In residential renovation, the digital twin is the digital replica of a physical dwelling that is kept updated (i.e., not static) over time. It holds geometry, design, cost, schedule, material, energy, condition, and other data, across each stage of the project life cycle. Its purpose is to facilitate multi-stakeholder interactions, supporting all life cycle processes and making it possible to integrate domain-specific tools in support of decision-making. This can improve productivity and communication, improve quality, and help reduce implementation risks.

Approach

A Common Data Model is essential to ensure interoperability across tools and a seamless flow of information across software components and stakeholders. The BIMERR Data Model comprises the open BIMERR ontology[**2**] covering non-geometric domains, supplemented by a BIM (Building Information Model) model for geometry and geometry-related aspects. As part of the research undertaken within BIMERR, we have developed, deployed and

demonstrated an ICT set of tools (see **Figure 1**) to support activities related to (i) digital building model creation, (ii) design support for renovation designers and (iii) construction work planning and workflow management.

Ensuring good quality data is critical. The BIM Management platform (a cloud-based tool) implements several approaches to data management that can support accelerating the (information) modelling process. The BIM models were created in the IFC (Industry Foundation Classes) to ensure better interoperability as per the ISO 16739 openBIM standard. We describe the process in the context of the demonstration sites that were part of the project.

Results

Shown in **Figure 2** is an example from one of the pilot sites. On the left is the building to be renovated (a residential block in Spain). To accelerate the BIM model's generation process, we explored two pathways: 1) perform an on-site survey and collect point cloud data. A Scan-to-BIM algorithm developed within the project can automate extracting a good quality BIM model from the point cloud data. When floor plans or other such information exists, modelling can happen within any BIM authoring tool.

We found that the approach of creating the models could vary significantly between BIM modellers; for this reason, we produced modelling guidelines to ensure

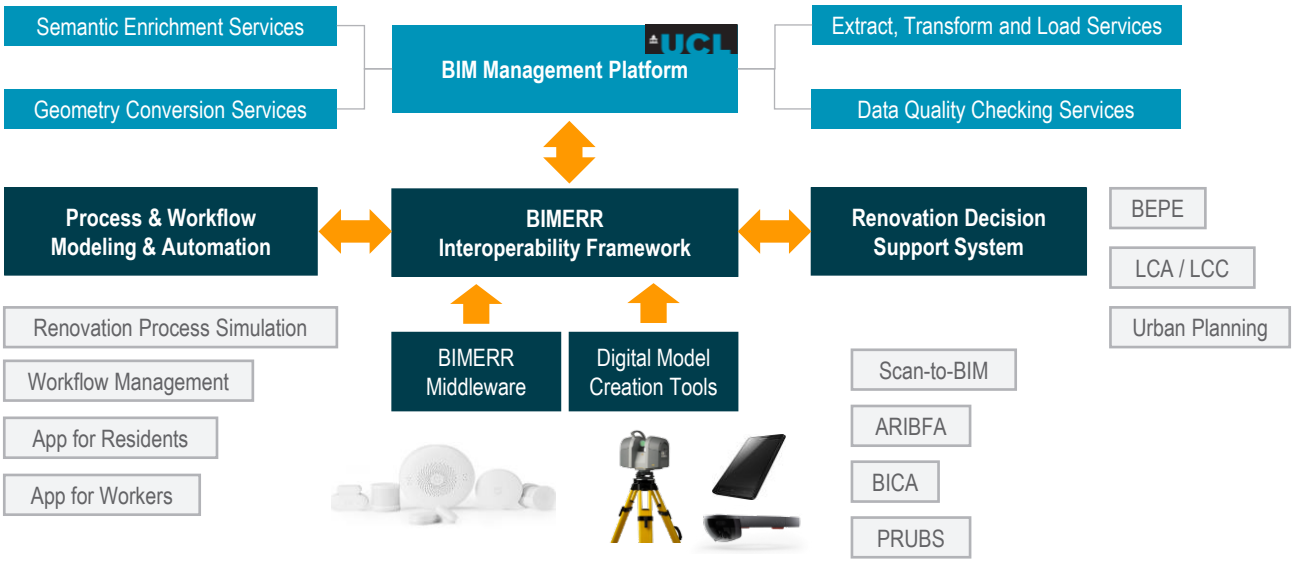

Figure 1. BIMERR High-level architecture.

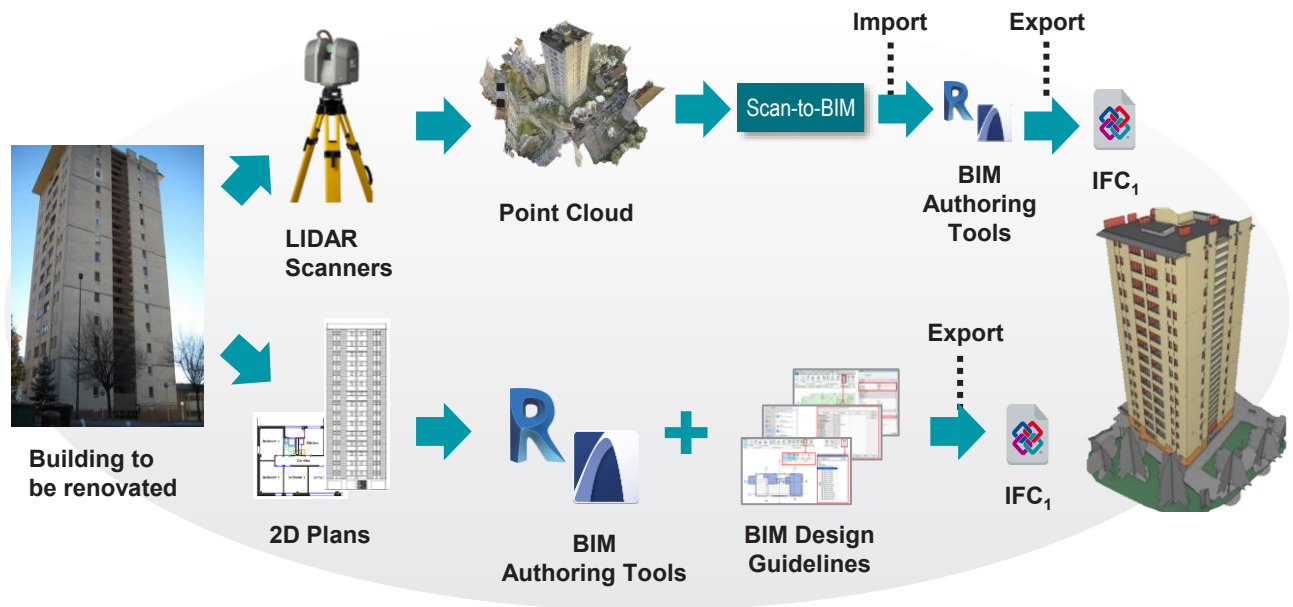

Figure 2. BIM Modelling process.

modellers can build good quality models. We found that importing and exporting IFC models with commercial editors was imperfect and created BIMERR-specific versions of IFC exporters for our requirements.

Whatever approach we adopt to create the model, the resulting model may still have errors or be incomplete in terms of having all the required information. A rigorous model checking procedure should ensure all needed information is present – this is an example of completeness checking. Shown in **Figure 3** is an example of such a check. Given a set of checking rules (in the form of specific Model View Definitions defined by buildingSMART), the platform ensures the model has all the required information. Once these completeness tests have passed, further geometric tests can take place, like clash detection using the platform's cloud-based tools. **Figure 3** shows an example of the model missing thermal properties or a containment relationship for a thermostat.

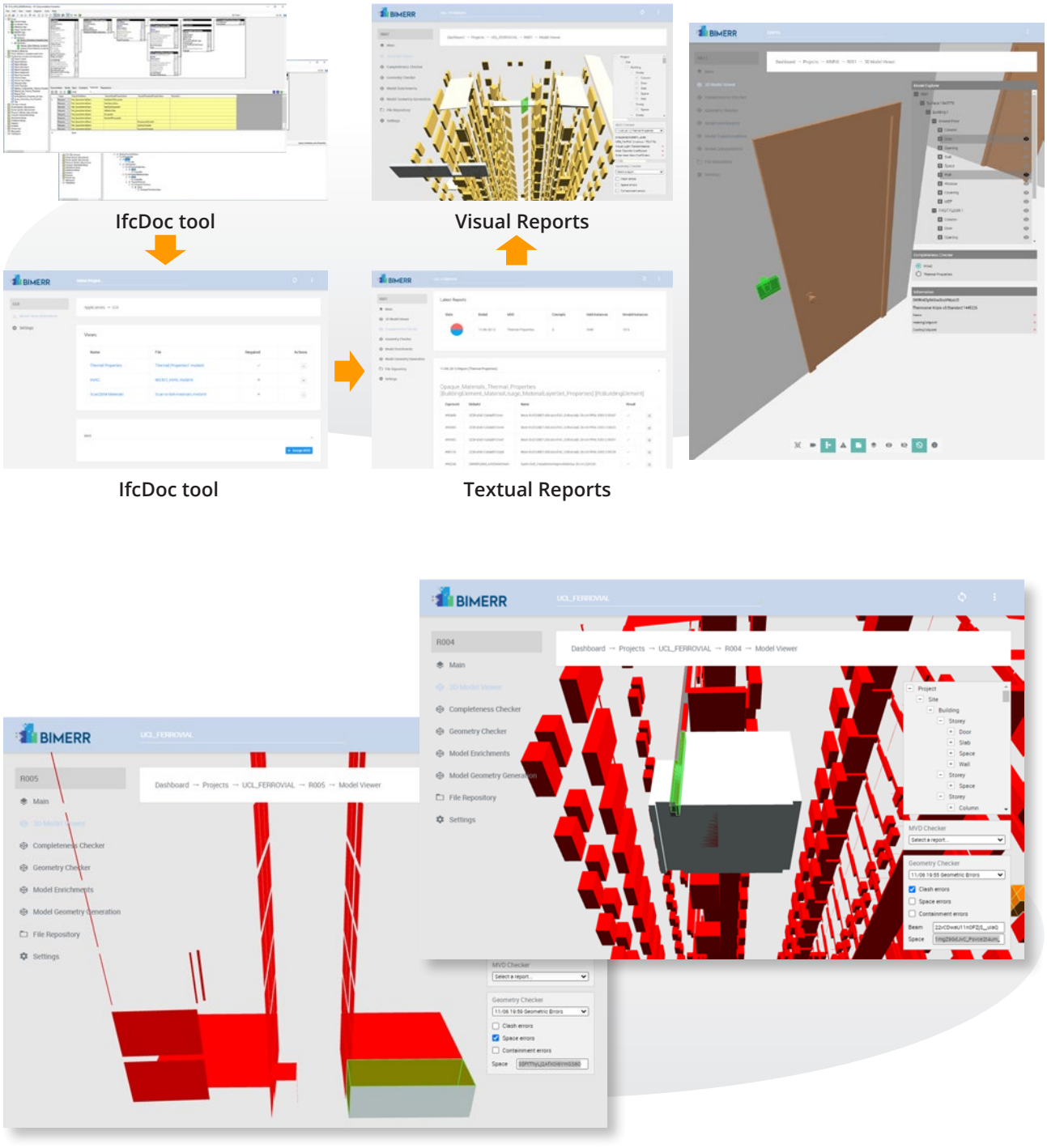

Figure 3. Model completeness checking (top) and Geometric model checking and clash detection (bottom).

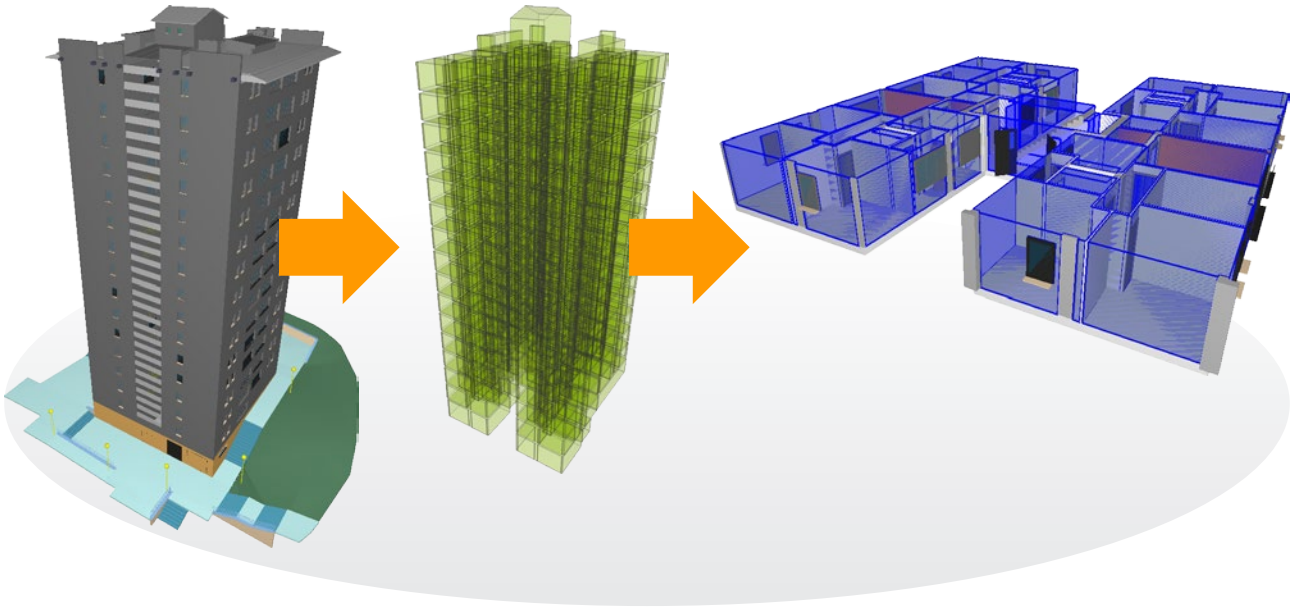

Figure 4. Semantic enrichment.

The data might be further post-processed to be useful for specific applications. Shown in **Figure 4** is the case where algorithms automatically generate spaces and extract thermal transfer surfaces required for energy modelling (2nd-level space boundaries).

This automated procedure can extract this information and enrich the model. The space boundary information can then be easily serialised to create inputs for energy modelling tools (using the E+ data dictionary in our case). The same applies to other details like thermal properties, construction, glazing, schedules, etc. Only a small additional manual effort is required to generate energy simulation models. In a past project, we explored the approach to creating parametric energy models that could be used in an optimisation context to evaluate possible retrofitting alternatives [**3**].

The approach presented allows for a significantly reduced modelling time by up to 50% (in the BIMERR demonstration sites). Perhaps more importantly, the process leads to high-quality data that can be useful for various purposes in the planning and construction phases. ■

Key Messages

For renovation planers, the work highlights potential new tools for planning and implementing energy efficiency renovations.

For policymakers, this research shows digital engineering tools that can improve renovations' quality and encourage investment in energy efficiency changes. Expected impacts include accelerating the renovation rate, helping meet climate targets, and enhancing energy security.

Acknowledgement

The contribution of K. Katsigarakis and G. Lilis (UCL), who developed the platform and geometric tools, F. Bosché (U of Edinburgh) for the Scan-to-BIM tool, and M. Poveda (Univ Poly Madrid) for the BIMERR ontology, is gratefully acknowledged. The work would not have been possible without the support of the European Commission H2020 programme under contract #820621 (BIMERR).

References

[1] BIMERR: BIM-based tools for Energy-driven renovation of existing residences, https://bimerr.eu/

[2] https://bimerr.iot.linkeddata.es/

[3] OptEEmAL (Optimised energy-efficient platform for refurbishment at district level) Available online: https://www.opteemal-project.eu/

How accurate are current CO_2 and PM sensors used in Dutch schools?

This article is based on the EngD project report of Vinayak Krishnan [1]





VINAYAK KRISHNAN
Kropman Installatietechniek

HAILIN ZHENG
Department of the Built Environment, Eindhoven University of Technology, Eindhoven, the Netherlands

MARCEL LOOMANS
Department of the Built Environment, Eindhoven University of Technology, Eindhoven, the Netherlands

SHALIKA WALKER
Kropman Installatietechniek

WIM ZEILER
Department of the Built Environment, Eindhoven University of Technology, Eindhoven, the Netherlands

There is a growing need for accurate low-cost indoor air quality (IAQ) sensors in schools. Therefore, a climate chamber performance study is conducted to evaluate the current scenario of low-cost sensors or monitors (LCMs) capable of measuring CO_2 and particulate matter (PM). Finally, the LCMs are compared using grading criteria to find out the best performing ones.

Keywords: Low-cost monitors, sensors, indoor air quality, performance study, schools

Introduction

Many schools in the Netherlands have insufficient ventilation [1]. At this moment, one of the pieces of advice by the Dutch government [2] for improving school ventilation is appropriate airing (i.e., opening doors and windows) based on the activities in poorly ventilated classrooms. If one can understand what exactly is happening in a classroom in terms of IAQ on a real-time basis, then appropriate interventions like these can be implemented to improve ventilation. Moreover, due to variable demand during the day in schools, demand-controlled ventilation helps to reduce energy consumption. Therefore, monitoring classroom IAQ is crucial for appropriately applying IAQ-improving interventions and effectively controlling the ventilation for a more energy-efficient system.

The Dutch government has also recognized this need and has decided to supply low-cost CO_2 sensor units for all school classrooms in the Netherlands [3] and make their presence obligatory. This is a good first step; however, how reliable are market available IAQ parameter measuring LCMs when applied on a large scale?

With this question, a study was conducted at the Eindhoven University of Technology (TU/e) with the following aims:

- To test the performance of market-available LCMs capable of measuring CO_2 & PM as compared to research-grade instruments (RGIs).
- To identify the advantages and limitations of LCMs when applied to monitor and control classroom ventilation, based on the results of the performance assessment.

This study was part of the RVO TKI Urban Energy and Eindhoven Engine project Efficient Comfortable School Indoor Air Quality (ECoS-IAQ).

Method

The LCMs were tested in a climate chamber setting (see **Figure 1**). The LCMs performance was compared to research-grade instruments (RGIs) using statistical metrics defined in the United States Environmental protection agency (U.S. EPA) guideline [4]. Later an overall performance assessment of the LCMs was conducted using rating criteria. For details on the method refer to [1],[5].

In total 16 LCMs (two units per brand) measuring multiple IAQ parameters were tested in this study. 7 out of 16 LCMs have not been tested in previous scientific literature yet [5]. In this article we focus on LCMs measuring CO_2 and/or PM. A GRIMM aerosol spectrometer (Model 11-D) was used as an RGI for PM and an SBA-5 CO_2 gas analyser was used as a reference for CO_2.

The study [5] tested LCMs performance for typical day care centre activities, which are similar to schools. However, the LCMs could not detect accurately the low concentrations of PM released. Therefore, in this study the focus has been on selecting activities which generate enough pollutants that can be detected by the LCMs. Three types of PM events were conducted which included, ultrasonic humidifier, candle burning and vacuum cleaning. Two types of CO_2 release events were conducted which included CO_2 dosing and human occupancy. Two different climatic conditions were considered for each event. These are hot and humid (T= ≈ 26°C, RH= ≈ 70%) and cold and dry (T= ≈ 20°C, RH= ≈ 40%), which are the indoor conditions commonly observed in the Netherlands. A total of 11 events for CO_2 and PM pollutants were conducted.

The four aspects as per [4] that were used to check the LCMs performance are as follows:

Precision: This is to check how repeatable the measurements are when comparing the two units of the same brand. This is checked by comparing the coefficient of variation (CV) values for the LCMs. The lower the CV value, the better the equipment's precision.

Bias: This metric estimates the systematic disagreement between the LCM and the RGI. Based on the research [4], the linear regression model is recommended to fit LCM data to RGI data. This regression can help determine the slope (m) and the intercept (c) computed with the LCM data plotted on the y-axis and the RGI data plotted on the x-axis. The closer the slope is to 1 and the intercept is to 0, the lower the LCM's bias.

Linearity: This metric explains how much the LCM results can explain the RGI measurements. This was quantified using the R^2 value. The higher the R^2, the better the fit of the data points to the linear regression line.

Error: This is a measure to quantify the disagreement in the values between the LCM and the RGI for a specific event. This was quantified using the root mean squared error (RMSE) and normalized root mean squared error (NRMSE). The lower these values, the

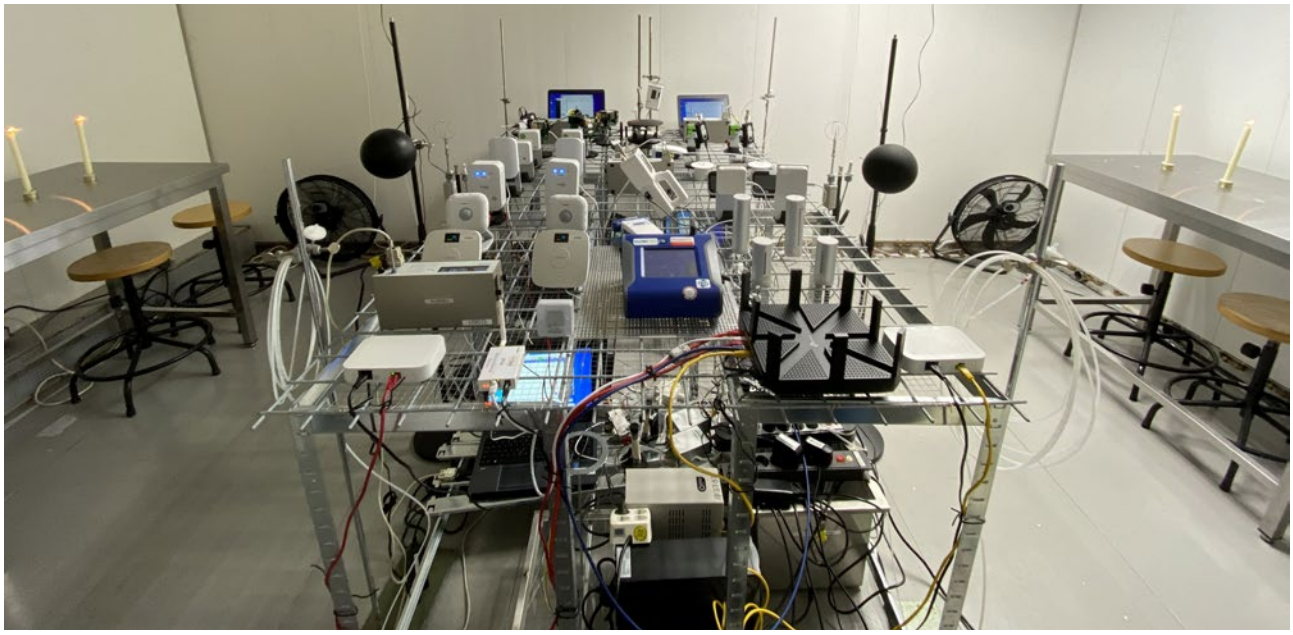

Figure 1. The Climate Chamber setup for the candle burning experiment is shown. The sensors are placed in the middle on a wire mesh table, and the pollutant sources are placed on the two tables around the sensors

lower the total error between the LCM and the RGI in an event.

It should be mentioned that each performance assessment metric was computed for each event. The metrics computed are plotted in a box plot, with each point representing a metric outcome for one event. This gives an idea of the spread of the data. Also, the limiting values are plotted to check the LCMs performance. The equations used to compute the metrics can be found in [1]. In the box plots the LCMs are indicated with the numbers as per the LCMs list in [1]. The grading criteria for the LCMs are shown in **Table 1**. These grading criteria incorporate three main aspects: precision, linearity, and error. The bias is not considered as it is already part of the error. Each LCM can be rated based on the parameter it can measure using these rating criteria.

Results and discussions

In **Figure 2**, **Figure 3**, **Figure 4**, and **Figure 6**, the CV, R^2, slope, and RMSE values for each event are plotted in a box plot for CO_2, and $PM_{2.5}$. The limiting values as per [4] are also indicated with a blue dashed line in the plot. The red dashed line indicates the ideal value. Although there were 3 types of PM sizes analysed in the study, only $PM_{2.5}$ results are shown. The LCMs performance of other PM sizes have been found to be similar [1].

Precision: Based on the results shown in **Figure 2**, it can be concluded that the precision is within acceptable limits for almost all LCMs for both CO_2 and $PM_{2.5}$. This also means that different LCMs of the same type will have reasonably consistent readings.

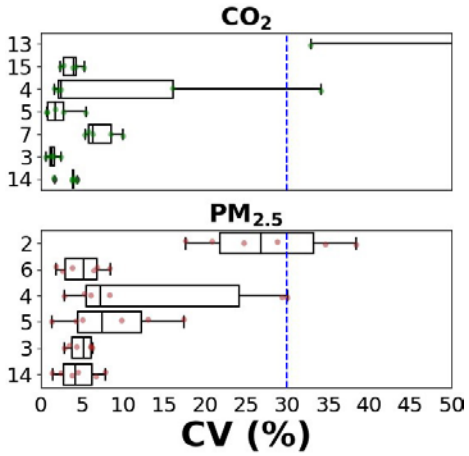

Figure 2. CV values for CO_2, and $PM_{2.5}$, are plotted in a box plot with each point denoting one event. The blue dashed line indicates the limiting value as per [4].

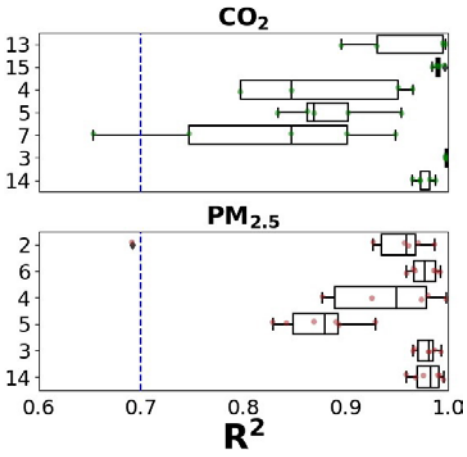

Figure 3. R^2 values for CO_2, and $PM_{2.5}$, are plotted in a box plot with each point denoting one event. The blue dashed line indicates the limiting value as per [4].

Table 1. *Grading criteria defined for each parameter of the LCMs for evaluating Precision (CV), Linearity (R^2), and Error (NRMSE & RMSE). The grade ranges from 5 (very good) to 1 (very poor).*

Parameter	Ranking grade	5 (Very good)	4 (Good)	3 (Moderate)	2 (Poor)	1 (Very poor)
CO_2	CV (%)	CV≤2.5%	2.5<CV≤5%	5%<CV≤7.5%	7.5%<CV≤10%	CV>10%
	R^2 (-)	R^2≥0.95	0.95>R^2≥0.9	0.9>R^2≥0.85	0.85>R^2≥0.8	R^2>0.8
	NRMSE (%)	NRMSE≤10%	10%<NRMSE≤20%	20%<NRMSE≤30%	30%<NRMSE≤40%	NRMSE>40%
PM	CV (%)	CV≤5%	5%<CV≤10%	10%<CV≤20%	20%<CV≤30%	CV>30%
	R^2 (-)	R^2≥0.95	0.95>R^2≥0.9	0.9>R^2≥0.85	0.85>R^2≥0.8	R^2>0.8
	NRMSE (%)	NRMSE≤15%	15%<NRMSE≤30%	30%<NRMSE≤45%	45%<NRMSE≤60%	NRMSE>60%

Linearity: Based on the results shown in **Figure 3**, it can be concluded that all the LCMs and the RGIs readings have a linear relationship with each other. The linear regression is a good fit for the data.

Bias: From **Figure 4** it can be observed that the slope values are within limits for CO_2 LCMs. From **Figure 5** it can be observed that the intercept for CO_2 can be quite variable depending on the LCM. Therefore, the bias for CO_2 LCMs can range from acceptable to significant. For almost all LCMs which measure $PM_{2.5}$, the bias values are significant, refer **Figure 4** and **Figure 5**. Particular attention must be placed on correcting the bias of the LCMs.

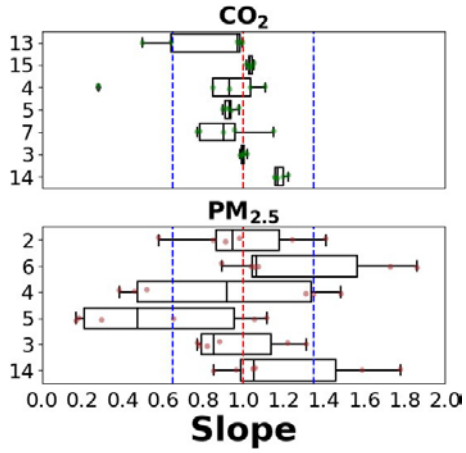

Figure 4. Slope values for CO_2, and $PM_{2.5}$, are plotted in a box plot with each point denoting one event. The blue dashed line indicates the limiting value as per [4] and red dashed line the ideal value.

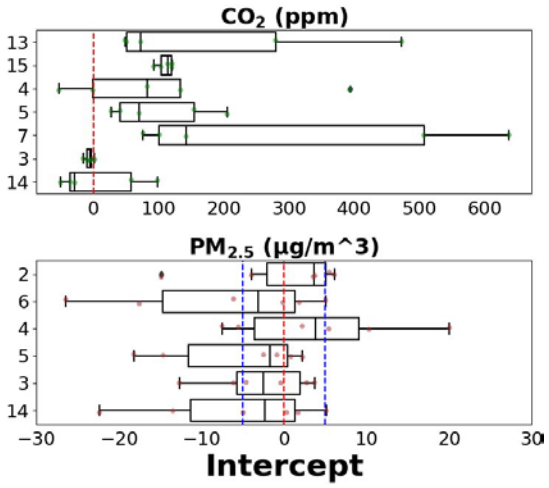

Figure 5. Intercept values for CO_2, and $PM_{2.5}$, are plotted in a box plot with each point denoting one event. The blue dashed line indicates the limiting value as per [4] (only for PM) and red dashed line the ideal value.

Error: Based on the results shown in **Figure 6**, it can be observed that the RMSE values are significantly high for almost all LCMs and both parameters. Interestingly, the average RMSE for CO_2 varied between 32.5 ppm and 415.4 ppm (except for LCM 13 as it was way too erroneous compared to the other LCMs), and for $PM_{2.5}$ almost all values were above the limits. Most manufacturers quote accuracy below these values; hence, every LCM's accuracy must be questioned and verified.

LCMs comparison

The LCMs used in the experiment can be compared using the rating criteria presented in **Table 1**. When comparing LCMs that measured CO_2, LCM 3 performed the best; refer to **Table 2**. Additionally, when comparing LCMs that measured $PM_{2.5}$, again, LCM 3 and also LCM 14 performed the best; refer to **Table 3**. LCM 3 was also the best performing LCM when comparing criteria across multiple parameters like $PM_{2.5}$, CO_2, TVOC, T, and RH in the study presented in [5]. Therefore, the results are consistent.

LCMs applicability

The main observations in terms of LCMs application from this study are:

General

Based on the spread in data for all the boxplots for the different metrics, it can be concluded that the LCM performance can be significantly dependent on the event itself. This indicates the activity dependence on the performance of the LCMs, which was also noted

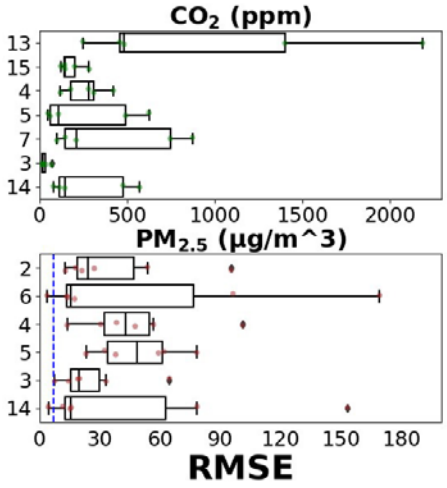

Figure 6. RMSE values for CO_2, and $PM_{2.5}$, are plotted in a box plot with each point denoting one event. The blue dashed line indicates the limiting value as per [4].

in [5]. Additionally, the systematic error or bias is significant, and is generally time dependent. Therefore, all LCMs must be regularly calibrated for the specific environment in which they will be installed. Despite the errors, all LCMs can follow the trends for the parameters based on the classroom activities and can be directly applied to detect events on a large scale and possibly initiate interventions to improve the ventilation. For this study, it was found that the LCM 3 performs the best overall. The metrics used and the grading criteria can be replicated from this study for other studies to evaluate LCMs in the future.

CO_2 LCM

As per the results, the main concern for CO_2 LCMs is the accuracy and variability across different activities. As an example, in the Netherlands, Frisse Scholen Classes [6] are defined in increments of 200 ppm. This increment is lower than the accuracy encountered by some LCMs, refer to **Figure 6**. This raises questions about the ability of these LCMs to distinguish between these classes. The accuracy quoted by the manufacturer and the actual performance was also noted to be different (lower) in most cases.

PM LCM

Regarding PM, it was observed that the LCMs readings could have a significant error and activity dependence compared to CO_2. The accuracy quoted by the manufacturer must be questioned, and from the results, it seems they are not yet mature enough to predict accurate absolute values for varying environmental conditions. For PM LCMs especially, the LCM must be calibrated for the specific pollutant generated in the application for which they will be used. However, it is expected to be a complex procedure because the types of particles generated in any indoor environment can vary a lot. It is also to be noted that currently available LCM technology cannot monitor particles less than 0.25 µm [5], which are considered the most dangerous for human health.

Table 2. *Ranking for the CO_2 LCMs in the experiment based on the rating criteria mentioned in* ***Table 1.***

LCM number	CO_2			Average rating	Rank
	CV	R^2	NRM-SE		
13	1	5	1	2.33	5
15	4	5	4	4.33	2
4	1	1	3	1.67	7
5	5	3	4	4.00	3
7	3	2	2	2.33	5
3	5	5	5	5.00	**1**
14	4	5	3	4.00	3

Table 3. *Ranking for the $PM_{2.5}$ LCMs in the experiment based on the rating criteria mentioned in* ***Table 1.***

LCM number	$PM_{2.5}$			Average rating	Rank
	CV	R^2	NRM-SE		
2	4	5	2	3.67	3
6	2	4	3	3.00	4
4	3	2	2	2.33	6
5	4	3	1	2.67	5
3	5	5	3	4.33	**1**
14	5	5	3	4.33	**1**

Conclusions

The LCMs measuring PM and CO_2 can detect variations in measured parameters in a classroom. However, the absolute accuracy of the LCMs needs to be questioned in practice. It was also observed that the performance depended on the environment and the pollutants they were exposed to, especially for PM. In most cases, for the CO_2 measurement results, the accuracy was lower than quoted by the manufacturer. The PM measurement results indicate that the current low-cost PM technology is not yet able to measure accurately in varying environmental conditions. However, overall, the LCMs could follow the trend of the exposed pollutants.

Recommendations

It is recommended to check how significantly can correcting the bias help in reducing the total errors. The frequency of this bias correction or calibration needs to be also checked. Also, since the calibration needs to be conducted on a large scale, a feasible and effective calibration method must be developed. Additionally, this study could be used as a start for creating a standardized performance test for selecting LCMs in the future. E.g., within the Brains 4 Buildings project (brains4buildings.org). This project is aimed at data driven Fault detection and Diagnosis.´■

Acknowledgements

This study was financially supported by RVO TKI as well as Eindhoven Engine. Furthermore, we would like to thank Ph.D. candidate Srinivasan Gopalan, Ph.D. candidate Karzan Mohammed, and EngD trainee Petros Zimianitis who were involved in the processing and analysis of the data.

References

[1] Krishnan, V. 2022. *Methodical School Ventilation Design to improve Efficiency, Comfort, and Health: Design Concepts for Air Handling units and Performance assessment for Low-cost sensors*. PDEng report, Eindhoven University of Technology Available: https://research.tue.nl/files/216623288/2022_08_30_Krishnan_V._SBC.pdf.

[2] Landelijk Centrum Hygiëne en Veiligheid, Binnen- en buitenmilieu voor basisscholen. May 2016 https://www.rivm.nl/sites/default/files/2018-11/Binnen-%20en%20buitenmilieu%20voor%20basisscholen%20-%20mei%202016.pdf.

[3] "gezamenlijk-actieplan-voor-snelle-verbetering-van-ventilatie-op-scholen @ www.rijksoverheid.nl." [Online]. Available: https://www.rijksoverheid.nl/actueel/nieuws/2022/02/03/gezamenlijk-actieplan-voor-snelle-verbetering-van-ventilatie-op-scholen.

[4] R. Duvall *et al.* 2021. Performance Testing Protocols, Metrics, and Target Values for Ozone Air Sensors: Use in Ambient, Outdoor, Fixed Site, Non-Regulatory and Informational Monitoring Applications. p. EPA/600/R-20/279, 2021, [Online]. Available: https://cfpub.epa.gov/si/si_public_record_Report.cfm?Lab=CEMM&dirEntryId=350784&Lab=CE%MM.

[5] Zheng, H., Krishnan, V., Walker, S., Loomans, M., & Zeiler, W. 2022. Laboratory evaluation of low-cost air quality monitors and single sensors for monitoring typical indoor emission events in Dutch daycare centers. Environment International, 166, 107372. https://doi.org/10.1016/j.envint.2022.107372.

[6] Netherlands Enterprise Agency. 2021. Program of requirements – fresh schools, [Online]. Available: https://www.rvo.nl/sites/default/files/2021/06/PvE-Frisse-Scholen-2021.pdf.

Lindab introduces

App controlled, **wireless ventilation**

Lindab **UltraBT**™

Room control system made easy

The Ultra BT system allows you to upgrade room by room, it requires no reconstruction of walls, no long-term shut down of offices and will result a huge reduction of ventilation costs and energy consumption.

The UltraLink Demand Controlled Ventilation regulator, Bluetooth sensors and Lindab apps on your smartphone – that is all you need to get a cost-effective ventilation upgrade with full operation control at room level.

www.lindab.com

Lindab®

New possibilities with EPBD revision for ventilation systems

JAN BEHRENS
Manager
Project and Support Center
Lindab Ventilation AB

Building renovation and inspection of ventilation systems is a welcoming addition in the proposed revision of EPBD [**1**]. It's important to consider the various stakeholders involved in the process of designing, implementing, and monitoring a well performing ventilation system. The revised and consistent regulatory, together with interdisciplinary collaboration, new technology and user behavior, are significant factors in making energy-efficient buildings and healthy indoor environments that work both in theory and practice.

Best-case performance for worst-case buildings

Collectively, buildings account for 40% of Europe's energy consumption [**2**]. Building operations, including heating, cooling and electricity, account for 27% of all global energy-related carbon emissions [**3**]. Optimizing energy performance in buildings is an essential factor in cutting emissions, lowering energy consumption and reducing vulnerability to prices in Europe [**1**]. It should be the task of everyone involved to achieve the goal of carbon-neutral buildings by 2050 [**4**], without having to forgo a good indoor climate. In particular, the restrictions caused by the COVID-19 pandemic have shown that adequate ventilation in buildings is of great importance for health. The upcoming winter could reveal the challenge of the circumstances. Will there be time to choose between good indoor climate or energy saving?

Modern control technics optimize energy requirement based on user behavior, which means that a good indoor climate can be combined with the lowest energy performance. Studies have shown that modern control procedures in ventilation systems, demand-controlled ventilation systems (DCV) in particular, can reduce energy consumption of the building while also improving the overall air quality and indoor environment. Using this control method for ventilation is an indisputable alternative for energy efficiency in new buildings but should also be considered for energy efficient renovation and refurbishments.

A case study made by Lindab Innovation Hub in 2020-2021, showed how modifying an existing ventilation system and adding a wireless DCV system at room level in an office building in Bargteheide, Germany, saved as much as 68% energy after installation.

The system consists of ultrasound measurement technology for the flow controllers, Bluetooth room sensors for CO_2 and presence detection and mobile applications that give access for commissioning but also for the user of the room to control and monitor the system and the indoor air quality. The return on investment for the upgrade was calculated to be 4.5 years but this number would probably be more drastic

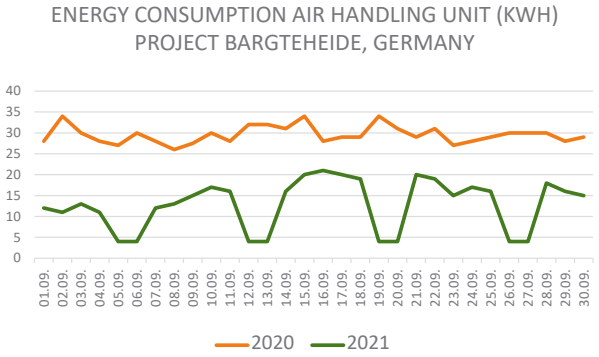

Energy consumption of an Air Handling Unit in comparison of September 2020 and September 2021, Office project in Bargteheide, Germany. Orange line shows the energy consumption before renovation (constant airflow according to design) and green line shows the energy consumption after renovation (Variable airflow with DCV).

if calculated with today's energy costs. As many as 100 million adults and children live, study and work in unhealthy houses in Europe [**5**] and around 75% of the EU's building stock is not considered energy-efficient [**6**]. Modifying existing ventilation in worst-case buildings with smart systems can be essential for indoor air quality, lowering energy consumption and cutting both direct, and indirect emissions of the building.

The double-edge sword of control systems in ventilation

To understand the accepted indoor climate in relation to energy performance, Lindab Innovation Hub made several long-term examinations in existing buildings with different control ventilation systems. The results showed in nearly all projects that the systems had failures, wrong settings, missing balancing adjustment or warning messages from the building management system that were ignored or not seen by the person responsible. Our conclusion is that without precise installation, well-functioning sensors and control, there is a high risk that the designed energy performance of a system will not be reached. In worst cases, an energy-saving system becomes a high-energy consumer that cannot guarantee a sufficient good indoor climate.

Since 1991, ventilation control has been mandatory in Sweden [**7**] and should be carried out by a certified inspector. It is a well-functioning system which is controlled regularly in most buildings, to show that the indoor climate is good, and that the ventilation system is working as it should. According to The Swedish National Board of Housing, Building and Planning the inspector must give suggestions on how the energy consumption can be reduced for the ventilation, without this resulting in a worse indoor environment [**3**]. With smart ventilation systems, it must be considered how the system as a whole is designed to perform on a daily basis. DCV systems are based on the presence of people to provide energy efficiency and ensure healthy indoor air. The system's capacity is worth considering when handing over to facility managers and for future controls and inspection. In Lindab Innovation Hub's case study from an office building in Otelfingen, Switzerland, a facility manager of a DCV system had the opinion that it was not performing well and that the energy costs had been too high. The investigation included an examination of the system drawing, re-calculations of the system and building energy requirement, as well as a long-term observation of different factors that could affect the system. An analysis of the results revealed that errors had gone unnoticed during the practical handling of the ventilation system in the past years. After corrective adjustments, the energy requirement of the ventilation system was reduced by 71%, while maintaining good indoor air quality.

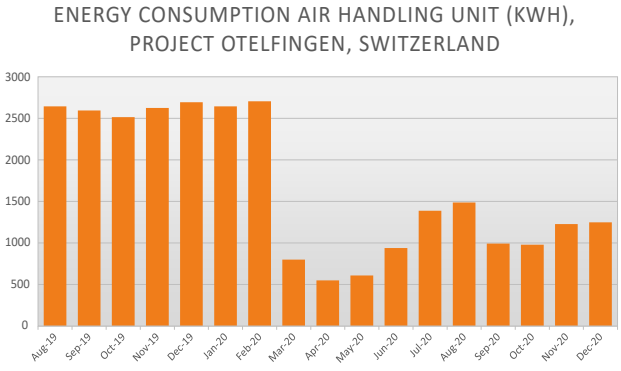

Energy Consumption of an Air Handling Unit in kWh, Project Otelfingen, Switzerland. Corrective adjustments fixed in March 2020.

The results clearly indicate the importance of regular and regulated inspection and monitoring of ventilation systems but also a need for accessible information, understanding of the consequences of errors and warning signals and a plan of action for correction. It also implies the importance of comparing inspections to the original and intended performance of the ventilation design, and that any configurations and suggestions of change should be documented for future reference and in a dialogue with facility manager, commissioner, and system designer.

Interdisciplinary collaboration and involvement of end-users

Targeting building renovations and inspections of ventilation systems is a welcomed act in the proposed revision of EPBD and an important step to take on the ongoing challenges of energy consumption and carbon emission in the real estate industry. The need for action is clear while time for action is running out. A new Global Retrofit Index report (2022) finds that less than 1% of existing buildings in major economies are given the necessary retrofitting upgrade. To meet the IPCC 1.5-degree scenario, the average annual retrofitting rate should be 2.5% by 2030 while reduction in energy intensity should be 45% [**3**].

National regulations aside, to meet the ongoing building requirements and environmental targets there is a need to reconcile the building industry with smart systems and interdisciplinary collaboration of all stakeholders involved. Property owners must receive

advice to understand the consequences of their decisions so that indoor climate and energy performance meet their expectations. Maintenance and servicing need to be done by organizations that take authority of proper operation. Designers should have the facility to make sure that all technical equipment fits together and operates optimally according to performance and design. Briefing the contractor is also important so that the system is installed as designed and that it operates as intended.

Possibilities of communication between system designer, ventilation system, monitors and end-user.

Our experience with both Bargteheide in Germany and Otelfingen in Switzerland is a lesson learned about actions, including the importance of clear documentation, smart solutions and easy to use products and systems that more extensively involve the end-user. It is guiding us towards new technological opportunities with better communication between the system designer, the ventilation system, sensors, and the actual end-user.

Developing digital solutions for constant and long-term monitoring, along with user behavior, design and experience is a way forward to better understand the effectiveness and impact of healthy indoor air and energy consumption of a building. Presenting data in user-friendly way is a path to improve satisfaction and trust - and encourages end-users to engage with performance and the effect a ventilation system can have on indoor environment and building energy consumption. ■

References

[1] European Commission, *Proposal for a Directive of the European Parliament and of the council on the Energy Performance of Buildings (recast)*, European Commission, 2021. EUR-Lex - 52021PC0802 - EN - EUR-Lex (europa.eu) [accessed 26 October 2022).

[2] European Commission, *In focus: Energy efficiency in buildings*, European Commission, 2020. In focus: Energy efficiency in buildings | European Commission (europa.eu) [accessed 26 October 2022).

[3] Robert Kilgour, Joshua Deru, Laura Watson and Michael Lord, *Global Retrofit Index*, 3Keel in association with Kingspan, 2022. https://www.3keel.com/wp-content/uploads/2022/10/Global_Retrofix_Index.pdf [accessed 01 November 2022).

[4] European Commission, *European Green Deal: Commission proposed to boost renovation and decarbonization of buildings*, European Commission, 2021. Renovation and decarbonisation of buildings (europa.eu) [accessed 26 October 2022).

[5] Velux, *Healthy Home Barometer*, Velux 2019. HHB_Main-report_2019.indd (azureedge.net) [accessed 26 October 2022].

[6] European Commission, *Driving energy efficiency in the European building stock: New recommendations on the modernisation of buildings*, European Commission, 2019. Driving energy efficiency in the European building stock: New recommendations on the modernisation of buildings | European Commission (europa.eu) [accessed 26 October 2022].

[7] Boverket, *OVK – oblikatorisk ventilationskontroll*, Boverket 2021 (link).

ISHRAE® informa markets

SHOWCASING ENERGY EFFICIENT HVAC-R PRODUCTS & SOLUTIONS

SOUTH ASIA'S LARGEST EXHIBITION ON AIR CONDITIONING, HEATING, VENTILATION AND INTELLIGENT BUILDINGS

ACREX® India 2023

14-16 MARCH 2023 | BEC, MUMBAI

ENGINEERING TOWARDS NET ZERO

The 22nd edition of ACREX INDIA is scheduled from 14th to 16th March 2023 at Bombay Exhibition Centre, Mumbai. The focus will be on engineering advancements and driving technological solutions towards net zero goals in the HVAC-R sector, which is pivotal in creating a better future.

ACREX INDIA 2023 shall stand tall as the most coveted & comprehensive conglomeration for industry professionals from around the globe. Experts from all over the world would come together to meet people, cultivate, expand networks and conduct business.

ACREX INDIA 2023 FEATURES

450+ Exhibitors	**35000+** Attendees	**32000 Sq m.** Gross Exhibition Space	Participation from **40 countries**	Technical Seminars and Workshops	Interactive Panel Discussions	ACREX Awards of Excellence	ACREX Hall of Fame

EXHIBITORS PROFILE

- Packaged Chillers
- Air Handling & Distribution Products
- Unitary Products (Air conditioners)
- Products (Refrigeration)
- Refrigeration Accessories
- Water Distribution
- Water Treatment

and many more...

SCAN QR CODE FOR VISITOR REGISTRATION

SUPPORTED BY

REHVA – Federation of European Heating, Ventilation and Air-conditioning Associations

PARTNERS

ACREX Award Night Partner: DAIKIN

ACREX Hall of Fame Partner: Danfoss

Curtain Raiser Partner: FUJITSU | ABS

Knowledge Partner: BLUE STAR – BUILT ON TRUST

Titanium Partner: Eurovent Certita Certification

Insignia Lounge Partner: Hisense HVAC – Reimagine your solution

IAQ Partner: ZECO – We breathe air into your life

Gold Partner: SANHUA

Silver Partners: AHRI | GANDHI Automations Pvt Ltd | Fascold | KEHEMS TECHNOLOGIES

Bronze Partners: aeropure | Munters

FOR MORE INFORMATION, CALL- M: +91 9833170240 | E: jivitesh.wadhwa@informa.com

www.acrex.in | www.informamarkets.com

Cracking the myths about propane

ALESSANDRO PINATO
Cooling & Heating Product Manager, Swegon

FABIO POLO
Cooling & Heating Product Management Manager, Swegon

Reducing our carbon footprint is currently on everyone's mind, but with the energy prices soaring, it's easy to get narrowly focused on kilowatt hours, and lose sight on other aspects of sustainability. For instance, there is a revolution ongoing when it comes to refrigerants, where EU regulations on synthetic refrigerants like CFC, HCFC and HFC have tightened, severely restricting or even banning their use. And a further tightening is underway with the update of the F-gas regulation which is currently under discussion. Within this scenario one of the earliest natural refrigerants ever tried – propane – has sailed up to become a smart replacement choice in many present and future HVAC applications. However, the knowledge in the business on using propane as a refrigerant is still scarce, and a number of myths emerging. Let us go through – and bust – some of them.

Myth: "Propane is not a refrigerant, it's a hydrocarbon and thus only good for burning."

This is definitely not true. Propane was one of the first candidates for refrigerants, has a long history, and is well-tested. It has excellent thermodynamic properties and can be used in a wide variety of HVAC appliances. And not to forget – it is smarted to use it in small quantity as a refrigerant in a heat pump instead of burning it in large quantity in a boiler (with 3 kg of propane you can heat a small building for a day by burning it in a boiler, or you can heat the building for 5 years if you use it as a refrigerant in a heat pump).

Myth: "The use of propane as a refrigerant is just a temporary fad pushed by the environmental movement."

In fact, Swegon now sees propane as a long-term solution that will not be displaced in the foreseeable future. Propane is already being used today as a refrigerant, for example, in supermarket display cabinets, domestic equipment and portable AC (have you ever check what is the refrigerant used in the refrigerator you have in your kitchen?). Its share is also growing fast in process and commercial comfort applications, and due to ongoing EU regulation updates, it will become widely used in the HVAC market.

Myth: "The use of propane as a refrigerant, results in low efficiency heat pumps"

Propane units' inefficiency has been one of the first myths to rise in the sector. However, associating the efficiency of a heat pump solely with the refrigerant is incorrect, it is a shortcut that can lead to mistakes. The unit's resulting efficiency derives from many factors: the product design, the available technologies and it is often a trade-off between different project targets such as compactness, silence, cost, etc. Therefore, comparing the unit overall figures, and associate the differences to the refrigerants only, is a source of gross simplifications.

That said, it is a fact that there are already propane heat pump ranges on the market with efficiencies comparable or even better than older product ranges with HFC refrigerants such as R32 and R454B.

Myth: "As natural refrigerant, CO_2 is better than propane."

CO_2 is definitely a good refrigerant with a Global Warming Potential of just 1. It is already in use for cooling in many commercial refrigeration applications where it has replaced some synthetic refrigerants. Nevertheless, if we look to heating and air conditioning appliances

Properties of refrigerants:

	R410A	R134a	R513A	HFO 1234ze	R454B	R32	R 290
GWP	1924	1300	573	<1	467	677	3
ASHRAE class	A1	A1	A1	A2L	A2L	A2L	A3
Flammability	No	No	No	Mildly	Mildly	Mildly	Flammable
Toxicity	No	No	No	No	No	No	No
PED group	2	2	2	1	1	1	1
Composition	Blend of HFC	HFC	Blend (HFC + HFO)	HFO	Blend (HFC + HFO)	HFC	HC
Glide	Almost zero	zero	zero	zero	Low glide	zero	zero
Suitable for W/W MT HP (LwT --> 45°C)	Yes	Yes	Yes	Yes	Yes	Yes	Yes
Suitable for W/W HT HP (LwT --> 60°C)	Yes	Yes	Yes	Yes	No	No	Yes
Suitable for A/W MT HP (LwT --> 45°C)	Yes	Yes	Yes	No	Yes	Yes	Yes
Suitable for A/W MT HP (LwT --> 60°C)	Yes	No	No	No	No	Almost	Yes

(*) GWP (AR5) according to IPCC V time horizon 100 years

then it has some significant drawbacks (extremely high operating pressure with poor efficiency) that makes it suitable only in high temperature lift applications.

Myth: "Propane is too risky to use."

To be fair, all refrigerants have drawbacks. Leaving aside the environmental effects of some synthetic refrigerants, even if we focus on natural refrigerants only, we can see that CO_2-based units need pressures of up to 90 bar, and ammonia-based units come with their own toxicity risks. In comparison to that, propane is relatively harmless. Yes, it is certainly flammable. But this can be properly addressed with guidelines and best practice instructions (think about how you properly deal with fuel pumps at a gas station for instance that is classified as an explosive area). And chances are that you already have propane in your home, happily burning it away on weekends: a cylinder for a propane-driven barbecue typically contains 5–10 times the amount of propane than what would be used in a chiller or heat pump for your residence. In HVAC applications, the propane is confined in a safe, closed system with monitoring of leakages and with component designs that prohibit fire or explosions. And as we mentioned above, you probably already have propane circulating in your refrigerator without having given it a second thought.

Myth: "The introduction of a new refrigerant in this phase could slow down the necessary transition from boilers to heat pumps."

It is true that propane cannot be used in all heating systems, such as rooftop units or direct expansion systems such as VRF / VRV. So, for specific applications we will still need synthetic refrigerants. But for most other heating systems propane is an excellent choice and will help support the boiler-to-heat pump transition. In particular, propane will be a key enabler in the European Commission Renovation Wave initiative, which will speed up the replacement of existing boilers with high temperature heat pumps. In newer buildings, the distribution system often works at low to medium temperatures, but radiators in older buildings often need water with higher temperature (60–75°C). In these buildings, heat pumps using propane, will be a perfect solution, thanks to their capacity to deliver water as hot as that from boilers. Heat pumps using synthetic refrigerants are not capable of this unless you choose more expensive cascade systems.

Myth: "This is just a refrigerants business. Next year there will be a new next gen refrigerant candidate in place of propane."

Over the last few years there has been a rush in the refrigerant business, with many chemical companies investing heavily into finding "the perfect refrigerant". So far, none have proven their worth. Furthermore, even existing synthetic refrigerants are increasingly being subjected to regulation revisions trying to mitigate their greenhouse effect. With the latest, low GWP synthetic refrigerant generation (HFO, hydrofluoroolefin), there are growing concerns about possible harmful compounds generated by decomposition in the atmosphere. The natural refrigerant propane has none of these problems. It is a mature solution, requiring no further long-running development work. It is already present in nature, and it is ready to use.

In short, propane is here to stay. ■

ISH 2023 – *Solutions for a sustainable future*

What kind of energy do we use for heating, what ensures hygienically clean air and how much water do we need? Against the background of scarce energy resources, pandemics and climate change, these questions are more relevant than ever before. Exhibitors will present solutions at the ISH from 13 to 17 March 2023 in Frankfurt am Main.

STEFANIE WEITZ
Director ISH Brand Management.
Tel.: +49 69 75 75-5188
stefanie.weitz@messefrankfurt.com
Messe Frankfurt Exhibition GmbH
Ludwig-Erhard-Anlage 1
60327 Frankfurt am Main
www.messefrankfurt.com

ISH
13.– 17. 3. 2023
Frankfurt am Main

In 2022, many related industries started again with trade fair presentations, showing how important and necessary personal exchange still is. ISH, the leading innovation show for Heating, Ventilation and Air Conditioning (HVAC) and Water will be back in March 2023.

We asked Stefan Seitz, Director ISH Brand Management ISH, five questions about the relevance of the upcoming international industry meeting place.

Question #1. The time until ISH 2023 is passing quickly. With what expectations are you looking forward to the upcoming event?

Stefan Seitz: Anticipatory, very attentive and excited - I think that sums it up quite well. There was an ISH digital in 2021, but the personal encounter was simply missing. In this respect, I am very much looking forward to visiting our exhibitors at their stands, discovering the innovations for a sustainable future for myself and entering in direct exchange about them. After all, the themes of the ISH absolutely hit the nerve of the times. At the leading international sanitary and HVAC event, national and international companies present the industry's marketable solutions for water, heating and air. But I am also realistic and know that we are currently influenced by external factors, whether geopolitical or economic. Therefore, I am at the moment very focused on how the situation will develop further, but my basic attitude is of course optimistic.

Question #2. What topics will be in focus?

Stefan Seitz: The motto of ISH 2023 is "Solutions for the future". Everything revolves around innovations that contribute to the achievement of climate protection goals and enable the responsible and efficient use of available resources. Sustainability is the very big topic. It is the connecting element between ISH Energy, consisting of heating, air-conditioning and ventilation, and ISH Water. In the Energy segment, this means that in the future we will have to become less dependent on fossil fuels and quickly increase the share of renewable energies. However, sustainable use and security of supply is also necessary with regard to our drinking water. The last extremely dry and hot summers have clearly shown this to us.

In the area of Water, however, sustainability also refers to the materials used - both in production and installation. It includes an efficient hot water supply and extends to durable concepts for bathroom design. In the future, bathrooms should be designed for all generations and needs.

Question #3. What kind of ISH can we expect in 2023? Will the market leaders be there?

Stefan Seitz: The last regular ISH took place in 2019. A lot has changed since then. This concerns both the dynamics of the industry and the trade fair as a marketing instrument. Corona, geopolitical developments and the partly gloomy economic forecasts in submarkets of the ISH have led to the participation decision being made at much shorter notice by both visitors and exhibitors. For this reason, the planning work is still in progress and new enquiries are coming in daily. In parallel, it leads to individual exhibitors deciding at short notice to withdraw from their participation in ISH.

Unfortunately, this is currently the case, but only in the Water sector and mostly with national manufacturers. The main reasons given by the companies are the declining willingness to invest in the sanitation market, higher energy prices and the general global political situation. Nevertheless, they all continue to emphasize the importance of the ISH as the leading trade fair for the sector and that the decisions were very difficult for them. This development is of course very regrettable.

Fortunately, the majority of the leading companies are still present in all areas of ISH. Currently, 1,250 companies have already signed their contracts. This corresponds to 70% compared to 2019. In addition, there are 320 companies that currently have a placement proposal or will receive one in the next few days. Therefore, it is currently difficult to estimate the final number of exhibiting companies.

Today, I can say that we have the support of the majority of all ISH exhibitors. At the moment, the reporting will focus on which cancellations have to be announced. However, it is worthwhile to look at who will be there. Because that is still the majority of companies, and they are looking forward to ISH in March 2023.

The ISH Contactor at www.ish.messefrankfurt.com/contactor provides a daily update on all exhibitors taking part.

Question #4. What will ISH 2023 look like - what is new and what themes can be seen where?

Stefan Seitz: In the ISH Energy segment, we are placing an even stronger focus on the technologies of the future in the heating market. Electrification is progressing strongly in this segment. That is why we are concentrating suppliers of heat pumps, home energy management systems and energy storage, as well as manufacturers of complete heating systems, in Hall 12, whereas in Hall 11.0 we are focusing on suppliers of wood heating, waste gas technology as well as heat generation and heat transfer. In Hall 10, visitors will continue to find everything to do with home and building automation, energy management, together with monitoring, control and regulation technology, as well as testing equipment. As at the previous event, the focus in Hall 9 will be on solutions for heat distribution and in Hall 8 on refrigeration, air-conditioning and ventilation technology.

The Eastern part of the fair ground is all about Water. The absolute novelty here is Hall 5, where the ISH is one of the first events to feature the newly built hall with installation technology and software. Installation technology will also be on show in Halls 4 and 6. Tools and mounting materials are also to be found in Hall 6. The Bathroom Experience is at home in Halls 2, 3, 4 and the Forum. The International Sourcing section will be located in Hall 1. Thus, the unique, practical and international range of products for the sanitation, heating, ventilation and air-conditioning sector in March 2023 invites visitors to discover solutions for the most important questions of our time.

Question #5. How digitally is the industry positioned for March 2023?

Stefan Seitz: At the last ISH 2021, the industry came together purely digitally. That was a valuable experience, but it also showed that face-to-face meetings are indispensable. Messe Frankfurt has meanwhile tried out many different event formats. The learning from this is that digital offerings are a perfect complement to the physical event. That is why we are accompanying ISH 2023 in Frankfurt with a digital platform. Parallel to the industry meeting point in Frankfurt, we will provide the ISH Digital Extension. It will then be available for use for one week longer, until 24 March 2023. This means that everyone can make the most of their time at the fair and, for example, view missed programme items afterwards. Another advantage is the possibility to make targeted contact. Using AI-supported matchmaking, suitable business partners can be found and contacted at the fair or digitally. ■

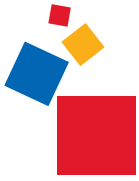

For more information, please visit our website at: www.messefrankfurt.com

Tomorrow starts today

Revolutionise your business with LG THERMA V

LG | Business Solutions

Did you know...

Annual heat pumps sales in Europe are set to increase x2 by 2025 and x5 after 2029

REPowerEU Plan EUR-Lex - 52022DC0230 - EN - EUR-Lex (europa.eu)

253 million dwellings across Europe will require an energy efficiency upgrade

BRG Products Market research https://www.brggroup.com/expertise/markets/brg-building-solutions/

LG Air Solution

LG Air Solution is a full scope heat pump supplier, with its comprehensive air-to-water heat pump line-up suitable to almost any building type and conforming to the EU regulation requirements.

LG AIR-TO-WATER PUMPS ARE...

- Energy efficient for cost reduction
- Easy to install, space-saving
- Regulation compliant
- Compatible with renewable energy systems (solar + storage)

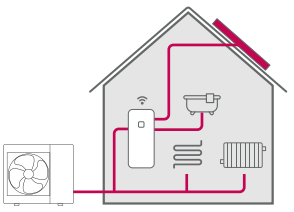

THERMA V MONOBLOC

THERMA V Monobloc S is a fully packaged AWHP that combines all functions in one outdoor unit allowing for a quick, easy and replicable installation with no refrigerant work.

Easily connectable with a pre-existing tank, Monobloc S is a perfect choice for smaller properties with the lack of living space.

Range capacity: 5 - 16 kW

Reliable heating at temperatures as low as -25°C

Operates at 100% capacity down to -15C

Low noise level (57 dB(A)) allowing high installation location flexibility

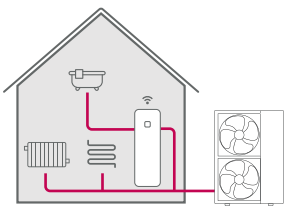

THERMA V HYDROSPLIT

THERMA V Hydrosplit is an AWHP that connects an indoor (IWT or Hydrobox) and outdoor unit through water piping, reducing the risk of indoor refrigerant leakage.

This all-in-one solution's hydronic and domestic hot water components are prewired, making it suitable for both renovation and new builds projects.

Range capacity: 12 - 16 kW

Provides reliable heating at temperatures as low as -25°C

Indoor Climate Systems Design in Times of Uncertainty

On November 11, 2022, Atze Boerstra was officially installed as the Chair of Building Services Innovation at the faculty of Architecture and the Built Environment at the Delft University of Technology. Below a short summary of the main statement that he made during his inaugural speech.

When indoor climate systems were first invented (think e.g. of air-conditioning) they were first and for all designed with end-user needs (specifically comfort needs) in mind. One could call this a human-centred approach. Since the 70's also energy use determines how HVAC systems are innovated. But generally speaking, anno 2022 we still don't really design systems with overall environmental impact in mind. Yes, factories that produce e.g. air handling units or air filters become more sustainable. And yes, systems nowadays are sometimes also designed with embodied energy of components in mind. And yes, recycled steel is part of the story when you talk about how indoor climate systems are built up. But how about the hidden landscape & ecological effects related to mining of the other raw materials that are used in different HVAC system components and the electronic components in their control systems? Think e.g. of critical materials or so called 'rare earth materials' (like for example those used in permanent magnets for motors and fans).

Decarbonizing the built environment implies that existing non-efficient heating, cooling and ventilation systems are replaced with state-of-the-art energy-efficient systems. But are we sure the materials that are used for this energy transition are available in plentiful enough amount and that these materials don't come with a lot of hidden environmental costs that could be avoided e.g. by designing future systems more with circularity in mind. What we do need in this context is to adopt a more humanity-centred design approach instead of the human-centred design approach as proposed e.g. by Don Norman of the University of California.

Further reading: Moving from Humans to Humanity (linkedin.com) ■

Atze Boerstra during his inaugural speech.

Lada Hensen Centnerová (Vice President of REHVA) and Jan Hensen (TU-Eindhoven) congratulates Atze Boerstra on behalf of the REHVA Board.

Atze Boerstra at the morning symposium on Building Services Innovation.

The REHVA Brussels Summit 2022

A brief summary of the REHVA Brussels Summit 2022 which took place in Brussels and online on Monday 14 and Tuesday 15 of November 2022.

The first day of the Summit, Monday 14th of November, was dedicated to REHVA Strategic activities with meetings of the standing committees (Publishing and Marketing Committee PMC, Education and Training Committee, Technology and Research Committee, and Supporters Committee).

New Chairs elected

During the Education and Training Committee, the members elected a new chair, REHVA Vice-President **Ivo Martinac** [2022–2024]. The members of the Supporters Committee elected REHVA Vice-President **Kemal Gani Bayraktar** [2022–2024] as chair. The chairs and co-chairs presented some reports of activities, and the members of the Committees had the opportunity to share their ideas and vision for the future of the organisation.

IVO MARTINAC
Education and Training Committee Chair (2022–2024), REHVA Vice-President

KEMAL GANI BAYRAKTAR
Supporters Committee Chair (2022–2024), REHVA Vice-President

REHVA Journal publishing plan for 2023

The members of the Editorial Board of the REHVA Journal also met. They discussed the upcoming issues for 2023 and drafted a publication plan for the upcoming year with themes including: Healthy built environment and energy security, Ventilation Commissioning, Transformation of educational building services in Europe in the context of the 21st century, Decarbonisation, EPBD Review, Ventilation, Energy Security. The publication plan is available on the REHVA Website. **Any of these themes attract you? Contact us to publish your** ad in the REHVA Journal.

The REHVA Dinner took place on Monday evening, where two big announcements were made:

#1 CLIMA 2025: the 15th REHVA HVAC World Congress in Italy, is official!

It is now official, Italy will host CLIMA World Congress 2025. During the REHVA Brussels Summit 2022, REHVA President Catalin Lungu and AiCARR President Filippo Busato signed the official agreement that entrusts AiCARR with the organization of this great event, in partnership with REHVA and LSWR Group. See you in Milan, in May 2025.

#2 Eurovent Certita Certification sponsoring REHVA Student Competition

During the REHVA Brussels Summit 2022, REHVA President Catalin Lungu and Sylvain Courtey, President of Eurovent Certita Certification, signed the agreement for the sponsorship of the REHVA Student Competition and the HVAC World Student Competition for the next three years.

REHVA is looking forward to working together toward our common goals and cooperating on these events.■

REHVA Brussels Summit Report: Policy Conference on Zero Emission Buildings & REPowerEU

JASPER VERMAUT
EU Policy & Project Officer at REHVA

On 15 November REHVA had the pleasure to host its annual Policy Conference during the Brussels Summit 2022 with a focus on two interlinked topics that preoccupied EU policy discussions for the building industry in the past year: **Healthy Zero-Emission Buildings** and **REPowerEU: Phase-out of fossil fuels in heating and cooling**. In this article you can read a summary of the discussions in both sessions with speakers from the European Commission, Parliament, industry stakeholders and REHVA experts. You can find the recordings and slide decks of the presentations on the REHVA website: https://www.rehva.eu/events/details/rehva-brussels-summit-2022

Morning Session on Healthy Zero-Emission Buildings

The morning session was opened and moderated by REHVA President **Catalin Lungu** who stressed that REHVA's role in the EU's policy area, as engineers & practitioners, is to provide our expertise on the technical and feasible solutions for the reduction in energy consumption and CO_2-emissions in buildings which is why the REHVA Policy Conference brought together a mix of experts.

Cristian Bușoi, MEP and Chair of the Industry, Research & Energy Committee (ITRE), highlighted in his keynote speech the priority areas for the ongoing negotiations within ITRE on the EPBD and links with other dossiers such as the revisions of the Renewable Energy (RED) and Energy Efficiency (EED) Directives. In particular, the energy efficiency potential of technical buildings should be optimally supported through the EPBD, complemented by the other Directives.

Heating and cooling play a central role in the energy transition and especially by increasing the share of renewables, which is related to the negotiations on the revision of RED II which are being finalised this month (*November 2022*) in the trilogue meetings between the Council and Parliament.

As a last point Mr. Bușoi highlighted the importance of district heating which ITRE is trying to strengthen

REHVA President Catalin Lungu opening the REHVA Brussels Summit: Policy Conference.

further in the Fit for 55 negotiations, as this allows Member States to best apply cost-effective solutions for the decarbonisation of the building stock with the support of their local & regional authorities who can develop targeted strategies. District heating greatly improves the flexibility for Member States to implement measures for further boosting renovations.

The keynote was followed by a presentation from **Paula Rey Garcia**, Deputy-Head of Unit Buildings & Construction at DG ENER in the European Commission, who gave an overview of the Commission's proposal and the ongoing negotiations. She stated the EPBD revision has to be seen in the framework of the Renovation Wave strategy and the Fit for 55-package, which aim to directly decrease GHG emissions by 2030 and set a long-term vision for a climate neutral building stock by 2050.

On **figure** below, you can see how Ms. Garcia showed that buildings with an EPC class of F or G consume 3 to 14 times as much energy as buildings with an EPC class A, depending on the Member State. This demonstrates that a lot of progress can be made in reducing energy consumption by tackling the worst performing buildings and explains why this is a priority area for the EPBD. The EPBD does this through the introduction of Minimum Energy Performance Standards (MEPS) that put the obligation on Member States to progressively improve their worst performing buildings and ensure that by 2033 all F & G class building have a better energy performance.[**1**]

The Council has adopted its general approach for the EPBD[**2**] negotiations on 25 October, where some parts of the Commission's proposal were preserved but Ms. Garcia stated that other parts were weakened to some extent (in particular the ZEB requirements). Currently there is a small delay within the Parliament to agree on their final position, which we now expect to be finalised in Q1 2023, while the trilogue negotiations between the institutions on the EPBD are expected to be finished in Q2 2023. There has been a push from some members in the Parliament to delay it further, but Commission has strong doubts about this given the central role of the EPBD in the ongoing energy crisis.

Jarek Kurnitski, Professor at TalTech University and Chair of the REHVA Technology & Research Committee, gave a presentation about the technical implementation of IEQ and primary energy aspects in ZEB within the EPBD recast as how it's currently worded in the Council's general approach. Articles 7 & 8 in the EPBD mentioned that Member States shall address healthy indoor climate requirements for new buildings & renovations, the question we can raise then is how serious the Member States will take these requirements as there will be different approaches and ambitions. The most significant change for IAQ requirements can be found in Article 11 which states that non-residential ZEBs should be equipped measuring & control devices for the regulation of IAQ.[**3**]

There are problems with the technical implementation of the calculation of energy performance of buildings however, as they're currently worded in the EPBD recast. There is a big difference when using *Total* Primary Energy (PE) for the calculation or *Non-renewable*. This is demonstrated when we compare the energy performance calculation between district heating and a condensed gas boiler. When calculating

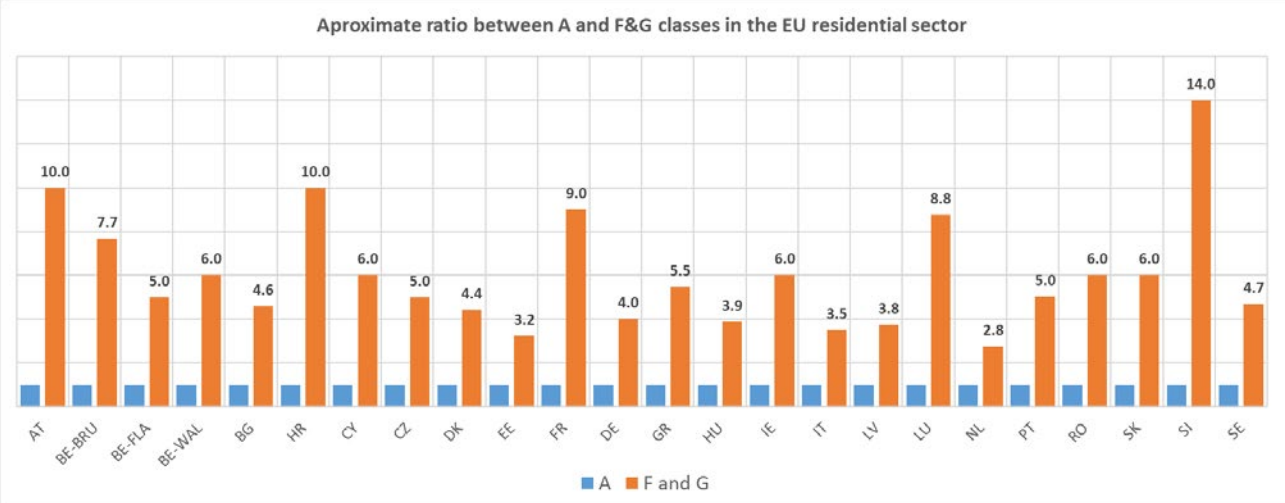

Rescaling of energy labelling for hydronic space heaters. (From the presentation by Paula Rey Garcia)

it with *total* PE, and excluding ambient heat and on-site PV, the gas boiler comes out as more efficient than district heating. When using *non-renewable* PE as the basis for the calculation, district heating is a lot more efficient.[**4**]

Benjamin Haas, Regulatory Affairs Director at Engie, talked about the implementation of EU measures for buildings in the French regulation, both in terms of the calculation of Primary Energy Consumption and limiting carbon emissions in LCA. In 2022 the RE2020 entered into force in France, which lays down new sustainable regulations for buildings. The RE2020 goes beyond the current EPBD as it includes LCA analysis for CO_2-emissions which requires a more holistic mindset. For example, from an LCA perspective, it's not enough to just ban fossil fuel boilers but also ensure that any indirect fossil fuel use through the electricity grid and district heating are phased out.

The final presentation of the morning session was given by **Ursula Hartenberger**, Secretary General of the Climate Positive Europe Alliance, on the role of green building certification. Ms. Hartenberger presented a framework reaching carbon neutral buildings & sites which exists out of two core elements that ensures more clarity and transparency for market actors. The first being a definition for carbon neutrality, while the second element explains what it means to have an effective approach for the reduction of GHG emissions.

Afternoon session on REPowerEU

In the afternoon the Policy Conference focused more on the REPowerEU ambitions and started with a statement by **Andrew Murphy**, Head of Buildings & Industry at ECOS, on demand reduction within the building sector. There needs to be a fundamental change in how we heat our buildings on all levels. For this to happen the European and national policies need to be closely aligned. On European level we have two big tools for reducing gas demand: the Ecodesign requirements and the EPBD. Ecodesign has proved very effective to reduce our dependency on fossil fuels in a large range of products, which is why the Commission has proposed to broaden it to a larger part of our economy and looks to phase out stand-alone fossil fuel boilers by 2029 through Ecodesign.[**5**]

Philippe Riviere, Policy Officer at DG ENER in the Buildings & Products unit, went deeper into the role of Ecodesign & energy labelling for HVAC products. On one hand we have Ecodesign requirements that act

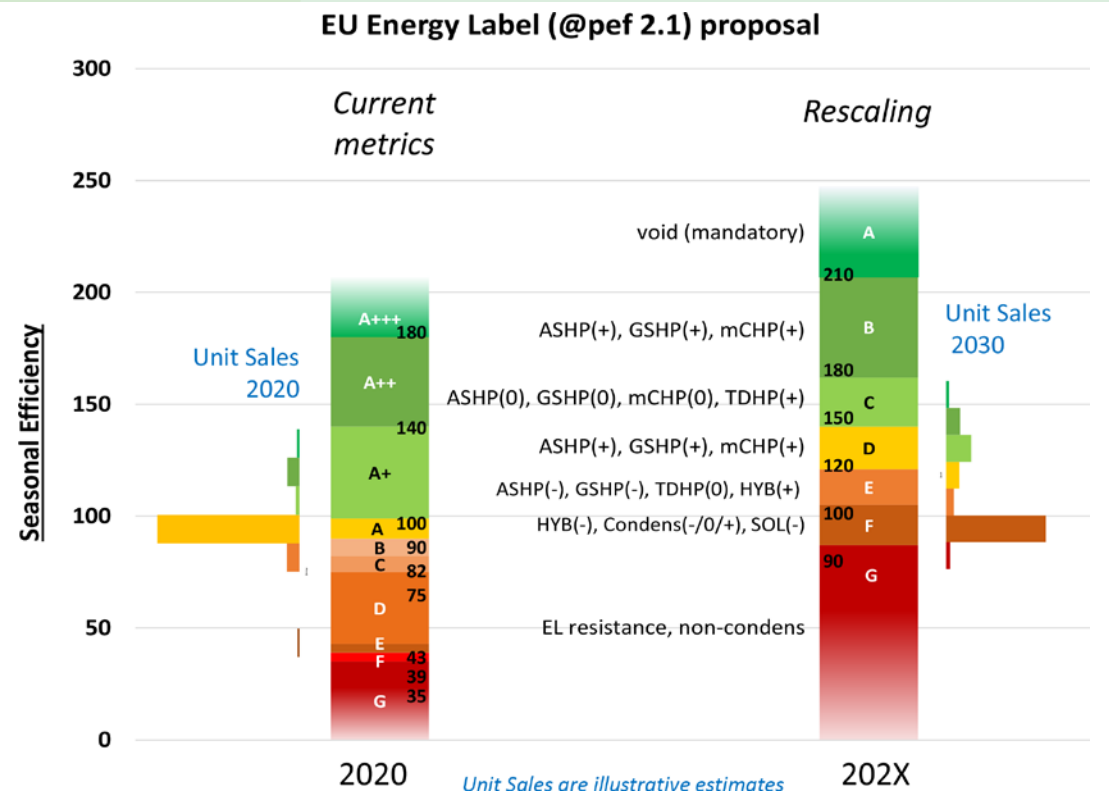

Energy consumption comparison between EPC Class A buildings and Class F & G buildings per Member State. (From the presentation by Philippe Riviere)

as a *push element* in the market to ensure minimum requirements on the lowest efficiency products on the market. On the other side, energy labelling acts as a *pull element* that aims to show which are the worst and best products on the market to drive up the sales of the best performing.

Currently energy labelling for both local/room heating and hydronic space heaters are being revised. For local/room heating there were 5 different scales in place depending on the product to improve efficiency within the products themselves. Now the Commission has proposed a single scale for all local/room heating products together to be able to better compare the efficiency between different energy products so that the most efficient product gets stronger incentives. This would, for example, allow to better compare the efficiency of heat pumps to gas boilers. The second revision focuses on hydronic space heaters for a rescaling of energy labelling for different energy products. With the current scaling condensing gas boilers have an energy label A while with the rescaling this will drop to F, while both ASHP & GSHP will have label B.

The last presentation of the day was by **Tomasz Cholewa**, chair of the REHVA Task Force on Building Decarbonisation, and presented on how to take on a holistic approach for deep energy renovations. The focus of renovations often lays on the building envelope, while the modernisation of HVAC systems can often bring bigger gains and should be a first step. This modernisation process for all HVAC systems is explained in REHVA Guidebook 32.[**6**] As a second step to complement the most efficient HVAC systems, the buildings should increase the use of RES.

The REHVA Policy Conference was closed by a panel discussion on the feasibility and readiness to ban fossil fuels in heating and cooling. The panel was formed by Philippe Riviere, Tomasz Cholewa, **Celine Carré** (President EuroACE), **Ilari Aho** (VP Sustainability & Regulatory Affairs Uponor), **Henk Kranenberg** (Senior Manager Daikin Europe), **Christian Schauer** (Director Water Competence Centre, Viega). We welcome you to watch the recording of the discussion: https://www.rehva.eu/events/details/rehva-brussels-summit-2022 ■

References

1 See Article 9 in the Commission Proposal: https://eur-lex.europa.eu/legal-content/EN/TXT/?uri=celex%3A52021PC0802.

2 Read more about the Council General Approach: https://www.rehva.eu/news/article/council-agrees-on-general-approach-for-the-epbd.

3 In the Commission's original proposal this requirement was put on all ZEBs, the Council proposes to limit this to only non-residential. See Article 11 in Council General Approach: https://data.consilium.europa.eu/doc/document/ST-13280-2022-INIT/en/pdf.

4 Read more about the technical comments on primary energy factor within the EPBD in the article by Dick van Dijk and Jarek Kurnitski for the REHVA Journal 04/2022: https://www.rehva.eu/rehva-journal/chapter/the-epbd-recast-how-to-come-to-a-transparent-and-fair-zeb-definition.

5 Find more information about the proposal for a Ecodesign for Sustainable Products Regulation, released on 30 March 2022: https://ec.europa.eu/info/energy-climate-change-environment/standards-tools-and-labels/products-labelling-rules-and-requirements/sustainable-products/ecodesign-sustainable-products_en.

6 Find more information about this Guidebook: https://www.rehva.eu/eshop/detail/energy-efficient-renovation-of-existing-buildings-for-hvac-professionals.

For a healthy and comfortable room climate.

Room units from Belimo

The new room units (sensors and room operating units) are the perfect addition to the existing product range. With the expansion of the product range for visible areas of the room, Belimo offers architects an aesthetic and timeless design. Installers appreciate quick installation and system integrators value easy commissioning with a smartphone. End customers enjoy not only a comfortable and healthy room climate but also the intuitive operation.

- Aesthetic, timeless design
- Room operating units with ePaper touch display
- Fast installation thanks to spring-loaded terminal blocks and snap-on cover
- Parametrisation and diagnosis of active devices via Belimo Assistant App

reddot winner 2022

Discover the advantages
www.belimo.com

BELIMO Automation AG
info@belimo.ch, www.belimo.com

BELIMO

The Seven Essentials of Healthy Indoor Air

What is important in building, renovating or operating an HVAC system to ensure healthy indoor air? Belimo identified seven essential factors for ensuring healthy indoor air in buildings.

1. Continuous and Reliable Measurement, Display and Monitoring of Indoor Air Quality

Ideally, air humidity, CO_2 content or VOC concentration are measured by sensors for the monitoring of air quality. This is because only measured variables can be controlled. From today's point of view, both the measurement and the display of these values should represent the minimum standard for indoor air quality measurement.

HUMIDITY

It is important that relative humidity indoors is held between 40–60%. Dry air droplets from an infected person speaking or sneezing easily evaporate and the contained virus travels further in the room as a light aerosol. If the humidity is higher, droplets do not evaporate as quickly and fall to the ground in a shorter distance. Thus, many bacteria and viruses are considerably more contagious in dry air conditions, which can dehydrate mucous membranes and weaken the immune system.

CO_2

CO_2 concentration of more than 1,000 ppm (parts per million) decreases the brain's ability to concentrate; starting at 2,000 ppm and higher, it can lead to fatigue or even headaches. CO_2 levels in indoor air is an excellent indicator of potential bio-contamination, an example is the COVID-19 viruses. If the CO_2 value is high due to increased occupancy and limited air exchange, high potential risk from infectious aerosols could result.

VOCS

Volatile Organic Compounds (VOCs) are organic compounds that originate from many different sources, including perfume, paint, printers, carpeting and building materials. Even low concentrations of VOCs can irritate the eyes, nose, or throat and indicate insufficient fresh air intake.

It is essential to measure these variables using suitable sensors so that appropriate measures can be implemented, for example, ventilation, air purification or humidification.

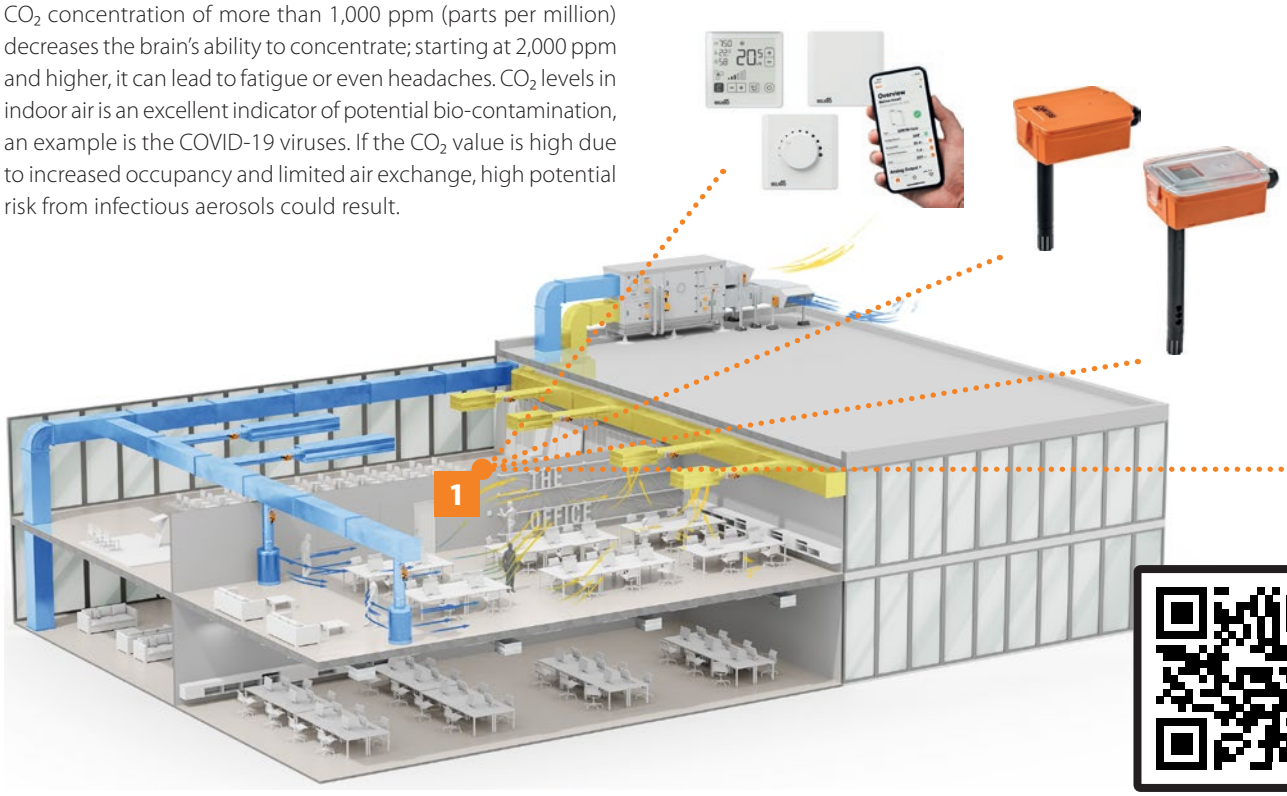

Learn more about Belimo's 7 essentials of healthy indoor air:
https://www.belimo.com/ch/en_GB/indoor-air-quality/7-essentials-iaq

Scan the QR code

Please send information of your event to Ms Nicoll Marucciova nm@rehva.eu

Exhibitions, Conferences and Seminars in 2023

February – March 2023		
4 – 8 Feb 2023	2023 ASHRAE Winter Conference (ashrae.org)	Atlanta, Georgia, USA
28 Feb – 3 Mar 2023	World Sustainable Energy days (wsed.at) [see more on page 81]	Wels, Austria
6 – 8 Mar 2023	HVAC Cold Climate Conference 2023 (ashrae.org)	Anchorage, Alaska
13 – 17 Mar 2023	ISH 2023 (ish.messefrankfurt.com)	Frankfurt am Main, Germany
14 – 16 Mar 2023	ACREX 2023 (acrex.in)	Mumbai, India
May 2023		
11 – 12 May 2023	REHVA Annual Meeting (rehva.eu)	Brussels, Belgium
18 – 19 May 2023	AIVC Workshop: "Towards high quality, low-carbon ventilation in airtight buildings" (iaqvec2023.org)	Tokyo, Japan
20 – 23 May 2023	IAQVEC 2023 (iaqvec2023.org)	Tokyo, Japan
June 2023		
11-14 June 2023	Healthy Buildings 2023 (isiaq.org)	Aachen, Germany
20-22 June 2023	European Sustainable Energy Week (europa.eu)	Brussels, Belgium
October 2023		
4 – 5 October 2023	43rd AIVC conference (aivc.org)	Copenhagen, Denmark

Due to the COVID-19 circumstances, the dates of events might change. Please follow the event's official website.

The World Sustainable Energy Days 2023

"Energy transition = energy security!" is the focus of the next World Sustainable Energy Days (WSED) in Wels/Austria from 28 Feb. – 3 March 2023.

The price crisis, multiplying signs of climate change, and threats to energy security urge us to act like never before. REPowerEU reflects this urgency and provides new momentum for the energy transition.

In 2023, the WSED show the critical role of the energy transition in securing our clean energy future and concrete policies, technologies and markets to get us there.

A comprehensive package

The WSED are a leading annual conference on the energy transition and climate neutrality with over 650 participants from more than 60 countries each year. They offer 6 dedicated conferences, more than 80 international speakers, a leading sustainable energy tradeshow, and hands-on experience through peer-to-peer exchange. Meet the entire energy transition world and enjoy Austrian hospitality!

Conferences and events:

- Industrial Energy Efficiency Conference
- Energy Efficiency Policy Conference
- European Pellet Conference
- Poster Presentation
- Tradeshow
- Innovation Workshops
- Smart E-Mobility Conference
- Young Energy Researchers Conference

World Sustainable Energy Days 2023

Upper Austria – a leader in the clean energy transition

The WSED are organised by the OÖ Energiesparverband, the energy agency of Upper Austria. Upper Austria, one of Austria's nine regions, is well on its way in the clean energy transition. Through significant increases in energy efficiency and renewable energy, greenhouse gas emissions from buildings were reduced by 39% in 10 years. 60% of all space heating and 33% of the primary energy in the region already come from renewables. Over 2.8 billion Euro are invested annually in the energy transition.

Mark your calendar for 28 Feb. – 3 March 2023 and join REHVA and the worldwide energy transition community at the World Sustainable Energy Days!

Professor Dr. Robert Gavriliuc in Memoriam

The REHVA Family very sadly announces the untimely passing of Professor Dr. Robert Gavriliuc, on December 1, 2022.

Born on June 20, 1959, Robert Gavriliuc graduated in 1984 at the Technical University of Civil Engineering of Bucharest (UTCB) as mechanical engineer, and got his PhD diploma in 1996. He won two post-doctoral scholarships at the Technical University of Karlsruhe (Germany) and the Oak Ridge National Laboratory (USA). In 2005 he became a full professor at UTCB.

As a professor at the Technical University for Civil Engineering from Bucharest (Faculty of Building Services Engineering), he made a remarkable contribution to the Romanian school for mechanical engineering, especially in the field of heat pumps and geothermal energy, being a prominent member of the thermodynamic academic community.

Robert Gavriliuc was president of the Romanian Geoexchange Society and active member of the Romanian Professional Associations AIIR & AGFR. He was also a member of ASHRAE and contributed substantially to EGEC activities.

Within REHVA, Robert Gavriliuc made numerous and valuable contributions, especially in the Education and Training Committee. In recognition, in 2012 Robert was granted the status of REHVA fellow and in May 2022, he received the REHVA professional award for Education.

In his private life Robert was a very devoted father and husband, and also a kind and generous friend to many of us. We express with sorrowful souls our heartfelt condolences to his family, friends and AIIR's colleagues.

Dr. Catalin Lungu, REHVA President

REHVA
Federation of European Heating, Ventilation and Air Conditioning Associations

MEMBERS

ATIC vzw–asbl – Belgium
www.atic.be

BAOVK – Bulgaria
www.baovk.bg

STP – Czech Republic
www.stpcr.cz

DANVAK – Denmark
www.danvak.dk

EKVU – Estonia
www.ekvy.ee

FINVAC – Finland
www.finvac.org

AICVF – France
www.aicvf.org

VDI–e.V. – Germany
www.vdi.de

ÉTÉ – Hungary
www.eptud.org

MMK – Hungary
www.mmk.hu

AiCARR – Italy
www.aicarr.org

AHGWTEL/LATVAC – Latvia
www.lsgutis.lv

LITES – Lithuania
www.listia.lt

AIIRM – Republic of Moldova
www.aiirm.md

TVVL – The Netherlands
www.tvvl.nl

NEMITEK – Norway
www.nemitek.no

PZITS – Poland
www.pzits.pl

ORDEM DOS ENGENHEIROS – Portugal
www.ordemengenheiros.pt

AFCR – Romania
www.criofrig.ro

AGFR – Romania
www.agfro.ro

AIIR – Romania
www.aiiro.ro

KGH c/o SMEITS – Serbia
www.smeits.rs

SSTP – Slovakia
www.sstp.sk

SITHOK – Slovenia
https://web.fs.uni-lj.si/sithok/

ATECYR – Spain
www.atecyr.org

SWEDVAC – Sweden
www.energi-miljo.se

DIE PLANER – Switzerland
www.die-planer.ch

TTMD – Turkey
www.ttmd.org.tr

CIBSE – United Kingdom
www.cibse.org

Network of 26 European HVAC Associations joining 120 000 professionals

REHVA Office: Rue Washington 40, 1050 Brussels - Belgium • Tel: + 32 2 514 11 71 - info@rehva.eu - www.rehva.eu

REHVA
Federation of European Heating, Ventilation and Air Conditioning Associations

SUPPORTERS

Leaders in Building Services

Daikin Europe – Belgium
www.daikin.eu

EPEE – Belgium
www.epeeglobal.org

EVIA – Belgium
www.evia.eu

Velux – Denmark
www.velux.com

Granlund – Finland
www.granlund.fi

Halton – Finland
www.halton.com

Uponor – Finland
www.uponor.com

Eurovent Certita Certification – France
www.eurovent-certification.com

LG Electronics – France
www.lgeaircon.com

Viega – Germany
www.viega.com

Aermec – Italy
www.aermec.com

Evapco Europe – Italy
www.evapco.eu

Rhoss – Italy
www.rhoss.com

Purmo Group – The Netherlands
www.purmogroup.com

Royal Haskoning DHV – The Netherlands
www.royalhaskoningdhv.com

SMAY – Poland
www.smay.eu

E.E.B.C. – Romania
www.eebc.ro

Dosetimpex – Romania
www.dosetimpex.ro

Testo – Romania
www.testo.com

Camfil – Sweden
www.camfil.com

Fläkt Group – Sweden
www.flaktgroup.com

Lindab – Sweden
www.lindab.com

Swegon – Sweden
www.swegon.com

Systemair – Sweden
www.systemair.com

Belimo Automation – Switzerland
www.belimo.com

Arçelik – Turkey
www.arcelikglobal.com

Friterm Termik Cihazlar Sanayi ve Ticaret – Turkey
www.friterm.com

Zoonex – United Kingdom
www.zoonexsystems.com

REHVA Associate Organisations:

EVHA – European Union
www.evha.eu

Enerbrain srl – Italia
www.enerbrain.com

Enviromech – United Kingdom
www.enviromech.co.uk

ISIB – Turkey
www.isib.org.tr

ECI – Belgium
copperalliance.org

OAER – Romania
www.oaer.ro

Network of 26 European HVAC Associations joining 120 000 professionals

REHVA Office: Rue Washington 40, 1050 Brussels - Belgium • Tel: + 32 2 514 11 71 - info@rehva.eu - www.rehva.eu

CLIMA 2025

REHVA 15th HVAC World Congress

SEE YOU IN ITALY

AiCARR
Cultura e Tecnica per Energia Uomo e Ambiente

REHVA
Federation of European Heating, Ventilation and Air Conditioning Associations